Heinrich Heine Universität Düsseldorf

Inaugural Dissertation

Unravelling tau-amyloid β crosstalk in Alzheimer's disease: insights into liquid–liquid phase separation and its role in neurodegenerative mechanisms

for the attainment of the title of doctor in the Faculty of Mathematics and Natural Sciences at the

Heinrich Heine University Düsseldorf

Submitted by

Tina Jacob

Kerala, India

Düsseldorf, December 2025

From the Institut für Physikalische Biologie at Heinrich-Heine-Universität Düsseldorf

Published by the permission of the Mathematisch-Naturwissenschaftlichen Fakultät at
Heinrich-Heine-Universität Düsseldorf

Supervisor: Jun.-Prof. Dr. Wolfgang Hoyer

Co-supervisor: Dr. Manuel Etzkorn

Date of oral examination: 05.03.2026

"If you can't fly, then run.

If you can't run, then walk.

If you can't walk, then crawl.

But whatever you do,

you have to keep moving forward."

- Martin Luther King Jr.

Declaration

Hiermit versichere ich an Eides statt, dass diese Dissertation von mir selbstständig und ohne unzulässige fremde Hilfe unter Beachtung der „Grundsätze zur Sicherung guter wissenschaftlicher Praxis an der Heinrich-Heine-Universität Düsseldorf“ erstellt worden ist. Die Arbeit wurde bisher keiner Prüfungsbehörde vorgelegt und auch noch nicht veröffentlicht. Ich habe bisher keinen erfolglosen Promotionsversuch unternommen.

Düsseldorf

02.12.2025 Tina Jacob

Acknowledgements

My heartfelt thanks to my supervisor, Wolfgang Hoyer, for his support and guidance throughout the journey. He supported me infinitely throughout the whole process, always there whenever I needed some help and always encouraged me whenever I wanted to do something scientific, like presentations or going for conferences. I couldn't ask for a better supervisor!

I would also extend my thanks to my second supervisor, Manuel Etzkorn for his help during this project.

I take this moment to thank all the people who helped to carry out different experiments in all the projects. Their scientific expertise in respective experiments helped to fasten all the projects and helped me to finish in time.

Far from my home, there were some people who made me feel home here. They made my life in Germany better, easier, comfortable.

My dearest Florian, I will always remember the time we spent together. All the writing sessions, crazy times, jokes that we shared will never ever fade away. The warmth you gave me as an international here in Germany is immeasurable. Thankyou for everything!

My dearest, Nazanin, you made me comfortable from the very beginning here. You are a precious person, and I will never forget you.

My dearest, Luis and Fernanda, thanks for everything, all the wonderful times that we all enjoyed together, ready to help me whenever, wherever.

Adding some more wonderful people to the list, whom I cannot leave out. Lora, Celina, Marie, Robin, Andrea, Joana, Hamed. They helped me always and I cannot thank you enough. The times that we shared together will always be close to my heart. Thanks to everyone who were and are part of IPB. Very nice and no stress working atmosphere was always helpful. My badminton people were my stress relievers outside work. I enjoyed so much playing with you and it would not be fair if I name some people because everyone there, were so nice and it was a lot of fun. Thankyou.

My family, Papa, Mummy, Chettayi, Jeenu, Maby are the people who supported me from miles away.

I would like to name out Taniya, Feby, Dibin, Atri, Remo, Jo, Athira, Littu, AK, Sanjay, Lena, Vinoth, Kartik, Harsha and everyone who made my PhD time better.

List of Abbreviations

1,6-HD	1,6-hexanediol
αS	α-Synuclein
Aβ	Amyloid-β
AD	Alzheimer’s Disease
ALS	Amyotrophic Lateral Sclerosis
APLP1/2	Amyloid Precursor-Like Proteins 1 and 2
APOE ε4	Apolipoprotein E ε4
APP	Amyloid Precursor Protein
ATP	Adenosine triphosphate
βS	β-Synuclein
Ca^{2+}	Calcium
CNS	Central Nervous System
C_{sat}	Saturation concentration
Cys	Cysteine
dimAβOs	Dimeric Amyloid-β Oligomers
DLS	Dynamic Light Scattering
DMEM/F-12	Dulbecco's Modified Eagle Medium / Nutrient Mixture F-12
DNA	Deoxyribonucleic acid
DTT	Dithiothreitol
EDTA	Ethylenediaminetetraacetic Acid
ELISA	Enzyme-Linked Immunosorbent Assay
ER	Endoplasmic Reticulum

FBS	Fetal Bovine Serum
FRAP	Fluorescence Recovery After Photobleaching
FUS	Fused in Sarcoma Protein
FTD	Frontotemporal Dementia
GAG	Glycosaminoglycans
HD	Huntington's Disease
HFIP	1,1,1,3,3,3-Hexafluoro-2-propanol
HMW	Higher Molecular Weight
HRP	Horseradish Peroxidase
Hsp	Heat Shock Protein
IDRs	Intrinsically Disordered Regions
IDP	Intrinsically Disordered Protein
IEC	Ion Exchange Chromatography
IMAC	Immobilized Metal Affinity Chromatography
IPTG	Isopropyl β-D-thiogalactopyranoside
kDa	Kilodalton
LCDs	Low-Complexity Domains
LDH	Lactate Dehydrogenase
LLPS	Liquid–Liquid Phase Separation
MAPT	Microtubule-Associated Protein Tau
MB	Methylene Blue
mRNA	Messenger RNAs
MTBD	Microtubule-binding domain
NaCl	Sodium Chloride
NaOAc	Sodium Acetate

NaPi	Sodium Phosphate
NDs	Neurodegenerative Diseases
NEAA	Non-Essential Amino Acids
NHS	N-Hydroxysuccinimide
NFTs	Neurofibrillary Tangles
NAC	Non-Aβ component
OD	Optical Density
PBS	Phosphate-Buffered Saline
PD	Parkinson’s Disease
PEG	Polyethylene Glycol
PFs	Protofibrils
PHFs	Paired Helical Filaments
ptau	Phosphorylated tau
PIPES	Piperazine-N, N'-bis (2-ethanesulfonic acid)
pI	Isoelectric Point
PBS	Phosphate Buffered Saline
PO_4	Phosphoryl Group
PD	Parkinson's disease
PDI	Protein Disulfide Isomerase
PPIase	Peptidyl Prolyl Isomerase
PPIA	Peptidyl Prolyl Isomerase A
PRD	Proline-Rich Domain
PrP	Prion Protein
PTMs	Post-Translational Modifications
PVDF	Polyvinylidene Difluoride

RBPs	RNA Binding Proteins
RNA	Ribonucleic Acid
ROI	Region of Interest
rpm	Revolutions Per Minute
RaPID	Random Non-standard Peptides Integrated Discovery
ROS	Reactive Oxygen Species
RP-HPLC	Reverse-Phase High-Performance Liquid Chromatography
SDS-PAGE	Sodium Dodecyl Sulfate Polyacrylamide Gel Electrophoresis
SEC	Size-Exclusion Chromatography
-SH	Thiol group
sHsp	Small heat shock proteins
SERF	Small EDRK-rich factor
SNARE	Soluble N-ethylmaleimide-sensitive factor Attachment Protein Receptor
SVs	Synaptic Vesicles
Tau	Microtubule-Associated Protein Tau
TBST	Tris-Buffered Saline with Tween-20
TCEP	Tris(2-carboxyethyl) phosphine
TDP-43	Transactive response DNA-Binding Protein 43 kDa
TIA 1	T-cell intracellular antigen-1
ThT	Thioflavin-T
VAMP2	Vesicle-Associated Membrane Protein 2
WHO	World Health Organization
WT	Wild-Type

Table of contents

List of figures

Chapter 1

Chapter 2

Chapter 3

Chapter 4

Chapter 5

Appendix

List of tables

Chapter 1

Chapter 2

Chapter 3

Appendix

Summary

Alzheimer's disease (AD) is among the leading causes of death worldwide, and its prevalence steadily increases with rising life expectancy and population aging. According to the World Health Organization, AD ranks among the top ten causes of mortality globally. The pathological accumulation of tau and amyloid-beta (Aβ) represents the principal hallmarks of AD. However, therapeutic approaches targeting either tau or Aβ individually have so far failed to yield curative outcomes, suggesting the involvement of complex and interconnected pathological processes in AD.

This thesis primarily focuses on investigating the interactions between tau and Aβ oligomers, proposing the central hypothesis that these interactions occur within the cellular environment and may play a pivotal role in disease progression. Understanding these interactions provides new insights into the mechanisms underlying AD and highlights the potential need for therapeutic approaches that target both tau and Aβ concurrently.

Chapter 1 presents a general introduction to neurodegenerative diseases and AD. It provides an overview of tau and Aβ proteins, their structures, physiological roles and mechanisms of pathological aggregation. The chapter also introduces dimAβ, the dimeric Aβ construct employed in this study to specifically investigate off-pathway Aβ oligomers. The chapter concludes a discussion of existing research exploring the interplay between tau and Aβ in AD pathology.

Chapter 2 reviews the concept of liquid–liquid phase separation (LLPS) of tau and α-synuclein and discusses how heterotypic LLPS can modulate protein aggregation. Emerging evidence indicates that different heterotypic LLPS partners of amyloidogenic proteins can influence their aggregation behaviour and potentially modulate disease pathways.

Chapters 3 and 4 describe experimental investigations into the interactions between tau and Aβ oligomers under LLPS and non-LLPS conditions. These studies demonstrate that tau and Aβ oligomers exhibit strong mutual affinity, leading to the formation of co-condensates and co-aggregates. While Aβ oligomers influence dynamics of tau in the heterotypic condensates, tau, in turn, modulates Aβ aggregation. These results provide new insights into the molecular basis of AD pathology and demonstrates that tau-Aβ oligomer interactions are influenced by crowding-induced solution conditions.

Finally, Chapter 5 integrates the results and highlights their broader implications. This work underscores the significance of studying heterotypic protein interactions and phase separation in neurodegenerative diseases. It proposes that targeting the synergistic

pathological behaviour of tau and Aβ may represent a promising direction for future therapeutic development in AD.

Zusammenfassung

Die Alzheimer-Krankheit (AD) zählt weltweit zu den häufigsten Todesursachen, und ihre Prävalenz steigt mit zunehmender Lebenserwartung und Alterung der Bevölkerung stetig an. Nach Angaben der Weltgesundheitsorganisation zählt AD weltweit zu den zehn häufigsten Todesursachen. Trotz intensiver Forschungsbemühungen existiert bislang keine kurative Therapie, was die dringende Notwendigkeit unterstreicht, die zugrunde liegenden Mechanismen der AD-Pathogenese besser zu verstehen, um wirksame therapeutische Strategien zu entwickeln. Die pathologische Akkumulation der Proteine Tau und Amyloid-Beta (Aβ) in Form amyloidogener Aggregate gilt als charakteristisches Kennzeichen der Erkrankung. Therapeutische Ansätze, die sich bisher ausschließlich auf eines dieser beiden Proteine konzentrierten, konnten jedoch keine kurativen Erfolge erzielen, was auf komplexe und miteinander verknüpfte pathologische Prozesse hinweist.

Diese Dissertation befasst sich mit der Aufklärung der pathologischen Wechselwirkungen zwischen Tau und Aβ. Die zentrale Hypothese lautet, dass die zellulären Interaktionen dieser beiden Proteine eine entscheidende Rolle im Krankheitsverlauf spielen könnte. Ein tieferes Verständnis dieser Prozesse könnte neue Einblicke in die zugrundeliegenden Mechanismen der AD-Pathogenese liefern und darauf hindeuten, dass therapeutische Strategien, die beide Proteine gleichzeitig adressieren, vielversprechender sind als Ansätze, die nur eines der Proteine anvisieren.

Kapitel 1 bildet eine allgemeine Einführung in die AD sowie verwandte neurodegenerative Erkrankungen. Neben einer Beschreibung der Strukturen und den physiologischen Funktionen der Proteine Tau und Aβ befasst sich das Kapitel mit den pathologischen Prozessen, die zu ihrer Aggregation führen. Darüber hinaus werden bisherige Studien zur Wechselwirkung zwischen Tau und Aβ im Kontext der AD-Pathologie zusammengefasst.

Kapitel 2 bietet eine Einführung in das Konzept der Flüssig-Flüssig-Phasentrennung (*liquid–liquid phase separation*, LLPS) von Tau und α-Synuclein und diskutiert, wie LLPS die Aggregation von Proteinen modulieren kann. Es beschreibt, wie heterotypische Phasentrennungen zwischen amyloidogenen Proteinen deren Aggregationsverhalten beeinflussen und möglicherweise krankheitsrelevante Signalwege beeinflussen können.

Kapitel 3 und 4 präsentieren die experimentell erzielten Ergebnisse zu den Interaktionen zwischen Tau- und Aβ-Oligomeren unter phasentrennenden und nicht-phasentrennenden Bedingungen. Die Ergebnisse zeigen, dass Tau und Aβ eine starke gegenseitige Affinität aufweisen, die zur Bildung gemischter Kondensate und Aggregate führt, welche die Aggregationsdynamik beider Proteine beeinflussen. Die Ergebnisse legen nahe, dass Tau die

Aβ-Aggregation modulieren kann und *vice versa*, wodurch neue Perspektiven für das Verständnis der molekularen Grundlagen der AD eröffnet werden.

Kapitel 5 fasst die erzielten Ergebnisse zusammen und diskutiert ihre übergeordnete Bedeutung im Kontext der aktuellen Literaturlandschaft. Die vorliegende Arbeit hebt die Relevanz von heterotypischer Protein-Interaktionen und Phasentrennung bei neurodegenerativen Erkrankungen hervor. Zudem deutet sie darauf hin, dass die gemeinsame pathologische Dynamik von Tau und Aβ ein vielversprechendes Ziel für zukünftige therapeutische Ansätze in der AD-Forschung darstellen könnte.

Publications included in this thesis

1. Jacob T, and Hoyer W *Heterotypic phase separation in aggregation: driver or deterrent?* Under revision at to *Biophysical chemistry* (2025)

2. Jacob T, Schützmann M and Hoyer W *Liquid-liquid phase-separated tau colocalizes with and stabilizes Aβ oligomers*. Under revision Nature *Communications* (2025)

Chapter 1: Introduction

1.1 Neurodegenerative diseases

Neurodegenerative diseases (NDs) are a wide group of chronic, progressive disorders that are characterized by the gradual loss of structure and function of neurons, resulting in significant cognitive and motor impairments (1,2). These conditions impact millions of individuals globally, posing a substantial burden on public health systems. An important feature of NDs is the deposition of misfolded proteins as amyloids with altered physicochemical properties (3). Frequent proteins involved in the pathogenesis of NDs are tau, amyloid-β (Aβ), prion protein (PrP), α-synuclein (αS), TAR-DNA-binding protein 43 kDa (TDP-43) and fused-in sarcoma protein (FUS) and their pathological deposits give rise to a wide variety of NDs (4). NDs can be classified based on the primary protein involved and the brain region affected (5). Table 1.1 gives an overview of important NDs and their key characteristics.

NDs can arise through a combination of genetic and non-genetic factors, and are broadly classified as familial or sporadic (6–8). Familial cases account for a smaller proportion of total cases and are caused by inherited mutations that follow clear patterns of genetic transmission, often autosomal dominant or recessive (9). These cases typically appear earlier in life and are linked to mutations in genes that disrupt cellular processes. In contrast, sporadic cases which represent the vast majority of NDs, occur in individuals with no known family history of the disease (10). The causes of sporadic NDs are often multifactorial, involving a complex interplay of age-related cellular decline, environmental exposures and common genetic risk variants that do not follow classic inheritance patterns.

Table 1.1: Key NDs and their key characteristics

ND	Key proteins	Affected brain regions	Clinical symptoms
Alzheimer's Disease (AD)	Aβ, Tau	Hippocampus, cortex	Memory loss, cognitive decline
Parkinson's Disease (PD)	αS	Substantia nigra	Bradykinesia, tremors
Frontotemporal Dementia (FTD)	Tau, TDP-43	Frontal/temporal lobes	Personality changes, aphasia
Amyotrophic Lateral Sclerosis (ALS)	TDP-43	Motor neurons	Muscle weakness, paralysis
Multiple Sclerosis	Autoimmune myelin attack	White matter tracts in CNS	Visual loss, paraesthesia
Huntington's Disease (HD)	Huntingtin	Striatum	Involuntary movements, dementia

1.1.1 Prevalence and social impact

Among all NDs, Alzheimer's disease (AD) is the most prevalent, accounting for 60–70% of dementia cases worldwide (11). According to the World Health Organization (WHO), more than 55 million people live with dementia globally, with nearly 10 million new cases each year (12). As life expectancy continues to rise, the prevalence of age-related disorders such as AD, Parkinson's disease (PD), and frontotemporal dementia (FTD) is expected to increase dramatically. Along with the financial implications, NDs profoundly affect the quality of life, leading to progressive cognitive decline, behavioural changes and ultimately causing death (13).

1.1.2 Common hallmarks of NDs and major risk factors

A key feature of neurodegenerative disorders is their selective targeting of specific brain regions, which underlies the diversity of clinical symptoms observed across diseases (14) (Fig 1.1 A). In AD, widespread cortical atrophy is observed, particularly in the hippocampus and temporal lobes, contributing to memory impairment (15). PD is characterized by the degeneration of dopaminergic neurons in the substantia nigra within the midbrain, leading to motor dysfunction (16). HD exhibits prominent atrophy in the striatum, associated with motor, cognitive and psychiatric disturbances (17). Multiple sclerosis is marked by demyelinating lesions within white matter tracts across the central nervous system, often involving periventricular regions, spinal cord and optic nerves (18). Despite their clinical and pathological diversity, many NDs share hallmark features at the molecular and cellular levels (19). These include protein aggregation, synaptic failure, disrupted proteostasis, mitochondrial dysfunction, oxidative stress and neuroinflammation (Fig 1.1 B).

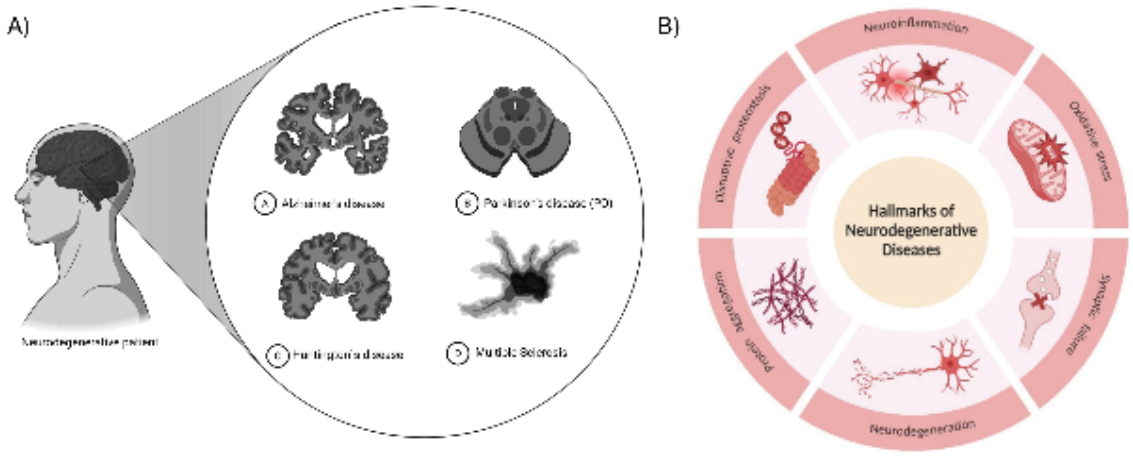

Fig 1.1: Different NDs and their hallmarks. A) Neuroanatomical regions impacted in different NDs. (Created with Biorender) B) Common pathological hallmarks of NDs (10).

NDs arise from a complex interplay between genetic, environmental and lifestyle-related factors (20). Although the precise etiology often varies across different NDs, several overlapping risk factors have been consistently identified. Among the risk factors, aging is widely recognized as the most significant non-modifiable risk factor for most of the NDs (21). While aging itself is not a pathological condition, it induces a range of biological changes that create a permissive environment for neuronal dysfunction and degeneration. Genetic mutations also play a significant role in the development and progression of various NDs, particularly in familial and early-onset cases (22). These mutations can interfere with essential cellular processes such as protein folding and clearance, mitochondrial function, RNA metabolism and synaptic regulation. Environmental and occupational exposures are increasingly recognized as important contributors to the risk of developing NDs, particularly in sporadic cases (23). Chronic exposure to certain environmental toxins such as pesticides, heavy metals, industrial solvents and air pollutants has been associated with elevated incidence of NDs. Lifestyle factors such as diet, physical activity, sleep quality, stress levels and cognitive engagement have been shown to modulate brain health over the lifespan (24). Sedentary behaviour, poor sleep hygiene and chronic psychological stress may exacerbate neuroinflammation. Furthermore, excessive alcohol consumption and smoking have been linked to increased risk of vascular dementia and other cognitive impairments.

1.2 Alzheimer's disease (AD)

AD is a progressive ND and the most prevalent form of dementia, characterized by gradual cognitive decline, memory impairment, behavioural disturbances which ultimately leads to death (25). AD was first described by Alois Alzheimer in 1906 (26) and now it is one of the leading cause of deaths worldwide imposing severe economic impact on the health care system (27). AD progresses through stages of mild memory deficits in the initial stages to severe impairment in executing daily functions, language and self-care abilities. Although advancing age remains the strongest risk factor, genetic mutations, polymorphism of apolipoprotein E gene (APOE ε4 allele), vascular comorbidities and lifestyle factors contribute significantly to AD susceptibility (28).

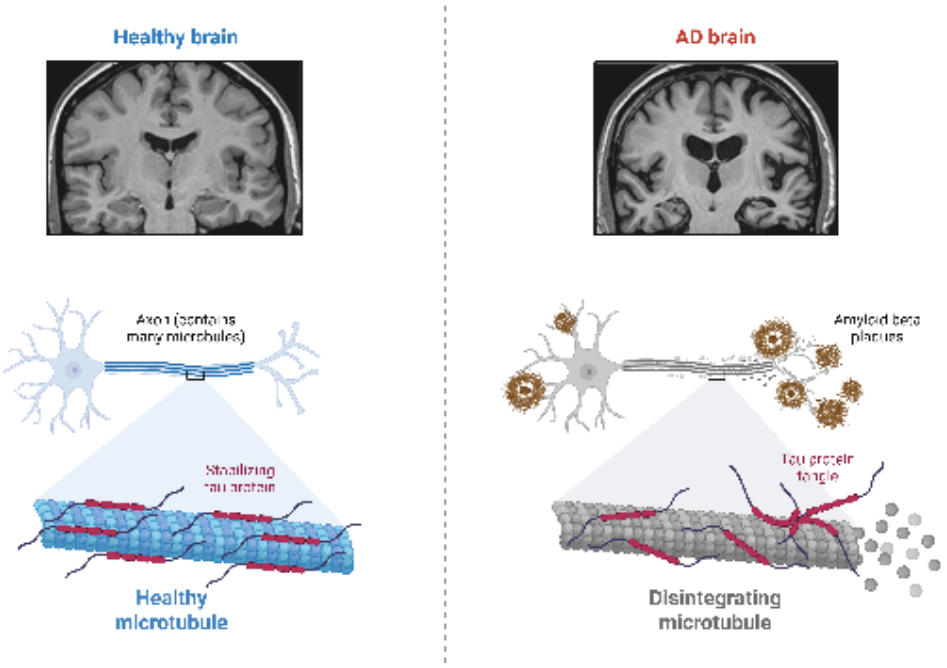

Fig 1.2: Pathology in AD. Comparison between a healthy brain and AD brain. (Created with Biorender)

Neurodegeneration in AD are attributed to cerebral atrophy, synaptic dysfunction, neuronal loss and mitochondrial dysfunction, particularly within the hippocampus and cortex regions of the brain (29). However, the pathology of AD is associated with 2 major hallmark accumulations; extracellular senile plaques composed of amyloid-β and intracellular neurofibrillary tangles composed of hyperphosphorylated tau protein (30) (Fig 1.2).

Till date there is no curative therapy for AD (31). However, several pharmacological interventions have been developed that primarily provide symptomatic relief in neurodegenerative diseases, whereas non-pharmacological strategies aim to delay cognitive decline and enhance quality of life in affected individuals (32,33). Lecanemab is one of the most effective treatment for AD in the current times that targets soluble amyloid-β protofibrils and thereby reducing amyloid plaque formation in the brain (34,35). It is a monoclonal antibody approved for the treatment of early AD and has been effective in slowing down cognitive and functional decline. But Lecanemab was associated with adverse events, indicating potential safety concerns that require longer trials and further investigation (36,37). Given its rising prevalence and profound socioeconomic burden, AD represents a major global health challenge necessitating continued research into disease-modifying treatments and preventive strategies.

1.3 Tau: structure, function and pathology

Tau protein is a critical microtubule-associated protein that plays a fundamental role in the development of AD and other tauopathies, which are a group of neurodegenerative disorders characterized by tau aggregation (38). In AD, tau undergoes hyperphosphorylation, leading to the formation of neurofibrillary tangles (NFTs), which are one of the key hallmarks of the disease (39). These tangles contribute to neuronal dysfunction and degeneration, ultimately resulting in cognitive decline and memory loss.

Tau was first discovered in 1975, as a heat stable microtubule-associated protein, that exists in highly soluble form in neurons throughout the central nervous system (CNS) (40). Tau is predominantly found in the axons of neurons, and the pivotal function of tau is to bind to microtubules, enhance the assembly and regulate the stability of microtubules (41).

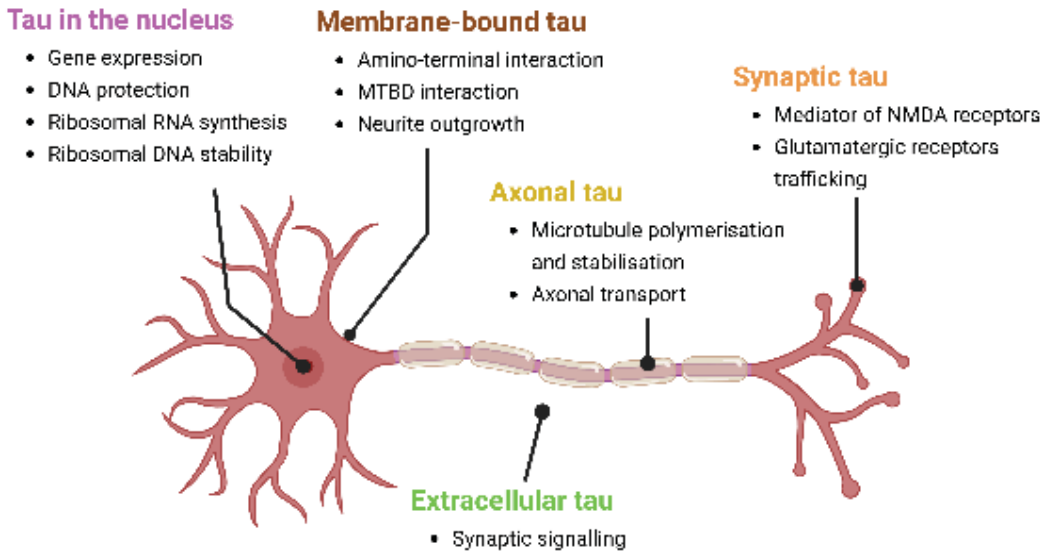

Fig 1.3: Functional roles of tau. Cellular functions of tau based on its occurrence.

Unlike other globular functional proteins, tau is an intrinsically disordered protein (IDP) (42). IDPs contain high proportion of polar and charged amino acids in their sequence, which results in the absence of a well-defined three-dimensional structure in their native form (43). Hence, being an IDP, under physiological conditions tau lacks a well-defined three-dimensional structure and instead, exists as an ensemble of conformations. This structural flexibility contributes to the interaction of tau with a wide variety of binding partners, supporting its physiological roles in microtubule stabilization (44,45). Further, tau is a versatile protein in neurons and highly multi-functional in nature (Fig 1.3). In the nucleus, tau

contributes to DNA protection and chromatin organization. As a membrane-bound protein, it interacts with plasma and organelle membranes, influencing signalling and structural stability. At the synapse, tau participates in regulating synaptic plasticity and signalling and additionally and extracellular tau has been implicated in cell-to-cell communication.

In the adult human brain, six isoforms of tau are expressed, generated through alternative splicing of the MAPT (Microtubule-associated protein tau) gene located on chromosome 17q21 (46). The longest human isoform of tau, 2N4R tau and consists of 441 amino acids. We refer to the full-length tau as "tau" in this thesis. Tau is characterised into distinct structural domains, each composed of specific amino acid compositions and charge properties (46,47) (Fig 1.4). At the N-terminus, tau contains a highly acidic projection domain that mediates interactions of tau with cellular membranes and other proteins. Next to the N-terminal region is the proline-rich region, which carries a net positive charge and contains multiple sites for phosphorylation and protein-protein interactions. The microtubule-binding repeats in the central region are critical for the assembly, nucleation, and stabilization of microtubules. They are highly basic and are dominated by positively charged residues that mediate electrostatic binding of tau to the negatively charged surface of microtubules. Finally, the C-terminal region is positively charged and supports microtubule stabilization and tau-tau interactions. Together, tau is a basic, hydrophilic protein and is highly stable under acidic and high temperature conditions (48).

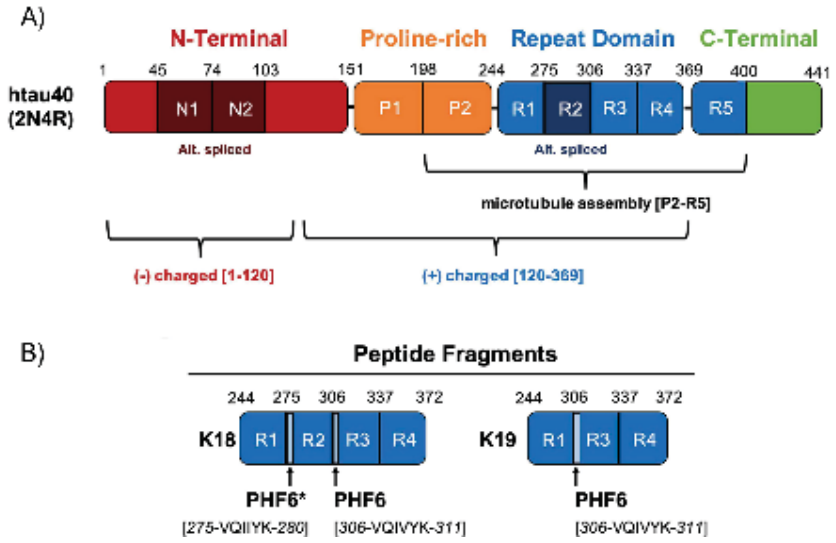

Fig 1.4: Domains of tau. A) shows the different domains in tau construct and their charges B) shows the K18 and K19 isoforms of tau. Adapted from (44)

The other two significant isoforms of tau are the K18 and K19 variants, which differ in their structural composition and pathophysiological implications (46). The K18 or 4R isoform of tau consists of four microtubule-binding repeats (R1–R4) but lacks the N-terminal region.

K18 retains important structural features that facilitate interactions with microtubules but lacks the regions that modulate phase behaviour and other functions associated with the full-length protein. In contrast, the K19 or 3R isoform contains only the first three repeat domains (R1-R3) of tau. In the normal human brain, the expression levels of 3R and 4R tau occur at a 1:1 ratio and several tauopathies are characterized by the alteration of this ratio of 3R:4R tau (49–51).

1.3.1 Post-translational modifications (PTMs) of tau

Post-translational modifications (PTMs) are one of the key mechanisms that drive AD pathogenesis and are also important for the regulation of cellular functions by tau (52). PTMs refer to the chemical alterations to a protein that occur at various stages of its life cycle. The homeostasis of such protein modifications are critical to human health but abnormal PTMs lead to changes in protein properties and loss of protein functions (53). PTMs are catalysed by enzymes and involve the addition of chemical groups or sugars to specific residues of the targeted protein (52). They alter the charge and electrostatics of a protein, inducing structural changes that influence protein function, protein-protein interactions and protein aggregation (54).

A wide variety of PTMs have been identified on tau that target different amino acids and multiple regions (55) (Table 1.2). Phosphorylation is one of the most common and important PTMs in the tau protein and is involved in both its physiological and pathological states (56,57). Tau has 85 potential phosphorylation sites, and this contributes to about 20 % of the whole protein that have the tendency to get phosphorylated (58). It involves the addition of a phosphoryl group (PO_4) to the polar side chains of amino acids and are carried out by a wide variety of kinases and phosphatases. Phosphorylation usually leads to increased polarity and hydrophilicity of the targeted amino acids enabling it to form intramolecular and intermolecular hydrogen bonding. While a normal phosphorylation of tau is critical for neuronal plasticity, a hyperphosphorylation interactions induce large conformational changes that may lead to aggregation or disaggregation of proteins (59). In the healthy brain, two to three amino acid residues on tau are phosphorylated. However, under pathological conditions the phosphorylation level of tau is significantly higher, with five to nine phosphates per tau protein (60). Ultimately abnormal hyperphosphorylation leads to aberrant aggregation, fibrillization and deposition into NFTs (61,62).

In addition to hyperphosphorylation, other types of PTMs of tau also contribute to the functions and dysfunctions of tau. Site-specific acetylation of tau has been observed in the brains of AD (63). However, acetylation has been shown to strongly attenuate aggregation of four-repeat tau protein while promoting amyloid formation of three-repeat tau (64). Similar

to acetylation, a site-dependent influence on tau aggregation has been observed in nitration. Depending on the residues that are modified, nitration can either promote or inhibit tau aggregation (65,66).

Table 1.2: PTMs of tau

PTM	Mode of action	Functional roles	Pathological roles
Phosphorylation	Addition of a phosphate group	Regulates tau's interaction with microtubules	Hyperphosphorylation reduces microtubule binding, disrupts axonal stability, and promotes aggregation into neurofibrillary tangles.
Acetylation	Addition of an acetyl group to lysine residues.	Modulates tau–microtubule interaction	Prevent degradation of tau leading to accumulation of tau
Ubiquitination	Covalent attachment of ubiquitin to lysine residues	Tags tau for proteasomal degradation	Impaired ubiquitination leads to inefficient clearance, favoring tau buildup and toxicity
O-GlcNAcylation	Addition of O-linked N-acetylglucosamine	Stabilizes tau and support microtubule binding	Reduced O-GlcNAcylation in Alzheimer's disease enhances hyperphosphorylation and aggregation
Nitration	Nitration of tyrosine residues	No specific roles studied	Promote tau aggregation; dependent on the residues targeted
Oxidation	Oxidation of cysteine/methionine.	No specific roles studied	Promote tau aggregation into paired helical filaments (PHFs)
Methylation	Addition of methyl groups to lysine or arginine residues.	Modulates tau–microtubule binding and structural conformation	Aberrant methylation increases aggregation propensity and mislocalization.

The role of methylation and ubiquitination in tau aggregation is controversial. Since they are observed in both healthy and diseased brains, their exact role in tau aggregation still needs to be explored (67,68). The oxidation of the cysteine residues promote tau aggregation into paired helical filaments (69). Other PTMs like glycosylation, glycation, ubiquitination and SUMOylation involve addition of large sugar groups or protein macromolecules. They impose steric hindrance on the native conformation of tau and hence strongly influence misfolding and aggregation (70). All major PTMs of tau, their mode of action, functional and pathological roles are listed in Table 1.2. The transition from functional to pathological tau is not likely a consequence of a single PTM, but rather a combination of the intrinsic structural alterations and extrinsic cellular conditions that leads to aberrant modifications and ultimately end in pathogenicity.

1.3.2 Pathology of tau

The functional nature of tau under physiological conditions is disrupted by pathological abnormalities including aberrant PTMs, mutations in the MAPT gene, hyperphosphorylation or enzymatic imbalance (71). Under these pathological conditions, tau undergoes misfolding and conformational changes, leading to its cytosolic accumulation and subsequent initiation of a pathogenic fibrillogenic cascade. Various tauopathies exhibit a diverse spectrum of pathological features, characterized by different types of tau inclusions that affect specific brain regions (72).

The aggregation pathway of tau initiates with the formation of dimers, oligomers from monomers, which further progresses into paired helical filaments (PHFs) and NFTs (73). Two hyperphosphorylated tau monomers can associate to form dimers, which serve as nuclei for the growth of larger aggregates. The addition of further tau monomers to these dimers gives rise to small, soluble oligomers that are structurally diverse and highly toxic. Tau oligomers represent a heterogeneous population of assemblies that differ in size, conformation, and stability (74). While the large insoluble NFTs have been the histopathological hallmark of AD and other tauopathies, it has been proposed that the soluble tau oligomers formed prior to fibril formation are the principal toxic species in these neurodegenerative disorders (75,76). These oligomeric intermediates cause synaptic dysfunction, mitochondrial damage, cellular cytotoxicity and can induce neurodegeneration in animal models (77–80). Tau oligomers can further assemble into protofibrils that mature into PHFs. PHFs are insoluble, less toxic than oligomers and exhibit a characteristic twisted double-helical morphology. Other filament types, such as straight filaments (SFs) and ribbon-like fibrils have also been identified in different tauopathies (81,82). PHFs can further associate into filamentous, β-sheet rich insoluble NFTs of tau. NFT deposition interfere will cell functioning and contributes to neuronal deaths. The extent of NFT deposition correlates with dementia severity and neuronal loss. Although the controversy surrounding the most neurotoxic species of tau persists, in recent years there is a shift in the therapeutic strategies to target toxic tau oligomers, rather than the large insoluble fibrillar aggregates (83–85).

A variety of negatively charged cofactors are known to induce tau aggregation *in vitro*, including polyanions like DNA, RNA and heparin (86–88). These anionic inducers bind to the positively charged regions of tau and disrupt its long-range intramolecular electrostatic interactions, thereby promoting aggregation. This disruption promotes local concentration of tau and facilitates its self-association into pathological aggregates. In 1996, Goedert *et al*. showed that heparin can stimulate tau phosphorylation and induce fibrillization (89). Structurally, heparin resembles sulphated glycosaminoglycans (GAG) that have been found

to colocalize with tau inclusions in AD and since then heparin has been widely used to study tau aggregation.

Recent studies have revealed that tau, particularly the full-length isoform exhibits a strong propensity to undergo liquid-liquid phase separation (LLPS) forming dynamic, protein-rich liquid droplets. The first experimental evidence of tau LLPS was reported in 2017 (90). Subsequent investigations by Wegmann *et al*. showed that LLPS can initiate the aggregation of tau into fibrils, while Kanaan *et al*. illustrated that LLPS is significantly enhanced in disease-associated forms of tau that further promoted pathogenic conformations of tau *in vitro* (91,92). This link between LLPS and aggregation of tau has been a great advancement in the study of pathology of tau. Further details on the general principles of LLPS and its relevance to tau are discussed in the next section.

One widely proposed mechanism for the propagation of tau pathology is the “prion-like seeding” enabling its spread to distinct parts of the brain (93). This was supported by the observation that brain extracts from tauopathies can induce tau aggregation in healthy neurons (94,95). Misfolded tau can act as pathological “seeds” that initiates aggregation pathway. They eventually disrupt neuronal structure and intracellular transport, contributing to cellular dysfunction. The misfolded tau that is released into extracellular space via dying cells are internalized by neighbouring. Internalized seeds convert native tau into misfolded forms and thus spreading pathology from neuron to neuron.

1.4 LLPS

Eukaryotic cells contain organelles that provide distinct chemical microenvironments for carrying out biochemical functions crucial for maintaining cellular homeostasis. These organelles can be classified into (i) membrane-bound organelles; facilitate spatially restricted biochemical processes and (ii) membraneless organelles; lacks a surrounding membrane yet exhibit distinctive organization within the cell (96,97). Nucleolus, Cajal bodies, P granules, stress granules, signalling complexes, processing bodies, and germline granules are critical membraneless organelles that carry out a range of distinct cellular functions in a confined space (97,98). These membraneless organelles, also known as "biomolecular condensates” and are formed through the process of LLPS. LLPS is a physiological process that drives the transition of a homogeneous solution components into a concentration-deprived dilute phase and a concentration-rich dense phase (99). Hence formed condensates exhibit liquid-like properties, enabling their components to diffuse, reorganize and fuse freely, thereby facilitating dynamic exchange with the surrounding cellular environment (100). They mediate critical processes in cells including gene expression, signal transduction and stress response (101). Several factors contribute to the

formation of these condensates, and these include multivalent, weak and transient interactions between protein-protein, protein-RNA and RNA-RNA interactions.

LLPS is particularly enriched in intrinsically disordered regions (IDRs) or low-complexity domains (LCDs) of proteins, which lack a stable secondary or tertiary structure, making them highly flexible and hence prone to phase separation (102). These regions enable interactions such as π-π stacking, dipole-dipole interactions, cation-anion interactions and π-cation interactions, which collectively facilitate the reversible formation of liquid-like droplets (103,104). LLPS is a tightly balanced process regulated by biomolecular composition, post-translational modifications, RNA interactions and cellular environmental cues such as temperature, pH and salt concentration (105).

An increasing number of proteins implicated in neurodegenerative diseases are now recognized to physiologically undergo LLPS (106). Over time, these dynamic and reversible condensates can gradually "age," transitioning from an initially liquid-like and mobile state into more viscous, gel-like assemblies, eventually giving rise to solid amyloid fibrils with pronounced cytotoxicity (92,107,108). This reflects how disturbances in phase behaviour bridge normal physiological organization and pathological aggregation. Consequently, LLPS is now regarded as an early molecular event in the cascade leading to neurodegeneration, offering a promising framework for identifying novel therapeutic strategies to restore or modulate healthy phase behaviour.

1.4.1 Thermodynamic basis of LLPS

LLPS arises from a balance between enthalpic attractions among biomolecules and entropic contributions from solvent reorganization. From a thermodynamic view, LLPS occurs when the total free energy change (ΔG) becomes negative, allowing spontaneous demixing of a homogeneous solution into a dense condensate phase and a dilute phase (109). Enthalpic gains arise primarily from multivalent weak interactions such as π-π and cation-π stacking, hydrogen bonding and electrostatic complementarity, which stabilize the condensed state (110). These interactions often involve aromatic and polar residues within IDRs of phase-separating proteins.

1.4.1.1 Flory-Huggins theory

Flory-Huggins (FH) theory explains the thermodynamic model of liquid mixing (111). It describes LLPS as a phenomenon that is driven as the competition of entropy of mixing and interaction energy between species involved (112,113). It is defined as:

$$\Delta Gmix = N1\phi 1 ln\phi 1 + N2\phi 2 ln\phi 2 + \chi\phi 1\phi 2$$

where:

ΔG_{mix} = Free energy of mixing

ϕ1, ϕ2 = Volume fractions of each component

N1, N2 = Degree of polymerization (size of the chains)

χ = FH interaction parameter

A high χ value reflects poor solubility and favors demixing. For large biomolecules (N → ∞), LLPS occurs when χ exceeds a critical value (~0.5), consistent with experimental findings for IDPs such as tau (114,115).

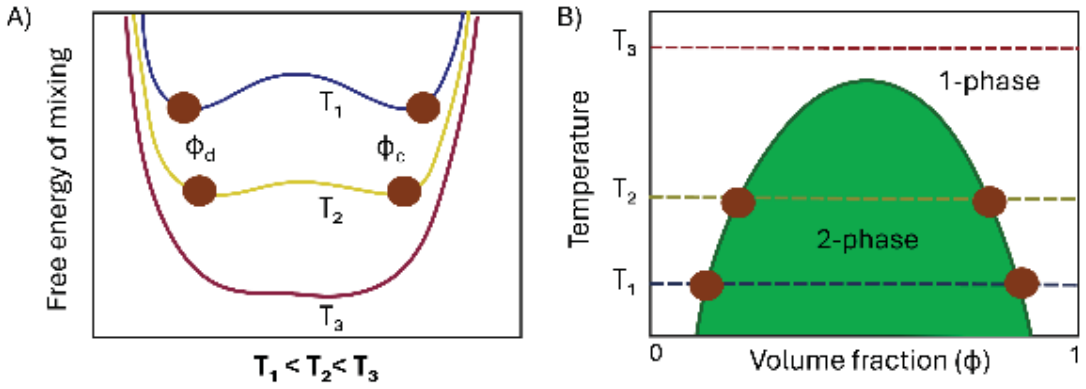

Fig 1.5: Phase diagrams of LLPS. A) shows free energy of mixing as a function of volume fraction (ϕ) for three representative temperatures (T1 < T2 < T3). Free energy surface at T_1 exhibits two minima corresponding to coexisting dilute (ϕd) and concentrated (ϕc) phases, separated by a barrier B) summarizes temperature versus volume fraction phase diagram of the different temperatures. The two-phase coexistence region (green area) is bounded by the binodal curve.

Fig 1.5 illustrates the phase behaviour based on effects of temperature and molecular composition on LLPS as described by the Flory-Huggins model (116,117). Temperature significantly alters the free energy landscape of phase separation. At lower temperatures, the profile becomes distinctly bimodal, reflecting the emergence of two thermodynamically stable states corresponding to dilute and dense phases. This transition marks the onset of demixing, where molecular crowding and attractive interactions drive the system into the two-phase regime. Importantly, the boundaries of this region in the phase diagram also define the temperature-dependent saturation concentrations (C_{sat}) (118). C_{sat} is the threshold concentration below which the system remains homogeneous and above which phase separation occurs. As the temperature increases, interaction strength decreases, free energy minimum merges and the two-phase region collapse, restoring miscibility and effectively raising the saturation concentration or eliminating phase separation altogether. This thermodynamic relationship encapsulates how environmental and molecular factors

converge to control both the propensity for phase separation and its saturation thresholds in protein solutions.

1.4.2 Key types of LLPS

In general three types of LLPS are defined; simple, complex and segregative LLPS (119–121). Fig 1.6 gives a schematic overview of the key types of LLPS described below.

1.4.2.1 Simple / Homotypic phase separation

Simple phase separation occurs when a single type of molecule self-associates into a dense phase through intermolecular interactions. Their coacervation is driven by a combination of π-π, cation-π, hydrogen bonding, dipole-dipole and charge interactions and strength of these interactions determine the rate at which they undergo coacervation. The stability of these LLPS systems is influenced by thermodynamic factors such as pH, ionic strength, and temperature, which in turn impact the intermolecular interactions. Such a phase separation system is often shown by proteins that have intrinsically disordered regions (IDRs) or low complexity domains (LCDs) (90,122).

IDRs are regions within a protein sequence that lack a defined three-dimensional structure and can exist in a variety of conformations. They can act as flexible linkers, mediate molecular recognition, binding interfaces for interaction partners and as cellular sensors (123–127). LCDs are a subset of IDRs wherein they lack structural definition and are characterised to have a very frequent amino acid composition (128). They often have a higher composition of amino acids such as glycine, alanine, serine, and threonine. While all LCDs are IDRs, not all IDRs are LCDs.

1.4.2.2 Complex / Associative / Heterotypic phase separation

A complex or associative phase separation is driven in a solution comprising of molecules that have high tendency to interact with each other. Several factors would govern these interactions similar to the simple phase separation. Often oppositely charged polymers, for as observed for RNA and tau (91), often show phase separation leading to a dense phase rich in both components. DNA is a highly charged polyelectrolyte and is prone to associate with multivalent cations, charged surfactants, proteins, polymers to undergo phase separation (129).

1.4.2.3 Segregative phase separation

In segregative LLPS, the repulsive forces between different molecules in a solution drive them to separate into two independent phases rich in each of the component. This creates a non-homogeneous system with two coexisting phases with differing molecular compositions (130). In this case, the thermodynamic factors such as pH, temperature and

the concentration of components play crucial roles and determine the state of the solution between co-solubility and phase separation.

A system demonstrating this phenomenon is the combination of the molecular crowders, polyethylene glycol (PEG) and dextran. They segregate into distinct two-phase system, PEG rich-phase and dextran-rich phase (120).

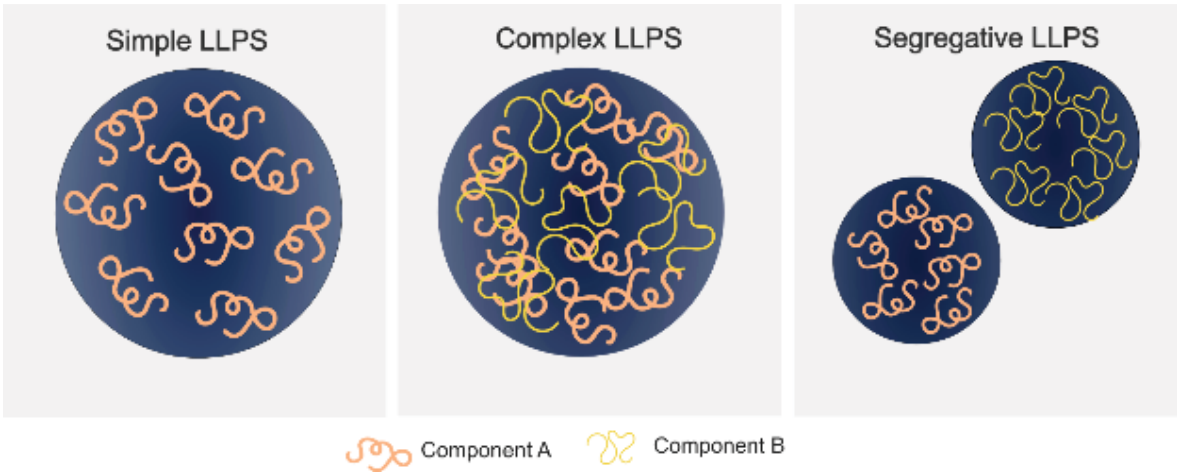

Fig 1.6: Types of LLPS. Schematic illustration of key types of LLPS

1.4.3 LLPS of Tau

Tau was studied to undergo LLPS, driven largely by electrostatic and hydrophobic interactions between its distinct charged regions (90). Upon LLPS, tau concentrates to form dynamic, reversible droplets and facilitates an increased multivalent intermolecular interactions and conformational changes within the protein.

Tau LLPS has been widely studied for its role in both cellular and pathological functions (131) (Fig 1.7). Recent findings show that, under LLPS conditions, tubulin dimers partition into tau condensates increasing their local concentration by several folds when compared to the surrounding (132). These enriched tubulin dimers have been shown polymerize and assembling into stable microtubule tubule networks, indicating that tau condensates could function as nucleation centres of microtubules. With time, these liquid droplets transform into less dynamic gel-like forms through the process of droplet aging and under pathological conditions this aging can result into the formation of amyloid aggregates for several proteins (133). Heparin, RNA, metal ions, pro-aggregation mutations and abnormal PTMs modulate LLPS of tau, promoting the liquid-to-gel transition of tau condensates (134). The charge distribution and net charge of different regions of tau are altered upon PTMs and induces conformational changes in tau. This further affects the electrostatic interactions and hydrophobic interactions within the droplets, thus leading to modulation of the LLPS behaviour. Interestingly, the functional role of tau LLPS was by inhibited by disease-

associated phosphorylation and acetylation of tau where these tau condensates could not recruit tubulin and hence failed to support microtubule nucleation (135,136). Similarly, the mutations that promote tau aggregation have also been shown to affect the LLPS behaviour of tau (91,92). Tau condensates also associate with other amyloidogenic proteins and stress

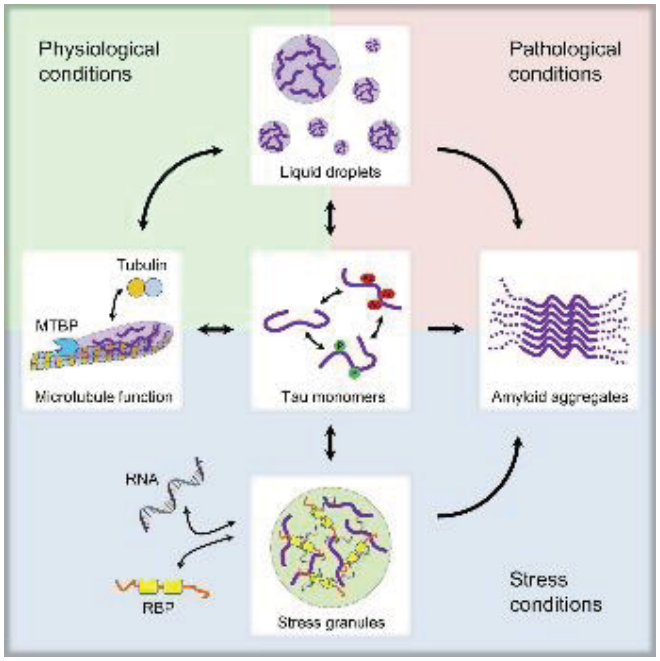

Fig 1.7: Tau LLPS in physiology and functions (107).

granule proteins such as TIA1, and these interactions often promote the maturation and aging of tau condensates (137,138).

Several recent studies suggest that tau LLPS leads to tau aggregation. Condensed phases increase the local concentration of tau and change the conformation of tau which in turn contributes to the aggregation. However, some studies also suggest that tau LLPS may be not necessarily on pathway to amyloid aggregation and rather they are two processes that occur under overlapping conditions (139). LLPS is a critical phenomenon in tau pathology that provides insight into the early stages of tau aggregation. However, despite growing interest, current studies have not yet fully elucidated the mechanisms underlying these processes and their connection to amyloid aggregation.

1.5 Amyloid-β (Aβ)

Amyloid beta (Aβ) is a 39-43 amino acid long peptide involved in the pathogenesis AD, together with tau (140). In humans, Aβ is produced through the sequential proteolytic cleavage of the amyloid precursor protein (APP) by β- and γ-secretases (141). Aβ was first identified as a constituent of the polymorphic deposits in patients with Down syndrome

(142). Later, Aβ peptides were found to aggregate extracellularly forming amyloid plaques, which are hallmark pathological features of AD brains together with NFTs by tau (143). These aggregates disrupt neuronal function by inducing synaptic toxicity, oxidative stress, calcium dysregulation and inflammatory responses, contributing to the neurodegenerative processes underlying cognitive impairments.

1.5.1 Origin of Aβ

APP protein is a member of transmembrane glycoprotein protein family and encoded by APP gene on chromosome 21 (144). They possess receptor-like structural features, but their cellular functions are not yet fully studied. APP can undergo cleavage through the non-amyloidogenic pathway, generating the neuroprotective sAPPα fragment and it is considered as a part of normal cellular functioning (145) (Fig 1.8). But the sequential cleavage of APP by β-and then γ-secretases leads to the formation of Aβ peptides. The family of APP also include two other isoforms, namely, amyloid precursor-like proteins 1 and 2 (APLP1/2) but they do not produce Aβ peptides upon cleavage. The cerebral cortex and hippocampus are regions that are enriched in Aβ and under normal functioning these peptides get degraded and removed by enzymatic degradation or other clearance mechanisms (146,147). Aβ40 and Aβ42 are the most abundant isoforms in humans and can be generated by neurons, astrocytes, neuroblastoma cells, hepatoma cells, fibroblasts or platelets. Aβ40 is the most abundant form of Aβ peptide but Aβ42 is the main component in the amyloid plaques. The presence of low amounts of the Aβ peptides in non-demented individuals indicates Aβ can be involved in normal physiology (148,149). However, net balance of this production and degradation of Aβ peptides will be very critical and the disturbance of these clearance mechanisms lead to their deposition as senile plaques (150).

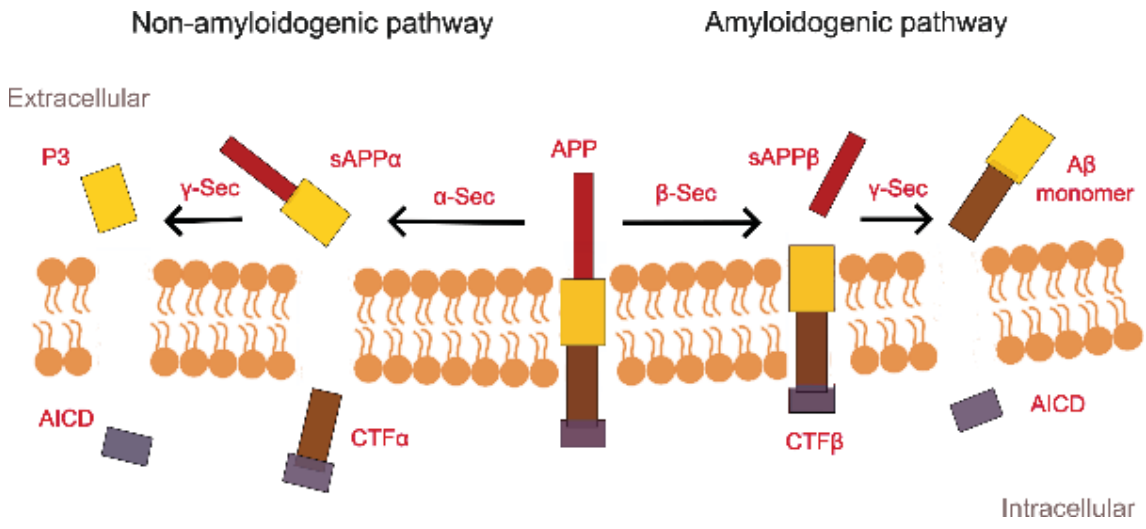

Fig 1.8: Origin of Aβ. During the amyloidogenic pathway, sequential cleavage of APP produces Aβ peptides. Adapted from (148).

The physiological roles of Aβ peptides are among the most intensively investigated topics in neurodegenerative research. Emerging evidence suggests that Aβ may serve important physiological functions, including modulation of synaptic activity, regulation of neuronal excitability and antimicrobial defence (151,152). However, when the production, clearance or structural integrity of Aβ monomers becomes dysregulated, they can transition from functional to pathological, aggregating into toxic forms that contribute to neurodegeneration.

1.5.2 Amyloid Cascade Hypothesis and Aβ Pathogenesis

Amyloid cascade hypothesis or Aβ hypothesis was first proposed by Hardy & Higgins in 1992 (153). They propose that deposition of Aβ is the main causative agent of AD pathology and that the neurofibrillary tangles, cell loss, vascular damage and dementia follow this deposition. Till date, there are several observations that support as well as contradict the Aβ hypothesis. The observations that mutations in the tau gene do not cause amyloid plaques and that amyloid buildup triggers tau aggregation are critical in supporting the Aβ hypothesis (154). There are also several concerns that are raised against Aβ hypothesis. The amount of amyloid plaques does not always match the severity of dementia and mouse models with amyloid buildup often lacks significant neuron loss (155). These observations indicates that amyloid accumulation alone may not fully account for the neurodegenerative features. Also, the amount of plaque deposition not correlating with the severity of dementia point out that rather than plaque themselves may not be toxic and there might be other critical intermediate species like monomers, oligomers or fibrils for Aβ plaques that are responsible for building up and spreading toxicity (156). Understanding these intermediate assemblies is critical to study neurotoxic pathway of Aβ.

Aβ peptides are produced under physiological conditions as soluble monomers, which represent the primary and most abundant species during the early stages of Aβ homeostasis. Structurally, Aβ monomers exhibit a predominance of α-helix and random coil conformations (157). Despite their inherent instability, Aβ monomers are not merely by-products of amyloidogenic processing but are increasingly recognized as possessing distinct physiological functions within the CNS (158). Under homeostatic conditions, Aβ monomers are implicated in cytoprotective and intracellular signalling pathways, including those related to synaptic modulation, metabolism and neurogenesis. However, the delicate equilibrium governing their production, solubility and clearance is critical for maintaining these physiological functions. Perturbations in Aβ homeostasis such as increased peptide concentration, post-translational modifications or isoform imbalance can shift Aβ

monomers toward pathological self-assembly (159). During the aggregation process, Aβ monomers dominate the lag phase, but due to their high aggregation propensity, obtaining a stable and homogeneous population of Aβ42 monomers has been challenging (160).

Aβ oligomers (AβOs) represent intermediate assemblies in the amyloidogenic cascade, formed by the self-association of Aβ monomers prior to fibrillization and are widely regarded as the most toxic and pathogenic form of Aβ (161). The identification of AβOs caused a major shift from the still popular amyloid cascade hypothesis towards AβO hypothesis, recognizing soluble oligomeric assemblies, rather than insoluble fibrils or plaques, as the principal neurotoxic species in AD (162). These soluble aggregates are structurally and biochemically heterogeneous, encompassing species ranging from dimers and trimers to higher-order assemblies with molecular weights from >50 kDa (141). Their soluble nature allows diffusion throughout the brain, resulting in a heterogeneous spatial distribution that distinguishes them from the insoluble fibrillar deposits. Membrane disruption, ion dysregulation, neuronal apoptosis, neural signal dysfunction are some of the toxic effects of AβOs, leading to severe cognitive deficits (163). In addition, their ability to disrupt Ca^{2+} homeostasis (164) and to induce endoplasmic reticulum (ER) stress (165) makes them central to the progression of AD. Structurally, oligomers can form via multiple pathways (166,167). On-pathway oligomers are transient intermediates leading directly to fibril formation, while off-pathway oligomers represent metastable assemblies that diverge from the fibrillogenic pathway. On-pathway oligomers accelerate fibril growth, whereas off-pathway oligomers, including globular species (>50 kDa) and associated curvilinear fibrils (~200 nm), persist longer within neurons and are linked to pronounced neurotoxicity (166,168,169). Studies indicate that most of the AβOs have the tendency to dissociate back to monomeric form while only a minority of them transition into fibrils (170) . This highlights the importance of studying the off-pathway oligomeric pathway of Aβ. The coexistence of these pathways contributes to the heterogeneity and persistence of toxic Aβ species within diseased tissue. AβOs occupy a critical position in the Aβ pathway between monomeric and fibrillar species. Their structural heterogeneity, high diffusibility and potent neurotoxicity render them central to the pathophysiology of AD. While traditionally been distinguished as an intermediate step en route to mature fibrils, Aβ protofibrils (PFs) can also be viewed within the broader spectrum of oligomeric assemblies (166,169). Recent studies suggest that Aβ can also undergo LLPS that affects its aggregation, but this research is still at its preliminary stage (171,172).

Aβ fibrils are the core components of the senile plaques in AD (173). They exhibit the canonical cross-β-sheet structure, with β-strands oriented perpendicular to the fibril axis and stabilized through extensive hydrogen bonding (174). Fibrils are insoluble, polymorphic,

and structurally heterogeneous, with their conformations influenced by peptide sequence (Aβ40 or Aβ42) and environmental conditions. Distinct fibril polymorphs display variable solubility, growth kinetics and neurotoxicity (175). *In vitro* and *in vivo* studies indicate that fibrillar Aβ assemblies disrupt synaptic architecture, impair neurogenesis and activate microglia, leading to chronic inflammation and neuronal loss (176). Structurally, fibril surfaces can catalyze secondary nucleation events, generating new oligomeric species that further propagate toxicity (177). While the traditional amyloid cascade hypothesis positioned fibril deposition as the principal driver of AD, the subsequent identification of soluble oligomers and protofibrils introduced complexity, enabling the shift of focus towards earlier, diffusible species as key neurotoxic entities. Nevertheless, Aβ fibrils remain central to AD pathology, both as a source of toxic oligomers and as a contributor to neurotoxicity.

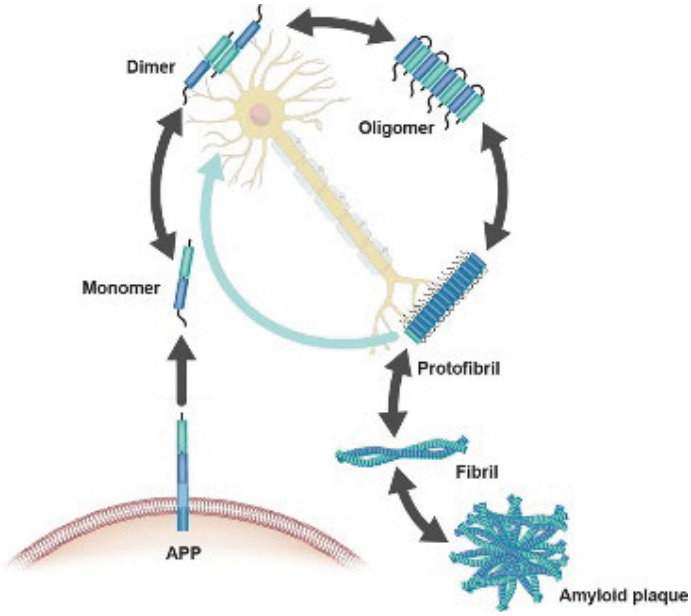

Fig 1.9: Aβ pathology. Key pathological species of Aβ (127).

1.6 DimAβ-a dimeric Aβ construct

The extraction of Aβ in its oligomeric state is very difficult due to its inherent metastability and heterogeneity (178). Most extraction protocols yield a mixture of many pathological species. DimAβ represents a recently developed dimeric Aβ variant that selectively forms homogenous population of off-pathway oligomers of Aβ (179) . In dimAβ, two Aβ40 units are linked in one polypeptide chain through a flexible glycine-serine-rich linker. DimAβ possess the same conformational properties as of free Aβ40 monomers (180). DimAβ brings together two Aβ units that mimics a concentrated environment for Aβ and triggers the formation of off-pathway oligomers. This allows the study of sole effects of AβOs with minimized

disturbance by Aβ monomers or fibrils. DimAβOs are of spherical and curvilinear shape and rich in β-sheet structure (169). Using cryo-EM and 3-D reconstruction it was determined the small dimAβOs consist of six dimAβ monomers which corresponds to twelve Aβ40 units. Such dodecameric AβOs species have been observed before in AD brains and have been associated with neuronal impairment (181).

There are several advantages in applying dimAβ for the study of AβOs. First, using dimAβ AβOs are formed above a critical oligomeric concentration (COC) of ~1.5 μM dimAβ at neutral pH (162,161). This is very low COC compared when compared to the COC of Aβ peptides and helps in preserving the protein during *in vitro* experiments. Second, the increased local Aβ concentration preferentially accelerates AβO formation. The specific formation of AβOs from dimAβ results in a well-separated kinetic phase for AβO and Aβ fibril formation. This helps us to extract oligomers free from disturbances from other Aβ species including monomers or fibrils.

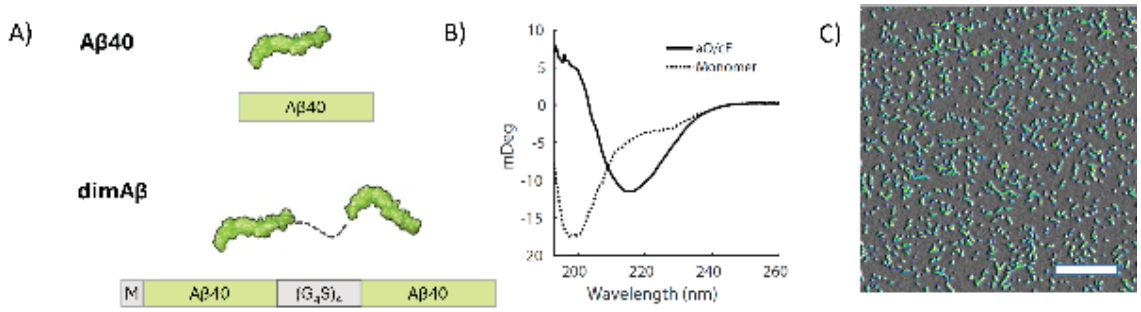

Fig 1.10: DimAβ. A) Schematic illustration of DimAβ construct B) CD spectra of dimAβ monomers and oligomers C) AFM images showing dimAβOs. Adapted from (156,162)

Importantly, dimAβOs recapitulate the biophysical and functional properties of native AβOs. DimAβOs cause missorting of tau into dendrites like native Aβ42Os (169). Tau which is normally localized into the axons become mislocalized into the somatodendritic compartments of neurons under pathological conditions. Tau missorting is a characteristic for several tauopathies (182) and dimAβOs could cause this like Aβ42Os but at lower concentrations. Also, like AβOs, dimAβOs were also observed to be concentrate inside the endo-lysosomal compartments which enhanced their oligomer formation (169). These observations point out that dimAβ is a relevant *in vitro* model that can be used to study the effects of AβOs specifically.

1.7 Interaction of tau and Aβ in AD pathogenesis

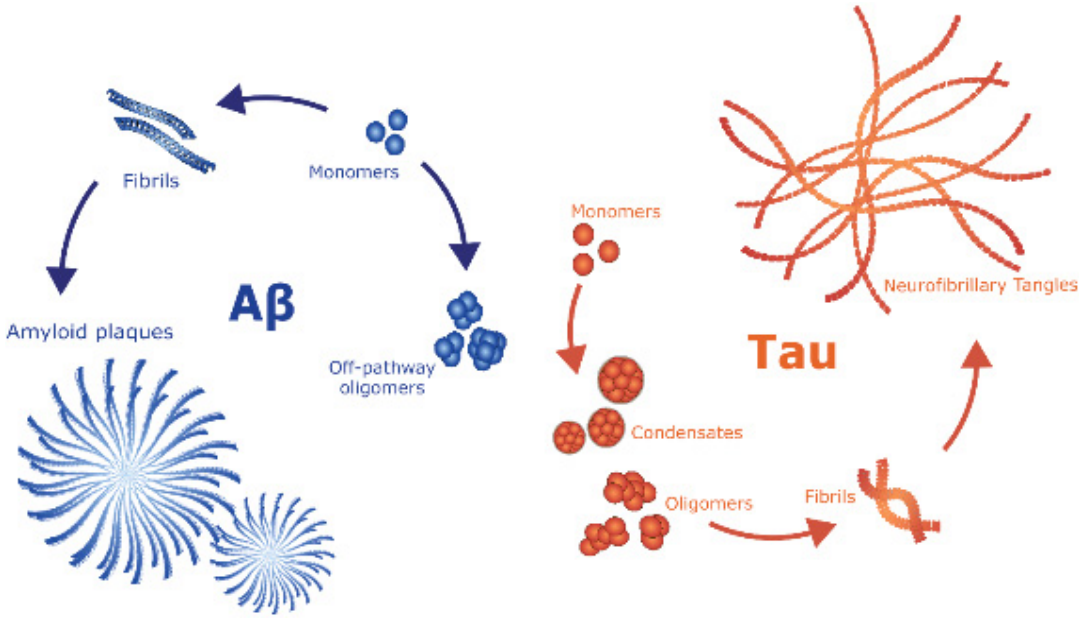

Fig 1.11: Disease associated conformers of tau and Aβ.

For long time, Aβ and tau have been extensively studied as distinct neurotoxic entities. As discussed, early studies identified Aβ as a trigger for the sequential events in AD pathology and tau as an effector of Aβ-mediated toxicity (140). However, emerging evidence highlights their critical interplay in AD pathogenesis. The development of many AD drugs that focused on the reduction of amyloid deposition and the clearance of AβOs and have not yielded satisfactory effect (183). Similarly, extensive studies focusing solely on the neurotoxicity of tau have also not shown significant efficacy in the treatment of AD.

Experimental studies demonstrate that Aβ-induced synaptic dysfunction, neuron death and cognitive deficits are largely tau-dependent, as demonstrated by tau knockout or reduction in transgenic mouse models, which protected against Aβ-mediated neurotoxicity (184–186). Conversely, Aβ promotes tau hyperphosphorylation via activation of kinases and interfere with the oligomer formation by tau (187,188).

In addition to their bi-directional regulatory effect, Aβ and tau synergistically impair mitochondrial function and oxidative phosphorylation system, contributing to neurodegeneration (189–191). Aβ aggregates accumulate within mitochondria, disrupting electron transport chain activity, increasing ROS and causing Ca^{2+} overload that triggers mitochondrial dysfunctions. Hyperphosphorylated tau further exacerbates this by impairing axonal and dendritic transport of mitochondria, disrupting fission-fusion dynamics, and interacting with key mitochondrial proteins. Interestingly, studies have also shown that Aβ has affinity to mitochondria that is comparable to tau and it displaces the mitochondria-

bound tau, promoting its aggregation and toxicity (192). Further, the combined presence of toxic Aβ and tau species amplifies oxidative stress, promotes mitochondrial fragmentation, and compromises synaptic bioenergetics, thereby accelerating neuronal vulnerability and degeneration (193,194). Also, both Aβ and tau and their misfolded forms exhibit prion-like propagation mechanisms, whereby misfolded aggregates acts to trigger conformational changes in native proteins, facilitating their trans neuronal spread (195). AβOs have been shown to interact with tau where it enhances the binding and internalization of tau oligomers at human synapses (196). Increased tau uptake in AD synaptosomes and in control synapses were observed when exposed to recombinant AβOs. Also, AβOs interact with phosphorylated tau in neurons affected by AD and these interactions progressively increases as the disease advances (197). This suggests that Aβ-tau interactions contribute to synaptic dysfunction and neuronal damage, ultimately leading to cognitive decline.

Together, these findings suggest that Aβ and tau engage in pathological cross-seeding and therefore, therapeutic strategies targeting both Aβ and tau, as well as their interaction pathways, are essential for effective intervention in AD. However, the understanding of the molecular association of Aβ and tau is still unclear and speculative, warranting further investigation.

Chapter 2: Heterotypic phase separation and protein aggregation

Manuscript Information

Title: Heterotypic phase separation in aggregation: driver or deterrent?

Authors: Tina Jacob and Wolfgang Hoyer

Journal: Biophysical chemistry

Status: Under Revision (November 2025)

Contributions: Conceptualization, literature analysis, manuscript preparation, figures and tables.

This chapter presents a review submitted to *Biophysical chemistry*, focusing on heterotypic LLPS. This review reveals the role of various heterotypic partners of tau and αS in modulating their LLPS and aggregation. It provides a relevant background on for understanding the interactions between AβOs and tau under LLPS conditions discussed in subsequent chapters.

2.1 Abstract

Liquid–liquid phase separation (LLPS) of proteins implicated in neurodegenerative diseases has gained growing attention in recent years, due to its potential role in driving the transition from functional protein monomers to pathogenic aggregates. However, the mechanisms by which phase separation contributes to the loss of protein function and promotes aggregation remain poorly understood. Recent studies show that multiple proteins or other biomolecules can colocalize within the biomolecular condensates, creating a highly interactive microenvironment that can modulate aggregation. In this review we look into the heterotypic phase separation of tau and α-synuclein, the two key proteins responsible for critical neurodegenerative disorders. By compiling recent findings, this review highlights the modulatory role of heterotypic condensates in disease progression and aims to provide an alternative perspective on regulation of protein aggregation in neurodegeneration.

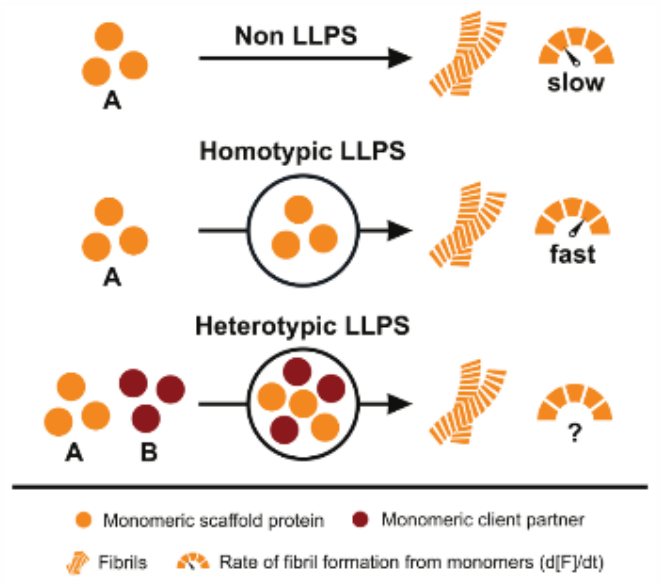

Fig 2.1: Investigation into modulatory role of heterotypic phase separation.

2.2 Introduction

2.2.1 Emergence and biological roles of LLPS

Liquid-liquid phase separation (LLPS) refers to the process by which distinct phases emerge from a homogeneous solution. In eukaryotic cells, phase separation serves as a crucial mechanism for the spatial organization of biomolecules into dynamic compartments to facilitate specific cellular functions (198–200). These compartments are distinct from conventional organelles, as they lack a membrane that allows selective regulation of

molecular transmission through it. Typically, they exhibit liquid-like characteristics and adopt a spherical shape, minimizing the interfacial surface energy (201). They show rapid molecular exchange with the surrounding cytoplasm and undergo physical processes such as Ostwald ripening and fusion, further reducing system energy (202). Strome and Wood et. al. were among the pioneers who recognised P-granule as a membraneless organelle with liquid-like properties (203). Since then, several other cellular systems, including nucleolus (204), Cajal bodies (205), stress granules (206) were found to be formed through LLPS.

Although still in the early stages of investigation, LLPS has emerged as a fundamental mechanism regulating a wide range of biological processes. LLPS plays critical roles in transcription and translation, signal transduction, stress responses, chromatin organization and DNA damage response (207,208). Recent studies have also underscored the role of LLPS in cancer biology, suggesting its potential as a therapeutic target for modulating drug efficacy and overcome resistance in tumor cells (209–211). LLPS is highly responsive to environmental conditions and is therefore strongly influenced by temperature, pH, post-translational modifications and interactions with small molecules (207,209,212). To maintain focus and avoid redundancy, this review will specifically explore phase separation in the context of proteins implicated in neurodegenerative diseases

2.2.2 The convergence of phase separation and protein aggregation

Protein aggregation poses a significant challenge to biological systems, often resulting in cellular dysfunction and neurodegenerative disorders (213–215). Upon aggregation, proteins misfold and form non-native structures that contribute to cellular toxicity. Recently, phase separation has gained attention as a potential intermediate in the transition from functional protein states to pathological aggregates (216,217). Several proteins associated with neurodegenerative diseases have been shown to undergo phase separation, particularly above a critical threshold concentration or in response to external stimuli (218).

The tendency of a protein to undergo phase separation depends significantly on its structure. Proteins with greater proportions of intrinsically disordered regions (IDRs) and low-complexity domains (LCDs) are more likely to phase separate. IDRs are multifunctional, highly flexible, unstructured regions of a protein that can critically contribute to the multivalent interactions during phase separation (219,220). LCDs are compositionally biased regions of a protein, often being a subset of IDRs. However, IDRs and LCDs are not strictly required for phase separation; phase separation abilities of proteins are also strongly influenced by post-translational modifications, environmental conditions, and heterotypic interactions (219). The saturation concentration (C_{sat}) represents the threshold concentration above which a molecule undergoes phase separation, serving as a key determinant of phase separation propensity. Several factors including temperature, pH,

ionic strength, intrinsic molecular properties and interactions with other molecules can influence C_{sat}. While self-association and phase separation of proteins have been extensively studied and implicated in various neurodegenerative diseases (133,198,221,222), this review will now focus on heterotypic LLPS, exploring how interactions between different molecular species drive or regulate condensate formation and aggregation.

2.2.3 Heterotypic LLPS

Membraneless organelles can contain dozens to hundreds of components, interacting through a wide spectrum of affinities and stoichiometries. Their formation is influenced by the relative strengths of homotypic and heterotypic interactions (200,223). When diverse biomolecules are recruited into a single condensed liquid phase, they create microenvironments that facilitate biochemical reactions and enhance cellular compartmentalization (224). This recruitment process establishes a two-, three- or multi-component system, resulting in a heterotypic organization, commonly referred to as heterotypic LLPS or multicomponent LLPS. While homotypic LLPS involves the self-association of identical molecules, heterotypic condensates arise from multivalent interactions between different types of molecules including electrostatic, hydrophobic, π–π or cation–π interactions between distinct molecular species (225).

We consider three possible cases for heterotypic systems; other cases have been discussed elsewhere (226,227). (i) Cooperative heterotypic phase separation; both components have strong self-interactions and phase separate. They also exhibit strong cross-interactions and efficiently form heterotypic condensates. (ii) Scaffold-client heterotypic phase separation; here the scaffold component can phase separate on its own while the client component, which does not have phase separating abilities but has strong affinity for the scaffold, gets recruited into scaffold condensates. This scaffold-client system will be elaborated in a later section. (iii) Cross-interaction driven heterotypic phase separation. In this system, neither of the components can phase separate on its own and phase separation occurs only through strong mutual cross interactions.

Recent studies have highlighted the ability of proteins implicated in neurodegenerative diseases to form heterotypic condensates with distinct biophysical properties (200,228). This phenomenon has gained significant attention due to its potential role in synergistic toxicity in cells, *in vitro* and in animal models. The recruitment of one protein into the condensates of another might also provide the basis for synergistic aggregation of proteins. For instance, the amyloidogenic proteins, αS and tau which are known to co-aggregate in various dementias, have also been shown to form heterotypic droplets that may contribute to the pathophysiology of Alzheimer's disease (AD) and Parkinson's disease (PD) (227,229).

Furthermore, studies demonstrating that the synergistic action of multiple proteins accelerates neurotoxicity (230–235) underscore the importance of studying protein phase behaviour in a heterotypic context.

2.2.4 Scaffold-client heterotypic phase separation

In scaffold-client heterotypic condensation, molecules are classified into scaffolds and clients. The scaffold component plays a crucial role by driving the formation of condensates, which then recruit client partners. Scaffolds have an intrinsic trigger to form condensates, driven by multivalent interactions or the presence of LCDs. The client partners do not favor condensation independently (223), but due to their affinity for the scaffold, they are recruited into the compartments formed by scaffolds and can significantly influence the stability and structural properties of condensates (223,236–239). Low-valency clients compete for scaffold-scaffold binding sites, reducing scaffold connectivity and condensate stability. Alternatively, high valency clients form additional client–scaffold interactions and increase condensate stability (238). However, the recruitment of client molecules by scaffold proteins may not be essential for condensate formation itself. One of the key determinants of client partitioning is the electrostatic interaction between charged scaffold and client components. Negatively charged molecules, such as RNA, exhibit a strong propensity for partitioning into condensates due to favourable electrostatic interactions with cationic scaffold proteins and this partitioning can be therefore regulated by the presence of ions (240). Additionally, the concentration of the components, phase separating conditions, specific amino acid composition and post-translational modifications of client proteins can modulate the partitioning into condensates (223,241). Importantly, the distinction between scaffold and client may be blurred for several systems and could vary with cellular conditions (237). Nevertheless, the scaffold-client distinction is useful for understanding condensate composition.

In the following sections, we aim to integrate two key areas of research: molecular interaction studies and phase separation studies. We discuss the heterotypic phase separation partners of tau and αS, analyse the driving forces underlying their interactions, their prior associations with the corresponding protein and their effects on the heterotypic condensates formed. We further classify the nature of each heterotypic system according to their effects on tau and αS aggregation.

2.3 Heterotypic phase separation of tau and the impact on its aggregation

2.3.1 Tau

Tau is a prevalent protein in the central nervous system (CNS) primarily responsible for microtubule stability and other vital cellular functions like axonal transport, synaptic plasticity, and cell signalling (45,242). Tau is an intrinsically disordered protein (IDP) that exists in six isoforms in the human brain, generated by alternative splicing of the MAPT gene (12). Structurally, tau can be divided into four distinct domains: an N-terminal projection domain, a proline-rich domain, a repeat region, and a C-terminal domain (243). The repeat domain, also known as the microtubule binding domain, is critical for tubulin binding and microtubule stabilization. Under normal physiological conditions, tau is predominantly bound to microtubules, and the concentration of unbound cytosolic tau remains in nanomolar range. This low abundance of free tau makes it particularly challenging to investigate the early molecular events that lead to tau pathology (244).

The abnormal aggregation of tau into large, insoluble protein assemblies is a hallmark of AD and other neurodegenerative disorders collectively known as tauopathies (245). The pathological cascade of tau involves several intermediate species; each associated with varied neurotoxicity. Kinases and phosphatases play vital roles in regulating tau under physiological conditions. However, dysregulated kinase activity, along with inhibited phosphatase function, can lead to tau hyperphosphorylation and misfolding. In response to these pathological triggers, monomeric tau aggregates into small, soluble oligomeric species. These oligomers have been implicated in a variety of neurotoxic effects and are considered key drivers of tau mediated toxicity (246). With time, these oligomers are replaced by higher molecular weight (HMW) species and fibrillar forms, which appear to be less toxic than the early-stage oligomers (247–249). This is supported by studies showing that tau oligomers, but not fibrils, cause neurotoxicity when injected into the mouse brain, despite both species being capable of propagating tau pathology (80,250).

The process of LLPS drives the local crowding of tau, raising its concentration well above the threshold required for aggregation. As a result, LLPS has been proposed to serve as a molecular bridge between physiologically soluble, monomeric tau and its pathological, aggregated forms. The finding that tau undergoes phase separation, first demonstrated *in vitro* (90) and confirmed *in vivo* (92), was a striking addition for understanding the early steps of tau pathology. Tau condensates have been shown to gradually transition into amyloid-like aggregates, indicating LLPS as a potential intermediate step in tau aggregation (92,251). Although the precise contribution of LLPS in the pathology of tau still remains under active research, LLPS provides a mechanistic basis for tau accumulation.

Interestingly, tau condensates are not exclusively linked to pathology. In a physiological context, they can recruit tubulin and function as microtubule nucleation sites (132), highlighting potential functional roles of tau phase separation. However, disease-associated phosphorylation of tau has been shown to impair its microtubule-nucleating ability, even though tubulin still partitions into tau condensates (135). These findings suggest that disease associated modifications, interactions or mutations may disrupt the balance between the functional and pathological roles of tau condensates.

As discussed generally earlier, tau LLPS is mediated by a combination of electrostatic forces, hydrophobic interactions, and thermal modulations (90,92,228,252,253). The presence of IDRs and sequence-based charge anisotropy, confers tau with a strong propensity for phase separation (254). High tendency for post-translational modifications and the presence of flexible IDRs, enable tau to adopt multiple conformations allowing interactions with a wide range of binding partners including proteins, nucleic acids and membranes (255). This versatility of tau in binding diverse partners, together with its ability to undergo LLPS, facilitates its incorporation into different heterotypic systems (252,256,257). In many of these systems, tau acts as the scaffold component, recruiting client molecules into its condensates and conferring properties distinct from homotypic tau condensates.

Here, we bring together the key systems in which tau undergoes heterotypic phase separation and summarise their effects on tau phase separation and aggregation.

2.3.2 Tau and RNA

The interaction between tau and RNA is among the most extensively studied heterotypic LLPS systems, explored under diverse thermodynamic conditions (228,252,253). RNA acts as a multivalent binding partner promoting tau assembly and phase separation. Interestingly, the phase separation boundary in the phase diagram of tau:RNA LLPS lies close to physiological conditions, highlighting its potential *in vivo* relevance (115). The net positive charge of tau at physiological pH and ionic strength facilitates its interaction with negatively charged polyanions such as RNA through long-range, weak, multivalent electrostatic interactions. Consequently, cellular ionic strength is a critical regulator of tau:RNA LLPS. The repeat domain of tau, enriched in positively-charged lysine and arginine residues, exhibits the strongest propensity for RNA association (253).

Zhang *et al*. were the first to demonstrate that tau undergoes RNA-driven phase separation and that tau binds to RNA in cells (252). This entropically driven heterotypic condensation maintains a dynamic and disordered structure of tau within condensates. Tau did not undergo any conformational changes upon coacervation with RNA and the resultant condensates were resistant to any change in charge distribution on RNA or disease-

associated mutations (256,258). Najafi *et al*. showed that tau forms reversible, RNA-mediated condensates with higher viscosity and stability compared to homotypic condensates of tau (228). Compared to tau LLPS, tau:RNA LLPS is less influenced by hydrophobic interactions and has reduced tendency for percolation into irreversible aggregates (92). However, other studies revealed that tau:RNA condensates, while being stable and non-percolating, show enhanced higher-order tau accumulation and elevated intracellular seeding potential compared to tau LLPS (138,259). These observations suggest a balance between two competing forces: (i) increased local tau concentration, which promotes aggregation, and (ii) high-viscosity of the environment which restricts diffusion and slows aggregation kinetics (256). Nonetheless, the precise behaviour of these systems in the complex cellular context remains to be fully elucidated.

RNase treatment of these heterotypic condensates leads to RNA degradation and dissolution of tau:RNA condensates, underscoring the essential role of RNA in stabilizing these condensates (260). Tau:RNA condensates are also involved in microtubule organization. Although RNA reduces the amount of tau directly binding to microtubules, it promotes tau-mediated microtubule bundling by sequestering tubulin into tau:RNA condensates. These condensates scaffold and organize microtubule polymerization through wetting interactions (259).

Phosphorylation is a major post-translational modification for tau, regulated by over 20 different kinases (261). With more than 80 potential phosphorylation sites, tau becomes more negatively charged and hydrophilic upon phosphorylation (259,262). Phosphorylation attenuates the overall positive charge of tau and weakens its electrostatic interactions with RNA. But not all phosphorylation sites have the same effect; phosphorylation at serine 262 (S262) enhance coacervation with RNA, whereas phosphorylation at threonine 205 (T205) suppress it (259). Phosphorylated tau (ptau) tends to undergo LLPS faster than unmodified tau. However in the presence of RNA, both ptau and tau show a similar delay in the formation of condensates (260). Also, ptau:RNA condensates disassembled at lower salt concentrations and were more sensitive to ionic strength than the unmodified tau:RNA LLPS. While enhancing the stability of ptau condensates, RNA promoted their aging into gel-like states (260).

Together, studies to date indicate that tau:RNA LLPS is less associated with amyloid aggregation than tau LLPS, and both of the systems appear to follow distinct mechanistic pathways (258). Nevertheless, under certain cellular conditions, these mechanisms may intersect or influence one another. The primary role of tau-RNA coacervation in cells may be to spatially organize tau and its cofactors, potentially facilitating aggregation under permissive conditions without necessarily being a direct driver.

2.3.3 Tau and amyloidogenic proteins

One of the most intriguing coacervate partners of tau is αS and several studies have reported their co-localization (108,263–265). αS is an extensively studied protein due to its critical role in the development and progression of PD. The presence of tau aggregates in PD and αS aggregates in AD and other tauopathies indicate overlapping pathological mechanisms (235,266,267). Siegert *et al*. were among the pioneers who study that monomeric αS is recruited as a client molecule into tau droplets, as αS showed limited homotypic LLPS under physiological conditions (265). The recruitment of αS into tau droplets was driven primarily by electrostatic interactions, specifically between the negatively charged C-terminal domain of αS and the positively charged proline-rich P2 region of tau. Interestingly, Gracia *et al*. showed that αS can also act as a scaffold, forming condensates with positively charged polypeptides and subsequently recruiting tau, including non-LLPS tau mutants (108). The heterotypic tau:αS LLPS formed dynamic, liquid-like droplets with high electrostatic surface potential due to charge imbalance. These droplets showed a high rate of coalescence into larger condensates to compensate for charge imbalance and exhibited increased resistance to high salt concentrations. Diffusion studies revealed no major effect of αS on tau dynamics upon co-localization (265), although some studies reported that the mobility of both proteins was reduced in comparison to their respective homotypic condensates (108,268). The maturation of these heterotypic condensates involves a gradual reorganization of their complex protein network, driven by both homotypic and heterotypic interactions. Over time, some tau:αS condensates may undergo valence exhaustion, become gel-like and fusion-incompetent whereas the larger, still liquid-like droplets serve as nucleation sites for amyloid aggregation (108). ATP acts like a protective agent on these heterotypic condensates by increasing protein dynamics, reducing both tau and αS partitioning into the condensates and solubilizing the proteins. The presence of polyamines also suppresses tau:aS condensation, but, in contrast to ATP, polyamines promote the formation of heterotypic amyloid-like aggregates. Interestingly, α-synuclein fibrils, like monomers, can also be incorporated into tau condensates (265). However, unlike monomers, fibrils distorted droplet morphology and destabilized the condensates. Collectively, these findings support a biophysical model in which αS accumulates inside tau condensates and forms fibrils that disrupt and deform the tau matrix, potentially leading to their release into the cellular environment.

Human prion protein (PrP) is widely expressed in various organs and tissues, particularly in the central nervous system. Misfolding of PrP leads to a group of fatal and transmissible prion diseases (269). Elevated PrP levels in AD suggest a potential role for PrP in disease progression (270). PrP also interacts with Aβ by acting as a receptor for Aβ oligomers, and

together they synergize with tau to promote synaptic disruption (271,272). PrP lowers the C_{sat} of tau and gets recruited into the tau condensates via electrostatic interactions (273). PrP enhances the number of condensates of tau and promotes smaller, more spherical complex coacervates. Stronger tau:PrP interactions within condensates are reflected by slower tau diffusion. These tau:PrP condensates are highly sensitive to RNA concentrations. Increasing RNA levels leads to several multiphasic rearrangements in tau:PrP condensates and excess RNA ultimately cause their dissolution. PrP also accelerates the maturation into gel-like state and transition into solid-like co-aggregates and fibrils. The protective role of RNA in dissolving the heterotypic condensates into individual protein monomers warrants further investigation and could be employed to target tau:PrP interactions.

2.3.4 Tau and RNA binding proteins (RBPs)

RNA-binding proteins (RBPs) bind to RNA through one or multiple RNA-binding domains and play crucial roles in regulating RNA metabolism (274). Many RBPs associate with RNA via LLPS, leading to the formation of ribonucleoprotein (RNP) granules such as stress granules, P-bodies, germ granules. These RNP granules are essential for various cellular functions, including RNA processing, storage of messenger RNAs (mRNAs), localization of RNAs and RNA degradation (275).

Stress granules (SGs) assemble in the cytoplasm during cellular stress to mediate a pro-survival adaptive response. The formation of SGs helps minimize cellular energy demands, and their disassembly upon stress removal is essential to restore normal cellular metabolism (276,277). Many protein components of SGs, including TDP-43, TIA-1, PABP-1, and TTP, have been extensively studied and these proteins are often mutated or mislocalized in neurodegenerative diseases (278,279). Several stress granule proteins exhibit unique interactions with tau and are thus closely associated with AD, with TIA-1 being a prominent example (253,280). Colocalization of TIA-1 with tau aggregates has been observed in AD, and knockdown of TIA-1 results in suppression of TIA-1 mediated tau aggregation (281–284). Tau supports the normal cellular functions of TIA 1, including its interactions with other RBPs and stress granule formation. In contrast, overexpression of TIA1 promotes tau misfolding and neurodegeneration, while reducing TIA-1 levels mitigates tau toxicity (282).

The heterotypic coacervation of tau with RBPs is strongly influenced by several factors, including the domain structure of the RBPs, the relative concentration of RBPs to tau, electrostatic interactions, thermodynamic factors and the balance between homotypic and heterotypic interaction enthalpy. Among all RBPs studied, TIA-1 exhibits a uniquely potent influence on tau phase separation and aggregation. TIA-1 was the most effective in driving tau phase separation, even in the absence of artificial crowding (138). TIA-1 driven

condensates were smaller but higher in number. Upon heterotypic coacervation with TIA 1, tau showed a reduced mobility and accelerated maturation into a gel-like state (285). Tau also showed multiphasic organisation within the condensates. At higher TIA-1 concentration, tau formed concentrated microdomains inside TIA-1 condensates, suggesting that homotypic tau-tau interactions override heterotypic tau:TIA-1 interactions, leading to internal immiscibility. However, these condensates of tau were not toxic even at high concentrations of both proteins.

In the presence of RNA, TIA-1 selectively promoted the formation of oligomeric tau species (138). Oligomeric tau has been studied to be more toxic than the fibrillar tau causing numerous neurotoxic effects (80). TIA-1 together with RNA triggered the formation of oligomers of tau at a faster rate than compared to RNA alone but did not induce the formation of HMW or fibrillar tau species. Interestingly, these oligomers of tau formed in the presence of TIA-1 showed higher toxic effects than the fibrillar forms formed in the presence of RNA alone. However, a parallel study showed that TIA-1 couldn't trigger tau aggregation in the presence of artificial molecular crowders, indicating the influence of environmental factors. Overall, TIA-1 promotes tau phase separation and the formation of toxic oligomeric aggregates, but this process could be sensitive to cellular context, highlighting the need for further investigation.

Among other tested RBPs, G3BP1 was able to recruit condensates of tau in the presence of RNA, but to a lesser extent than TIA-1 (138). Several other RBPs, including DDX6, HNRNP1, RP11, EIF4A1, and EIF4E, formed heterotypic condensates with tau only in the presence of both RNA and PEG, suggesting that they act as weaker scaffolds. DDX6 showed a concentration-dependent shift in condensate morphology, indicating a dynamic balance between homotypic and heterotypic interactions. HNRNP1 formed distinct microdomains within tau condensates. EIF4A1 exhibited pH-dependent partitioning, driven by changes in net charge and electrostatic interactions.

However, none of these RBPs other than TIA-1 triggered the formation of neurotoxic oligomers or any other accumulations of tau. Hence, the role of these RBPs which co-localize with tau condensates still needs to be explored in the context of tau aggregation.

2.3.5 Tau and molecular chaperones / regulatory proteins

Molecular chaperones are a diverse group of proteins that regulate essential cellular functions. They assist in protein folding under both physiological and stress conditions, and are therefore critically implicated in the context of neurodegenerative diseases (286,287). The protective roles of several classical chaperones against neurotoxic protein deposits have been well studied (288). Notably, Hsp70 has been shown to disaggregate tau fibrils,

converting them back into monomers (289). Recently, chaperones have been recognized for their ability to regulate phase separation, particularly in preventing the transition of protein condensates into solid-like aggregates (290,291). Several heat shock proteins (Hsp) modulate condensation behaviour of disease-related proteins and protect them against pathological aggregation (290,292). In this section, we explore how various chaperone and regulatory proteins interact with tau and modulate its phase separation and aggregation behaviour.

Small heat shock proteins (sHsp) are stress-induced chaperones characterized by their low molecular weight and ability to prevent protein aggregation (293). Hsp22 is one of them and was recruited into the condensates of tau. Hsp22 significantly enhanced the number of smaller condensates (294). Importantly, Hsp22 significantly slowed the aggregation of tau and prevented its maturation into amyloid-like aggregates.

Another key chaperone, heat shock protein 40 (Hsp40), plays a central role in regulating tau aggregation and has been linked to pathological nucleation events in AD and other neurodegenerative diseases (295). The yeast homolog of Hsp40, Ydj1, was found to be enriched within tau condensates (296). Ydj1 promoted tau phase separation at lower critical concentrations, and its interaction with tau is mediated by both electrostatic and hydrophobic forces and results in dense co-condensates. Ydj1 inhibited tau aggregation even at sub-stoichiometric levels. Instead of toxic amyloid fibrils, Ydj1:tau co-condensates formed non-amyloidogenic heterocomplexes. These findings highlight a condensate-mediated chaperone mechanism, in which proteins like Ydj1 enhance tau LLPS while preventing its pathological maturation, offering a promising therapeutic approach.

S100B is a Ca^{2+} binding protein known for its chaperone activity, particularly in binding to AD proteins and preventing their misfolding (297,298). The chaperone activity of S100B is regulated by Ca^{2+} and it binds to proteins in a Ca^{2+}-dependent manner. S100B has been shown to interact with tau *in vivo* and inhibit the seeding ability of tau oligomers (298). Ca^{2+}-bound S100B (Ca^{2+}-S100B) was recruited into tau LLPS and slowed down tau phase separation (299). In the presence of Ca^{2+}-S100B, a higher level of molecular crowding was required to induce tau LLPS. This inhibitory effect increased with rising concentrations of Ca^{2+}-S100B. In contrast, Ca^{2+}-free S100B had minimal impact on tau LLPS and aligned with the previous study that S100B- tau interaction is regulated by Ca^{2+} levels (298). Importantly, excess calcium alone did not influence tau LLPS, ruling out a direct role of Ca^{2+} itself. Ca^{2+}-S100B did not alter the internal dynamics of tau after incorporation into condensates. Interestingly, although high-molecular-weight (HMW) tau oligomers formed early, their levels decreased at later time points in the presence of Ca^{2+}-S100B. These findings suggest that Ca^{2+}-S100B acts as a regulator within tau condensates, dampening both condensation and subsequent aggregation processes.

14-3-3 proteins are a family of multifunctional regulatory proteins widely expressed in the central nervous system. They typically interact with target proteins at their phosphorylated sites, and these interactions are crucial in a variety of cellular processes (300). 14-3-3 proteins have been found to associate directly with tau (301–303) and are present in neurofibrillary tangles (NFTs) in the brains of AD patients (304). 14-3-3ζ, one of the seven isoforms, plays a particularly important role in tau regulation. Several studies have shown that 14-3-3ζ binds tau and enhances its phosphorylation and aggregation *in vitro* (305–307). 14-3-3ζ is recruited into condensates formed by both phosphorylated and unphosphorylated tau, interacting with the proline-rich domain (PRD) and the microtubule-binding domain (MTBD) of tau. These co-condensates are stabilized by a combination of hydrophobic and electrostatic interactions (257,308). 14-3-3ζ regulated tau LLPS in a concentration-dependent manner, where the droplet number increased initially and then dropped with increasing 14-3-3ζ concentration. In phosphorylated tau condensates, 14-3-3ζ reduced molecular mobility, while it had no significant effect on unphosphorylated tau dynamics (257,308). However, despite being present in the droplets, 14-3-3ζ did not promote the maturation or aging of these co-condensates. The protective role of 14-3-3ζ in preventing tau aggregation is context-dependent, influenced by the phosphorylation state of tau and the cellular environment, as has been previously observed in 14-3-3ζ-mediated regulation of tau aggregation (308,309). Hence, the exact role 14-3-3ζ in LLPS-mediated aggregation of tau is not fully understood and demands further studies.

Protein disulfide isomerase (PDI) is a multifunctional chaperone primarily located in the endoplasmic reticulum (ER), where it plays a crucial role in protein folding, particularly during ER stress (310,311). PDI binds preferentially to misfolded proteins through hydrophobic interactions and has been implicated in various neurodegenerative diseases, especially AD (312–314). In AD brains, PDI colocalizes with tau in neurofibrillary tangles (NFTs) and is upregulated in AD mouse models (315,316). PDI directly interacts with tau, inhibiting its phosphorylation and aggregation (317). PDI undergoes heterotypic condensation with tau and suppresses phase separation of tau (317). PDI diminishes the number of condensates and in the resulting co-condensates, PDI enhanced the liquid nature of tau. PDI slows down the maturation of tau condensates into hydrogels or mature fibril filaments. However, S-nitrosylation of PDI, an aberrant modification observed in AD and PD, impairs its protective role. S-nitrosylated PDI fails to be recruited into tau condensates and does not inhibit phase separation. Instead, it is associated with increased formation of tau droplets, hydrogels, and fibrils. This highlights how post-translational modifications of PDI can convert a protective factor into a contributor to tau pathology.

EFhd2 is a highly conserved calcium-binding protein predominantly expressed in the central nervous system and implicated in various pathological conditions, including cancer and neurological disorders (318). In AD, EFhd2 colocalizes with pathological aggregated forms of tau and is increasingly detected as neurodegeneration progresses (319,320). Also, *in vitro* studies demonstrate that EFhd2 promotes tau amyloid formation, suggesting a critical role in AD progression (321). EFhd2 alone exhibits phase separation in the presence of molecular crowding and in response to calcium ions (Ca^{2+}), forming dynamic liquid condensates. However, in the absence of Ca^{2+}, EFhd2 formed solid-like amorphous aggregates (322). EFhd2 also modulates LLPS of tau at sub-molar concentrations and in a Ca^{2+}-dependent manner. In the presence of Ca^{2+}, EFhd2 forms co-condensates with tau, whereas without Ca^{2+}, EFhd2 disrupts tau phase separation and together they accumulate into solid-like structures (322). While the solid-like accumulations of EFhd2 with tau could potentially influence tau's transition toward pathological states, the study does not directly demonstrate this, and the role of EFhd2 in neurodegeneration remains unclear (323).

Peptidyl prolyl isomerases (PPIases) or cyclophilins are a family of molecular chaperones that facilitate protein folding by catalysing the cis–trans isomerization of proline residues (324). PPIases are essential for proper protein conformation and function, and have been implicated in a range of pathological conditions, including cancer, neurodegenerative diseases, viral infections, and psychiatric disorders (325–327). Peptidyl prolyl isomerase A (PPIA) is vital for numerous biological processes, including those linked to neurodegenerative diseases (328,329). PPIA has been shown to reduce tau aggregation, and high proline content of tau enhances its interaction with PPIA. PPIA is recruited into tau condensates and becomes enriched within them (330). PPIA does not alter the liquid-like properties or dynamics of tau in co-condensates. However, when added to pre-formed tau droplets, PPIA induces their dissolution, releasing monomeric tau into solution. Although the effects of PPIA on the maturation of tau condensates remain to be fully characterized, these studies suggest a potential chaperone-like role in regulating tau LLPS and preventing pathological aggregation. Given its chaperone-like role in regulating tau aggregation (331), PPIA enzymes represent promising candidates for developing therapies for AD.

2.3.6 Tau and small molecules

Suramin is a polyanionic compound with broad pharmacological activity and has been used for treating various diseases, including neurodegenerative disorders (332). Suramin has been previously shown to inhibit the aggregation of amyloidogenic proteins, including Aβ (333,334). Suramin strongly enhances tau LLPS, resulting in the formation of larger condensates (335). Like RNA, suramin interacts electrostatically with tau through its multiple negative charges. Interestingly, suramin disrupts pre-formed tau condensates with

RNA and heparin by outcompeting these polyanions for tau binding. Moreover, it inhibits the formation of seeding competent species from tau:suramin condensates and tau:heparin condensates. These findings suggest that suramin may serve as a therapeutic candidate to interfere with tau condensation and its pathological maturation.

Methylene Blue (MB) is a well-known redox-active dye with established clinical applications across various diseases and infections (336). In the context of neurodegeneration, MB reduces hippocampal amyloid-β levels and inhibits tau aggregation *in vitro* (337,338). MB directly binds to tau and enhances its phase separation, even in the absence of crowding agents (339). MB increases droplet turbidity and size and lowers the C_{sat} for LLPS. This modulation of tau LLPS by MB is independent of its redox activity on tau cysteine residues and is instead mediated through electrostatic and hydrophobic interactions. MB significantly reduces the internal dynamics of tau within the condensates, suppresses droplet fusion, and promotes a transition from a liquid-like to a gel-like state. Importantly, MB does not interfere with tau's functional role in tubulin polymerization. While MB-induced condensates mature into non-toxic amorphous aggregates, they deviate tau from forming Thioflavin T (ThT)-positive amyloid fibrils. Thus, MB protects against pathogenic tau aggregation by redirecting it toward alternative, less cytotoxic pathways.

Table 2.1 provides an overview of heterotypic LLPS partners of tau discussed in this study. Each system is classified according to the type of LLPS based on the information from original publications. Due to its strong intrinsic phase-separating propensity, tau predominantly functions as the scaffold component driving phase separation in most systems. Depending on their influence on driving tau into toxic aggregates, the interacting partners have been categorized as either drivers or deterrents of tau aggregation.

Table 2.1 : Effect of hetero phase separation on tau aggregation

Partner	LLPS type	Effect on LLPS	Effect on tau aggregation	Enhance (+) Suppress (–)	Reference
RNA	tau (scaffold) RNA (client)	promotes heterotypic LLPS, increases droplet viscosity and stabilitv	decreases aggregation tendency, context-dependent	+/–	(228,252,253)
αS	both tau and αS can act as scaffolds	promotes heterotypic LLPS, retains liquid-like state, more resistant to electrostatic screening	enables nucleation of amyloid aggregation, forms heterotypic aggregates with polyamines	+	(108,264,265)
PrP	tau (scaffold) PrP (client)	promotes heterotypic LLPS, increases number, forms smaller	Accelerates maturation into solid-like fibrils	+	(137)

		and more spherical condensates			
TIA 1 (RBP)	Cooperative LLPS	forms heterotypic condensates, increases number, smaller in size	accelerates gelation, with RNA promotes toxic tau oligomer formation	+	(138,285)
Efhd2	Cooperative LLPS	heterotypic phase separation regulated by Ca2+, forms dynamic co-condensates with tau	can trigger formation of solid-like co-aggregates with tau	+/–	(322)
Hsp22 (chaperone)	tau (scaffold) Hsp22 (client)	Hsp22 is recruited into tau LLPS, increases number of condensates	prevents maturation and inhibits tau aggregation	–	(81)
PDI (chaperone)	tau (scaffold) PDI (client)	reduce number of condensates, regulated by nitrosylation of PDI	inhibits tau aggregation, nitrosylation impairs the neuroprotection	–	(317)
14-3-3ζ (chaperone)	tau (scaffold) 14-3-3ζ (client)	14-3-3ζ recruited into tau condensates, concentration-dependent regulation of tau LLPS	no effect on maturation or aging of co-condensates	+/–	(257)
S100B (chaperone)	tau (scaffold) S100B (client)	slows down tau LLPS	reduces formation of HMW tau oligomers	–	(299)
Ydj1 (chaperone)	tau (scaffold) S100B (client)	lowers critical concentration of tau LLPS, enhances phase separation	forms non-amyloidogenic heterocomplexes	–	(296)
PPIA	tau (scaffold) PPIA (client)	PPIA recruited into tau LLPS, maintains dynamic state of condensates	dissolves the condensed phase into single mixed phases	–	(330)
Suramin	tau (scaffold) Suramin (client)	enhances heterotypic LLPS, promotes bigger droplets	inhibits formation of seed competent tau species	–	(335)
Methylene Blue	tau (scaffold) MB (client)	binds to tau in condensates, enhances phase separation	accelerate liquid-to-gel-like transition, redirects tau into less cytotoxic pathways	–	(339)

2.4 Heterotypic phase separation of αS and the impact on its aggregation

2.4.1 αS

Parkinson's disease (PD) is a prevalent neurodegenerative disorder characterized by the progressive loss of dopaminergic neurons. The hallmark feature of PD pathology is the aggregation of alpha-synuclein (αS), a presynaptic protein, into Lewy bodies. Genetic mutations and altered expression of the *SNCA* gene, which encodes αS, are the key contributors to disease progression (340–343).

αS is a 140-amino acid protein predominantly expressed in neurons of the central and peripheral nervous system. αS plays crucial roles in synaptic function and neurotransmitter release and is predominantly localized at presynaptic terminals (344,345). In its native state, αS is inherently disordered, which allows it to interact with various cellular membranes and proteins. However, this structural flexibility can also contribute to its pathological accumulation in neurons. The resultant toxic assemblies disrupt neuronal homeostasis and define a group of disorders known as synucleinopathies (346,347).

The structural properties of αS contribute significantly to its function and role in disease. αS is comprised of three major domains: an N-terminal domain involved in membrane binding, a central hydrophobic non-Aβ component (NAC) region responsible for fibril formation and a flexible C-terminal domain (348). αS exists as an unstructured monomer, resistant to fibrillization within healthy neurons (349). In contrast, pathological conditions induce a conformational shift toward β-sheet-rich oligomers and fibrils that accumulate into Lewy bodies. These structurally diverse species including oligomers and mature fibrils can interconvert and contribute differentially to toxicity (350). Increasing evidence implicates prefibrillar oligomers as the primary toxic intermediates mediating pathology primarily through membrane disruption, organelle dysfunction and neuroinflammation (351,352). Nonetheless, mature fibrils also contribute to toxicity and together with αS oligomers, they drive disease progression (353–357).

Recent studies have highlighted that αS can undergo LLPS, majorly driven by the N terminus and NAC region, to form liquid droplets that may serve as precursors to amyloid fibrils (358–360). Although αS exhibits relatively low LLPS propensity at physiological pH, the phase separation behaviour of αS was regulated by various PD-associated factors such as local concentration of αS, pH shifts, metal exposure, lipid interactions and mutations (263,361). Initially, αS droplets show liquid-like properties and undergo a time dependent liquid-to-solid transition, progressively forming rigid, insoluble assemblies enriched in fibrillar and oligomeric species (358). Fibrillization of αS is accelerated when mediated through LLPS. Conditions that suppress LLPS delay or inhibit α-synuclein aggregation, suggesting a

potential implications of αS condensation in PD progression (362). However, some disease-associated αS mutants form fibrils without undergoing LLPS, and fibrils formed under LLPS conditions exhibit structural properties distinct from those formed under non-LLPS conditions (363). Together, these findings point towards the complex nature of αS phase separation and highlights the need for further investigation within the broader landscape of neurodegenerative diseases.

αS interacts with a diverse array of biomolecules, including enzymes, chaperones, and cytoskeletal proteins and these interactions significantly impact its biological functions, aggregation propensity, and contributions to neurodegeneration (364). More than 70 of these different interacting partners are identified within Lewy Bodies (365). Moreover, other neurodegenerative disease-associated proteins such as tau, Aβ, prion proteins, TDP-43 and Huntingtin, are often found to cross-seed and co-deposit with αS aggregates (366–368). Heterotypic interactions between these proteins may underlie the co-occurrence of multiple pathologies and their synergistic contribution to disease progression (369,370).

In the following sections, we review the interacting partners that undergo heterotypic phase separation with αS and discuss their influence on αS aggregation.

2.4.2 αS and amyloidogenic proteins

Tau is a major amyloidogenic interaction partner of αS, and their heterotypic condensation has been discussed in section 2.3

Transactive response DNA-binding protein 43 (TDP-43) is a critical pathological protein implicated in various neurodegenerative diseases, predominantly in amyotrophic lateral sclerosis (ALS) and frontotemporal dementia (FTD) (371). TDP-43 functions as a nuclear RNA-binding protein involved in RNA processing as well as a cytosolic regulator of stress granule dynamics. Under pathological states, TDP-43 undergoes nuclear depletion and cytoplasmic aggregation, a hallmark of ALS and FTD pathology (372,373). Previous studies indicate a direct interaction between TDP-43 and αS. They co-deposits in glial cytoplasmic inclusions and synergistically enhance cytotoxicity (374–376). αS also interacts with the prion-like domain of TDP-43 (TDP-43PrLD), seeding its aggregation and forming cytotoxic heterofibrils (367). TDP-43PrLD shows a strong propensity to undergo coacervation with RNA and form highly dynamic condensates. Although, αS alone does not phase separate under these conditions, it was readily recruited into pre-formed TDP-43PrLD–RNA droplets (377). The interaction between αS and TDP-43PrLD were driven majorly by electrostatic interactions and occurred under cellular conditions as well. αS significantly reduced the liquid-like nature of TDP-43PrLD within the droplet. Together with RNA, αS localized asymmetrically to the droplet surfaces and prevented the coalescence between

condensates. αS exhibited low fluorescence recovery at the condensate periphery, indicative of a more solid-like state. αS significantly accelerated fibril nucleation and aggregation within these co-condensates, producing heterotypic fibrils with morphologies resembling both αS and TDP-43PrLD control fibrils. The formation of these heterotypic aggregates suggests a mutual promotion of aggregation between αS and TDP-43, indicating that their co-pathology in neurodegeneration might be mediated by LLPS.

As discussed earlier in this review, PrP undergoes heterotypic condensation with tau. Interestingly, PrP also interacts with αS and similarly forms heterotypic condensates. Several studies have demonstrated that PrP can act as a receptor for αS aggregates, promoting their internalization and enhancing their toxicity (378,379). The role of PrP in αS pathology appears to be complex and context dependent. While several studies support its involvement in αS propagation and toxicity, others report minimal or no contribution (380,381). Under physiological conditions, where neither PrP nor αS phase separate on their own, their mixture leads to the spontaneous formation of co-condensates rich in both PrP and αS (382). These PrP:αS condensates exhibit dynamic liquid-like properties and both proteins showed high mobility within the condensates. The heterotypic condensation is primarily driven by electrostatic interactions and is sensitive to higher stochiometric mixing. Spatiotemporal organisation within the PrP:αS condensates was modulated by RNA, leading to the emergence of multiphasic condensates (382). Under quiescent conditions, these droplets undergo a gradual liquid-to-solid transition; however, mechanical agitation triggers a rapid conversion into heterotypic amyloid aggregates. Notably, this conversion does not occur under non-LLPS conditions, highlighting the critical role of LLPS in facilitating aggregation. Given that the PrP:αS interaction is highly context dependent, further studies under *in vivo* contexts are needed to explore their LLPS-mediated interaction.

β-Synuclein (βS) is a member of the synuclein family, sharing 78 % sequence homology with αS (383). βS is found abundantly in the central nervous system and co-localizes with αS at the presynaptic terminals. Despite their structural similarity, βS is considerably less aggregation-prone and is generally considered neuroprotective, counteracting αS aggregation and associated toxicity. Studies have shown that βS inhibits both the initiation and amplification phases of αS aggregation by competitively binding to lipid surfaces and αS fibrils (384–386). βS, as a client component partitions into αS condensates through electrostatic interactions and co-localizes with αS under physiological and crowded conditions (387). Notably, αS alone undergoes phase separation under these conditions, whereas βS does not. The presence of βS enhances αS phase separation by increasing the size, number, and liquidity of the condensates. However, contrasting findings suggest that

βS can also negatively regulate αS phase separation and reduce condensate fluidity (388). Despite these opposing effects, both studies support a protective role of βS in modulating αS aggregation via LLPS. βS dramatically delayed the tendency of liquid-to-solid transition of the co-condensates and prevented the formation of amyloid fibrils. Yet, emerging evidence indicates that βS may gain toxic properties under pathological conditions. Altered expression levels or disease-associated mutations in βS have been shown to promote the maturation of αS condensates into gel-like, aggregation-prone states (389). These findings highlight a delicate balance in the modulatory role of βS, which may shift from protective to pathogenic in disease contexts.

S100A9 is a pro-inflammatory protein constitutively expressed by neutrophils, dendritic cells, and monocytes and has been implicated in the pathogenesis of various types of cancer, chronic inflammation, and neurodegenerative diseases (390). S100A9 is a potential initiator and amplifier of amyloid pathology in PD, primarily through its ability to co-aggregate with αS and significantly accelerate its fibrillation (391). Both S100A9 and αS independently undergo LLPS under conditions of molecular crowding at physiological pH, forming homotypic condensates. In the case of S100A9, these homotypic condensates often coexist with aggregates. Upon co-incubation of S100A9 and αS, the number of condensates were enhanced and these included S100A9:αS heterotypic condensates, as well as, S100A9 and αS homotypic condensates (392). The S100A9:αS interaction was driven by a combination of electrostatic and hydrophobic interactions. Within the mixed condensates, S100A9 aggregation is notably suppressed by αS, although it displays uneven, clumped distribution. Conversely, S100A9 strongly promotes αS aggregation, accelerating fibril formation and stabilizing a distinct fibril strain with enhanced seeding capacity. The cellular abundance of S100A9, its upregulation during neuroinflammation, and its propensity to seed α-synuclein aggregation collectively suggest that S100A9 may represent a therapeutic target for Parkinson's disease.

2.4.3 αS and synaptic/disordered Proteins

VAMP2 (vesicle-associated membrane protein 2) is a key component of the SNARE (soluble N-ethylmaleimide-sensitive factor attachment protein receptor) complex (393). VAMP2 mediates the fusion of synaptic vesicles (SVs) with the presynaptic membrane and facilitates exocytosis and plays a pivotal role in neurotransmitter release. αS has been shown to directly bind VAMP2 and regulate SNARE complex assembly (394). Recent studies have demonstrated that αS undergoes heterotypic condensation with VAMP2 (395), as well as with SVs containing VAMP2 (396). Under the corresponding experimental conditions, αS forms homotypic condensates, and the presence of VAMP2 significantly lowers the C_{sat} required for αS phase separation. VAMP2 also enhances both the size and number of αS

condensates. Within these heterotypic condensates, αS retains high liquid-like mobility, indicating the preservation of a dynamic phase. Importantly, VAMP2 markedly suppresses αS oligomerization upon heterotypic condensation and also inhibits αS fibrillation, highlighting a potential protective role for VAMP2 in αS pathology (396). Thus, beyond its established function in SV clustering and synaptic transmission (397), VAMP2 may act as a molecular modulator that mitigates the aggregation propensity of αS through LLPS.

Small EDRK-rich factor (SERF) proteins are evolutionarily conserved, highly charged and conformationally dynamic molecules that play a critical role in modulating cellular mechanisms that underpin stress granule formation and protein aggregation (398). Their intrinsic disorder, driven by extensive intrinsically disordered regions (IDRs), enables them to engage flexibly with a wide range of interaction partners (399). SERF proteins have been directly implicated in modulating the aggregation of amyloidogenic proteins (400–402). Specifically, SERF binds to αS in the cytoplasm, generating SERF/αS complexes (401). SERF competes with the protective intramolecular interactions within αS and promote the nucleation of αS aggregates (403,404). SERF undergoes electrostatically driven homotypic LLPS forming dynamic condensates both *in vitro* and *in vivo*. Although αS alone does not phase separate under these conditions, it is readily recruited into pre-formed SERF condensates, resulting in the formation of larger and denser heterotypic droplets (405). Interestingly, as these condensates mature, αS shows a dramatic reduction in fluorescence recovery, suggesting a transition to a solid-like state, whereas SERF retains its mobility. Over time, SERF exits the condensates, leaving behind solidified αS. This co-localization significantly accelerates the formation of ThT-positive aggregates. Notably, while SERF promotes αS fibril formation, it simultaneously suppresses the accumulation of toxic oligomeric intermediates. By redirecting aggregation toward less harmful fibrillar forms, SERF reduces αS-induced cytotoxicity, underscoring its dual role as both a pro-amyloid modulator and a mitigator of oligomer toxicity.

Synapsin proteins are integral to several functions in neuronal physiology, particularly in the assembly of SVs and regulation of neurotransmitter release (406). Phase separation underlies SV organization, and synapsins have been shown to form liquid-like condensates *in vitro* that incorporate liposomes mimicking SVs (407). Dysregulation of synapsin activity has been implicated in several neurological disorders (408). In the context of PD, synapsin and αS are co-dysregulated and co-deposited, and synapsin knockout has been shown to reduce αS aggregation and toxicity (409,410). Recent studies demonstrate that αS is recruited into synapsin1 condensates at synapses, where synapsin functions as the scaffold and αS as the dynamic client partner (411). Importantly, excess αS disrupts synapsin condensate formation, potentially interfering with the organization of synaptic vesicles and

contributing to early synaptic dysfunction. Current studies lack information on the role of synapsin in aggregation of αS via heterotypic LLPS. While the precise role of synapsin in modulating αS pathology remains incompletely understood, the findings point to a delicate stoichiometric balance between the two proteins that may be critical for maintaining synaptic integrity.

2.4.4 αS and polyphenols/small molecule modulators

Myricetin is a naturally occurring flavonoid within the broader class of polyphenolic compounds, widely distributed in fruits, vegetables, nuts, and plant-derived beverages (412). Myricetin exhibits a broad spectrum of biological activities, including antioxidant, antiviral, antidiabetic, anti-inflammatory, and neuroprotective effects. Notably, myricetin confers neuroprotection by mitigating oxidative stress (413) and inhibiting the aggregation of several amyloidogenic proteins implicated in neurodegenerative diseases, including Aβ (414), αS (415), insulin and superoxide dismutase 1 (416,417). Myricetin directly binds to the N-terminal region of αS which is critical for oligomerisation and thereby suppresses oligomer formation (415,418). Upon heterotypic condensation with αS, myricetin did not alter the morphology, number, or size of αS condensates, but slightly reduced the dynamics of αS within the co-condensates (419). Importantly, myricetin inhibited the liquid-to-solid transition of αS condensates and blocked amyloid fibril formation in a dose-dependent manner. Moreover, it demonstrated the ability to dissolve pre-formed αS aggregates, underscoring its therapeutic potential.

Curcumin, a natural polyphenolic compound derived from the rhizome of *Curcuma longa* (turmeric), is increasingly recognized for its broad therapeutic potential, particularly in chronic inflammatory and neurodegenerative disease (420,421). Curcumin exhibits potent antioxidant, anti-inflammatory, and neuroprotective activities (422,423). In the context of αS pathology, curcumin enhances the solubility of αS monomers and inhibits aggregation by binding preferentially to oligomeric and fibrillar species, thereby reducing their toxicity (424–426). αS undergoes heterotypic condensation with curcumin, where curcumin associates primarily with hydrophobic regions of αS within the condensates (427). Curcumin does not alter the morphology, size, or number of αS condensates but reduced the initial dynamics of αS in the condensates. However, curcumin slows the liquid-to-solid maturation, and significantly inhibits fibril formation, effectively disrupting αS aggregation. Strikingly, curcumin is also capable of disassembling preformed αS amyloid fibrils, likely through intermediate condensate states. Furthermore, it exhibits similar inhibitory effects on PD-associated αS mutants. The effect of curcumin on α-synuclein LLPS closely mirrors that of myricetin, suggesting that small polyphenolic molecules can modulate αS phase behaviour and aggregation.

Peptide-based molecular strategies to inhibit protein misfolding, aggregation, and neurodegeneration represent a rapidly advancing frontier in therapeutic research. Owing to their structural versatility, high specificity, and potent bioactivity, peptides can be precisely engineered to target pathological protein conformations, offering innovative avenues for intervention (428,429). The RaPID (Random Non-standard Peptides Integrated Discovery) system is a platform for identifying such therapeutic candidates, particularly against amyloidogenic targets (430,431). Using this system, two peptides FL2 and FD1 were identified that selectively bind to fibrillar states of αS. These peptides induced LLPS with αS in the presence of molecular crowding (432). The phase separation was concentration-dependent on both peptide and αS, and the resulting condensates displayed hallmark properties of fluid phases, including reversibility, fusion behaviour and surface wetting. Binding of the peptides to αS occurred via weak interactions or site-specific contacts. Interestingly, although peptide-induced LLPS facilitated nucleation by reducing the lag phase of aggregation, it concurrently promoted the formation of hydrophobic, non-amyloidogenic pre-fibrillar aggregates, inhibited seeded fibril elongation, and reduced the overall fibril load. Thus, by locally concentrating αS within condensates, these peptides exert a dual modulatory effect enhancing early nucleation while potently blocking downstream amyloid formation and misfolding.

Spermine is a naturally occurring polyamine that plays critical roles in a wide range of biological processes, including cellular growth, differentiation, gene regulation and stress responses. Dysregulation of the polyamine metabolic pathway has been implicated in the pathogenesis of neurodegenerative disorders (433,434). Biogenic polyamines are abundant in neurons and modulate the aggregation of amyloidogenic proteins. They exert differential effects on protein aggregation depending on their net charge, molecular length, and concentration, and have been shown to promote the aggregation of both αS (435) and Aβ (436). Under molecular crowding conditions, spermine forms heterotypic condensates with αS via electrostatic interactions (263,437). Notably, neither αS nor spermine alone, nor their individual combinations with PEG, underwent LLPS under these conditions. These αS:spermine condensates accelerated the aggregation kinetics of αS and promoted its conversion into β-sheet-rich fibrils that coexisted with aged droplets (437). In contrast, Rodríguez *et al*. reported that mesh-like aggregates formed during maturation lacked β-sheet signatures, suggesting variable structural effects (438). This heterotypic condensation is modulated by three factors: acetylation of spermine, ATP, and RNA. Acetylation of spermine impairs liquid–liquid phase separation, ATP promotes droplet solidification, and RNA dissolves condensates and delays αS aggregation. Together, spermine promotes both αS condensation and fibrillization, while acetylation, ATP, and RNA finely regulate this process.

The various heterotypic LLPS partners of αS discussed above are summarized in Table 2.2. Each system has been classified according to the type of LLPS, based on information reported in the original publications. αS can function either as a scaffold or as a client within these condensates and this can be influenced by αS concentration and various experimental conditions used in respective studies. Furthermore, depending on their influence on the formation of toxic αS assemblies, the interacting partners have been categorized as drivers or deterrents of αS aggregation.

Table 2.2 : Effect of hetero phase separation on αS aggregation

Partner	LLPS Type	Effect on LLPS	Effect on αS aggregation	Enhance (+) Suppress (–)	Reference
TDP- 43 (prion-like domain)	αS (client) TDP-43 (scaffold)	αS localized at droplet surfaces, reduces dynamics of TDP-43 condensates	accelerates amyloid formation, forms heterofibrils	+	(377)
βS	αS (scaffold) βS (client)	βS is recruited into αS condensates, can enhance or suppress phase separation	blocks aggregation of αS	–	(387,388)
PrP	Cross interaction driven LLPS	PrP formed highly dynamic heterotypic condensates with αS	rapid formation of heterotypic aggregates under agitation	+	(382)
S100A9	Cooperative LLPS	promote formation of heterotypic droplets	enhances aggregation and fibril formation.	+	(392)
Synapsin	αS (client) Synapsin (scaffold)	αS recruited into synapsin condensates, αS retains mobility.	no direct aggregation effects; excess αS disrupt condensates and causes synaptic dysfunction	+/–	(411)
SERF	αS (client) SERF1 (scaffold)	promotes heterotypic LLPS, increases droplet size and density	reduces oligomer-mediated toxicity of αS	–	(405)
FL2/FD1 (de-novo peptides)	Cross interaction driven LLPS	drives heterotypic LLPS, enhance fluid characteristics of condensates	reduces the overall fibril mass	–	(432)

Myricetin	αS (scaffold) Myricetin (client)	does not affect initial condensate formation, reduces αS dynamics	delays liquid-to-solid phase transition, blocks αS fibril formation, disassemble pre-formed amyloids	–	(419)
Curcumin	αS (scaffold) Curcumin (client)	recruited into αS condensates, reduces αS fluidity	delays liquid-to-solid like transition, inhibits amyloid aggregation	–	(427)
VAMP2	αS (scaffold) VAMP2 (client)	promotes heterotypic LLPS, increases size and number of condensates	prevents αS aggregation	–	(395)
Spermine (Sp)	αS (client) Sp(scaffold)	promotes heterotopic condensation with αS	accelerates fibrillization of αS	+	(263,437)

2.5 Quadrant plot summary

In this review, we brought together the heterotypic phase separation partners of tau and αS. Fig 2.2 (a) and (b) show the discussed phase separation partners of tau and αS in a quadrant plot. Each partner is positioned in the plot based on its effects on two aspect; (i) phase separation, as judged by the physical properties of heterotypic condensates, including number, size, and fluidity, and (2) protein aggregation, encompassing the kinetics of maturation, progression into aggregates, and the toxicity of the resulting aggregates. From the plots, it is evident that most amyloidogenic proteins that co-phase separates with tau or αS tend to enhance LLPS and the subsequent aggregation. This effect aligns with the observed co-pathology of these proteins in several neurodegenerative diseases**.** For tau, many molecular chaperones appear to suppress aggregation. Interestingly, this suppression does not necessarily equate to inhibition of phase separation. Rather, these chaperones often direct tau condensates towards less amyloidogenic pathways. Proteins like Efhd2 and 14-3-3ζ were not included in the tau plot due to limited data regarding their role in LLPS-mediated tau aggregation. In contrast, phase separation with molecular chaperones is less studied in the case of αS, likely due to the inherently low phase separation tendencies of

both αS and chaperones. Polyphenolic compounds have shown promise in inhibiting αS aggregation via LLPS mechanisms.

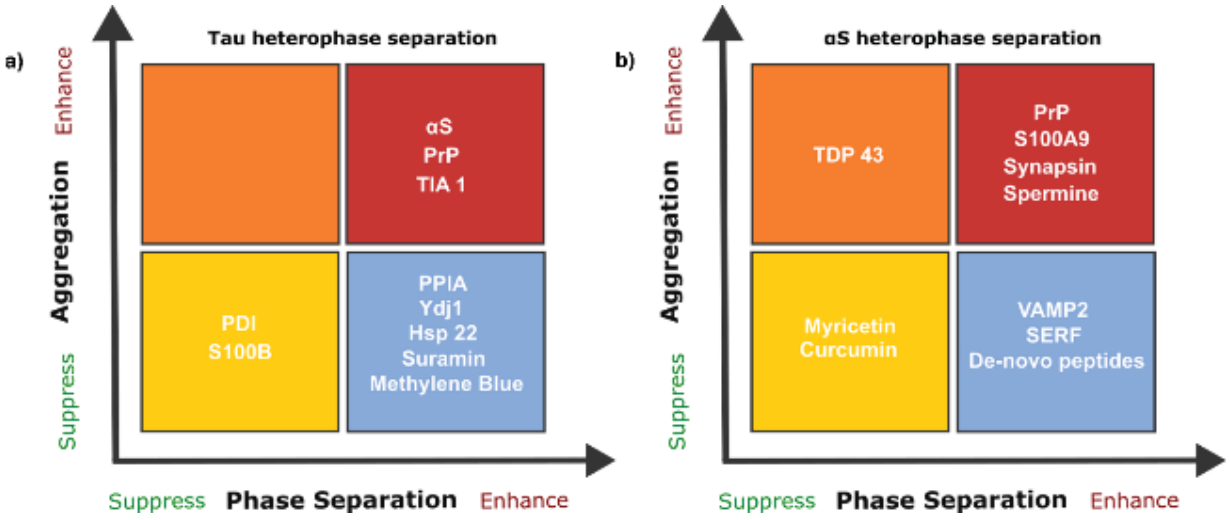

Fig 2.2: Quadrant plot showing the effect of different heterotypic LLPS partners on tau and αS.

Further exploration of similar small molecules against tau could present new opportunities to slow or prevent neurodegeneration. Peptide-based therapeutic strategies have demonstrated the potential to enhance the fluid properties of αS condensates while preventing their maturation into fibrils. These approaches could serve as valuable interventions at specific intermediate stages of the aggregation process. βS, although excluded from the quadrant due to its unclear role in phase separation, effectively inhibits αS aggregation and holds promise as a therapeutic agent due to its endogenous origin and favourable cellular distribution. These findings collectively underscore the potential of targeting heterotypic phase separation as a therapeutic strategy in neurodegenerative diseases.

2.6 Concluding remarks and future perspectives

In summary, heterotypic phase separation emerges as a pivotal mechanism modulating the aggregation behaviour of key neurodegenerative proteins including tau and αS. Our review highlights that heterotypic condensates formed through interactions with diverse partners can either enhance or suppress pathological aggregation, revealing a complex regulatory network within biomolecular condensates.

The interplay between scaffolds and clients within these condensates dictates the condensate properties and aggregation propensity. Moreover, the presence of cofactors and post-translational modifications can further modulate condensate dynamics and

aggregation pathways, emphasizing the multifactorial control of protein homeostasis via phase separation.

Looking forward, a deeper mechanistic understanding of the molecular determinants governing heterotypic phase separation will be critical. Key challenges remain in investigating how these condensates transition from functional assemblies to pathogenic aggregates *in vivo*. Advanced biophysical techniques, combined with cellular and animal models, will be essential to elucidate the temporal dynamics and structural features of heterotypic condensates.

Future research should also explore the therapeutic potential of modulating heterotypic phase separation. Targeting specific interaction interfaces or modulating condensate properties could provide novel strategies to prevent or reverse aberrant aggregation in neurodegenerative diseases. Overall, embracing the complexity of heterotypic phase separation offers promising avenues for understanding and ultimately intervening in progression of neurodegenerative diseases.

Chapter 3. Tau-AβO interaction under LLPS conditions

Manuscript Information

Title: Liquid-liquid phase-separated tau colocalizes with and stabilizes Aβ oligomers
Authors: Tina Jacob, Marie Schützmann and Wolfgang Hoyer

Journal: Nature Communications

Status: Under revision (September 2025)

Contributions: Transformation, expression, purification, FRAP assays, SDS-PAGE, fluorescent labelling, ThT kinetics, TIRF microscopy, Confocal microscopy, DLS and turbidity measurements, preparation of figures, writing and reviewing of the manuscript.

This chapter includes sections from the above manuscript that describe the interaction between tau and AβOs under LLPS conditions. It has been further expanded with additional experimental data to provide a more comprehensive understanding of these interactions under LLPS conditions.

3.1 Aim of the study

The aim of this study is to investigate the molecular interplay between tau and AβOs within the framework of LLPS, a biophysical phenomenon increasingly recognized as a key regulator of protein aggregation, subcellular compartmentalization, and proteostasis. Using biochemical labelling strategies in combination with advanced biophysical and imaging approaches, this work seeks to elucidate the mechanistic principles that govern tau-AβO interactions in a physiologically relevant, crowded environment.

Specifically, the study aims to (i) determine how AβOs interact with tau condensates and modulate their properties, and (ii) assess how pre-formed tau condensates influence the aggregation kinetics and pathological characteristics of AβOs. This bidirectional analysis is intended to clarify whether LLPS provides an active microenvironment that drives aberrant molecular association and modifications.

3.2 Materials and methods

3.2.1 Plasmid Isolation

Plasmid DNA was isolated using the NucleoSpin® Plasmid kit (Macherey-Nagel, Germany) in accordance with the manufacturer's protocol. For tau, a single colony of *E. coli* XL1-Blue cells containing the recombinant plasmid was inoculated into 5 mL LB medium supplemented with kanamycin (50 µg/mL) antibiotic resistance. Following overnight incubation at 37 °C with shaking at 160 rpm, 3 mL of culture was harvested by centrifugation. The bacterial pellet was resuspended in resuspension buffer A1containing RNase A, followed by the addition of lysis buffer A2. After few gentle inversions to ensure complete lysis, neutralization buffer A3 was added to precipitate genomic DNA, proteins and other cellular debris. The lysate was then centrifuged, and the clear supernatant was transferred to a NucleoSpin® column for plasmid binding. The column was washed sequentially with wash buffers AW and A4, and plasmid DNA was eluted using 50 µL of pre-warmed elution buffer. DNA concentration and purity were assessed using a NanoDrop spectrophotometer.

3.2.2 Determination of nucleic acid concentration

The concentration of plasmid DNA was quantified using a NanoDrop 2000 spectrophotometer (Thermo Scientific, USA). The system was first blanked with 2 µl of elution buffer under the nucleic acid analysis mode. Following the blank, 2 µL of each DNA sample was loaded onto the instrument pedestal, and measurements were recorded. DNA concentration was calculated from the absorbance at 260 nm. Sample purity was assessed using the A260/A280 ratio, with values of 1.8 considered indicative of high-purity DNA.

3.2.3 Bacterial transformation

The pET-28a and pACYCDuet-1 plasmids encoding tau and dimAβ, respectively, were transformed into chemically competent *E. coli* BL21(DE3) cells (Novagen) using the heat-shock method. Purified plasmid DNA (1-5 µL) was added to 50 µL of thawed competent cells and gently mixed, followed by incubation on ice for 20-30 minutes. Cells were then heat-shocked at 42 °C for 45 seconds to facilitate DNA uptake and immediately returned to ice for 2 minutes. Subsequently, 450 µL of pre-warmed SOC medium was added, and the cell suspension was incubated at 37 °C with shaking at 300 rpm for 1 hour to allow recovery and expression of antibiotic resistance. After recovery, 100 µL of the transformation mixture was spread onto LB agar plates containing kanamycin (50 µg/mL) and incubated overnight at 37 °C for colony selection. Individual colonies were selected the following day and inoculated into 50 mL of LB medium supplemented with kanamycin (50 µg/mL) to establish precultures. The cultures were incubated at 37 °C with shaking at 160 rpm overnight.

3.2.4 Expression and purification of tau

The preculture was inoculated into the main culture to achieve an initial optical density at 600 nm (OD_{600}) of 0.05. The cells in the main culture were grown in 2YT medium supplemented with kanamycin (50 µg/mL) at 37 °C until reaching an OD of 0.6. At 0.6-0.7 OD, the main culture was induced for protein expression by adding 1 mM isopropyl β-D-1-thiogalactopyranoside (IPTG). Following induction, the culture was incubated for an additional 4 hours under the same growth conditions and subsequently harvested using a Beckman JLA 10,500 rotor by centrifugation at 5,000 × g for 12 min at 4 °C. The resulting cell pellet was resuspended in lysis buffer composed of 20 mM PIPES, 500 mM NaCl, 2 mM dithiothreitol (DTT), pH 6.5, supplemented with a ethylenediaminetetraacetic acid (EDTA) protease inhibitor tablet (Roche Applied Sciences). Cells were lysed by Bandelin Sonopuls utilizing an VS 70T sonicator tip. The sonication was performed for a total of 5 minutes using 3 s pulse followed by 5 s pause and repeated for three cycles. Cell debris was removed by centrifugation using a Beckman JA-10 rotor at 40,000 × g for 40 min at 4 °C. Owing to the high thermal stability of tau, the supernatant was heated to 80 °C for 15 min and centrifuged again to remove precipitated, heat-denatured proteins. Tau was subsequently precipitated by adding ammonium sulphate to a final concentration of 54% saturation (from a 4 M stock) and incubating the mixture overnight on a roller shaker at 4 °C. The precipitated protein was collected by centrifugation, resuspended in deionised water, and dialysed overnight against 20 mM PIPES, 50 mM NaCl, 2 mM DTT, pH 6.5. Following successful dialysis, tau purification was continued using ion-exchange chromatography (IEC) on a HiTrap SP FF 5-mL cation-exchange column, and tau was eluted with a linear NaCl gradient (from 50 mM to 1 M) in 20 mM PIPES buffer, 2 mM DTT at pH 6.5. A final size-exclusion chromatography (SEC) step was

performed on a HiLoad 16/600 Superdex 75 pg column to remove truncated species. During SEC, buffer exchange was simultaneously performed to yield purified protein in 30 mM Tris, 50 mM NaCl, pH 7.4.

3.2.5 Sodium dodecyl sulfate polyacrylamide gel electrophoresis (SDS PAGE) for protein analysis

Protein analysis based on molecular weight was performed using sodium dodecyl sulfate polyacrylamide gel electrophoresis (SDS PAGE). Each gel consisted of a stacking gel (upper layer) and a resolving gel (lower layer). The choice of gel system depended on the size of the protein. Tris-glycine gels were used for proteins larger than 40 kDa, while Tris-tricine gels were used for proteins smaller than 40 kDa. In this study, tau (44 kDa) was evaluated using Tris-glycine gels, whereas dimAβ analysis (10.1 kDa) was performed on Tris-tricine gels. Tris-glycine resolving gels were prepared at 8% polyacrylamide, while Tris-tricine resolving gels were cast at 20% polyacrylamide.

Table 3.1 : Composition of 8 % tris-glycine gels

Components	Resolving gel	Stacking gel
1.5 M Tris-HCl, pH 8.8	2.5 ml	
0.5 M Tris-HCl, pH 6.8		1.5 ml
Rotiphorese Gel 30 (37.5:1)	2.6 ml	830 µl
Milli-Q H2O	4.7 ml	2.8 ml
10% SDS	100 µl	50 µl
TEMED	10 µl	10 µl
10% APS	100 µl	50 µl

Table 3.2 : Composition of 20% tris-tricine gels

Components	Resolving gel	Stacking gel
3 M Tris-HCl, 0.3% SDS, pH 8.45	10 ml	4.2 ml
Rotiphorese Gel 30 (37.5:1)	17 ml	2 ml
Glycerol	3.2 ml	
Milli-Q H2O	2.3 ml	2.8 ml
TEMED	50 µl	50 µl
10% APS	100 µl	100 µl

The resolving gel solution was prepared by combining all required components, adding APS and TEMED last to initiate polymerization. The mixture was gently but thoroughly mixed and immediately poured between the assembled glass plates. A layer of isopropanol was then added to the surface to create a smooth interface and prevent bubble formation during gel

polymerization. After complete polymerization of the resolving gel, the isopropanol overlay was removed. The stacking gel solution was prepared, with APS added last to initiate polymerization, and carefully layered on top of the resolving gel. A 10 or 15 well comb was inserted, and the stacking gel was allowed to polymerize. The gels were either used on the same day or stored at 4 °C for up to one week, wrapped in moist paper towels to prevent dehydration. Polymerized gels were assembled into a BioRad Mini-PROTEAN electrophoresis system. For Tris-glycine gels, 1x Tris-glycine running buffer was added to both the cathode and anode chambers. For Tris-tricine gels, 1x Tris-tricine cathode buffer was added to the cathode chamber and 1x Tris-tricine anode buffer to the anode chamber. Stock buffer preparation (10x) is described in Section 6.4.

Protein samples were prepared by mixing with 4x Laemmli loading buffer to a final 1x concentration in a total volume of approximately 20 µL. Samples were heated at 95 °C for 5 min, briefly centrifuged, and loaded into the wells. A pre-stained protein molecular weight marker (PageRuler™ or PageRuler™ Plus, Thermo Scientific) was loaded in an adjacent well. Electrophoresis was performed at a constant voltage of 120 V for 2 h, until the bromophenol blue dye exited the gel or, when colourless loading buffer was used, until the lowest marker band reached the bottom.

Following electrophoresis, the gel was removed from the cassette and processed either directly for western blotting, imaged for fluorescent proteins using a Gel Doc XR system, or subjected to Coomassie staining. For Coomassie staining, gels were incubated in colloidal Coomassie blue or READYBLUE® Quick Stain (Sigma-Aldrich) for 2 h under gentle agitation, followed by three washes with distilled water and overnight destaining in water with agitation. After 24 h, gels were rinsed again, and images were acquired using a Gel Doc XR imaging system.

3.2.6 Fluorescent labelling of tau

For confocal microscopy, fluorescent labelling of tau was required to enable its direct visualization within condensates and co-assemblies. N-hydroxysuccinimide (NHS) ester chemistry was used due to its high efficiency and specificity for primary amines under mild aqueous conditions (439). The 44 lysine residues in tau serve as the primary sites for NHS ester labelling (6.1). NHS ester reacts with the ε-amino groups of lysine side chains and the N-terminal amine through nucleophilic attack, forming stable amide bonds. This reaction is typically carried out in a slightly basic aqueous buffer (pH 7.5-8.5), which deprotonates the amine groups, enhancing their nucleophilicity while maintaining protein stability.

Tau was fluorescently labelled using Alexa Fluor 647 NHS ester (Alexa 647, Thermo Fisher Scientific, Cat. No. A20006). Alexa 647 is a far-red dye with an excitation maximum at 650

nm and an emission maximum at 668 nm, providing high photostability and minimal spectral overlap with commonly used green fluorophores. Briefly, 3 mg of lyophilized tau was dissolved in 90 mM HEPES/NaOH (pH 7.9) containing 10% (v/v) amine-free dimethylformamide (DMF) and incubated with an excess of dye for 70-90 min at 20 °C in the dark to prevent photobleaching. Free, unreacted dye was removed by reverse-phase high-performance liquid chromatography (RP-HPLC) using a Zorbax SB-300 C8 (9.4 × 250 mm) semipreparative column.
After successful RP-HPLC purification, the fractions that showed coincident signals for both Alexa 647 and the protein were collected and lyophilised (Fig 6.1 A).

The lyophilised aliquots were dissolved in 30 mM Tris, pH 7.4, and analysed by SDS-PAGE using a pre-stained protein ladder. Prior to loading, the samples were mixed with Laemmli buffer lacking bromophenol blue to avoid interference with fluorescent detection. Following electrophoresis, the gel was imaged directly without Coomassie staining. Images were acquired in both the standard channel and the Alexa 647 fluorescence channel, and the resulting images were overlaid (Fig 6.1 B).

3.2.7 LLPS of tau

Unless mentioned specifically, all tau condensates were prepared at a concentration of 10 µM in 30mM Tris, 50 mM NaCl, pH 7.4, with 10% PEG 6000 (SigmaAldrich-81260). To image the droplets, 5-6 µl of the solution were placed on a clean glass slide with a coverslip on top to prevent evaporation.

3.2.8 Expression and purification of dimAβ

Expression and purification of dimAβ were carried out according to previously established protocols (169). Bacterial expression of dimAβ was achieved by co-expression of ZAβ3, a chaperone-like binding protein that shields aggregation-prone sequence segments of Aβ. The gene encoding dimAβ, consisting of an N-terminal methionine followed by an Aβ40 sequence, a flexible $(G_4S)_4$ linker, and a second Aβ40 sequence, was obtained from Life Technologies and cloned into the pACYCDuet-1 vector using *NcoI* and *HindIII* restriction sites. The resulting co-expression plasmid contained both the dimAβ gene and the gene for His_6-tagged ZAβ3 arranged as follows: T7 promoter-1 – dimAβ – T7 promoter-2 – His_6-ZAβ3 – T7 terminator (6.2).

For the expression of dimAβ, M9 culture medium was used. The composition of M9 for 500 ml is as described in Table 3.3.

Table 3.3 Composition of M9 media for dimAβ expression

Components (stock concentration)	Final concentration	Volume for 500 ml
NH_4Cl (20 %)	0.1 %(w/v)	2.5 ml
Glucose (40 %)	0.2 %(w/v)	2.5 ml
$CaCl_2$ (0.1M)	0.1 mM	0.5 ml
Chloramphenicol (25 mg/mL)	25 µg/mL	0.5 ml
M9 salt (10 x stock)	1 X	50 ml
MQ water		441 ml

For protein expression, bacterial cultures were inoculated with 0.1% (v/v) of preculture and grown to an OD of 0.6-0.8, followed by induction with 1 mM IPTG. Following a 4 h incubation at 37 °C, cells were harvested using Beckman J2-21 centrifuge mounting a JA 10.500 rotor at 5000 rpm for 15 minutes. For purification, cell pellets were resuspended in 50 mM Sodium phosphate (NaPi), 0.3 M NaCl, 20 mM imidazole, pH 8, containing EDTA-free protease inhibitor (Roche Applied Sciences). The cell lysate was then lysed by Bandelin Sonopuls utilizing an MS72 sonicator tip. The pulse was applied for 5 min at 55% amplitude with a cycle of 3 s on and 5 s off. The cell debris was removed by centrifugation in a Beckman J2-21 centrifuge mounting a JA20.1 rotor at 40,000 RPM, 4 °C for 40 minutes. For capture of the dimAβ:ZAβ3 complex by immobilized metal ion affinity chromatography (IMAC), the supernatant was loaded on a HisTrap FF column (GE Healthcare). DimAβ was separated from the resin-bound ZAβ3 and eluted with 8 M urea, 20 mM NaPi, pH 7 in a step gradient. For further purification, including removal of residual ZAβ3, RP-HPLC was performed. For this purpose the IMAC eluate was concentrated in a Vivaspin 20 centrifugal concentrator (Sartorius), followed by addition of 5 mM Tris(2-carboxyethyl)phosphine (TCEP) to reduce the disulfide bond of ZAβ3, and loading onto a semi-preparative Zorbax 300SB-C8 RP-HPLC column (9.4 mm × 250 mm, Agilent) connected to an Agilent 1260 Infinity system with UV detection at 214 nm. Monomeric dimAβ was eluted in a gradient from 30% (v/v) to 36% acetonitrile in water, 0.1% (v/v) trifluoroacetic acid at 80 °C. DimAβ containing fractions were pooled, lyophilized, dissolved in HFIP (1,1,1,3,3,3-Hexafluoro-2-propanol), aliquoted in 1 mg portions, lyophilized again and stored at −20°C. Before use in experiments, monomeric nature of dimAβ was ensured either by SEC or by dissolving it in HFIP. For SEC, lyophilized dimAβ was reconstituted in 6 M guanidinium-HCl, 50 mM NaPi, 50 mM NaCl, pH 7.4, and sonicated for 30 minutes in a SONOREX RK100H sonicator bath. Subsequently, the solution was loaded onto a Superdex 75 10/300 GL column (GE Healthcare) equilibrated with corresponding buffer conditions. Alternatively, lyophilised dimAβ was first dissolved in HFIP

and re-lyophilised in aliquots. Each aliquot was then dissolved in 50 mM NaOH and the appropriate buffer, followed by brief sonication (30 s) to aid dissolution. An equal volume of 50 mM HCl, matching the volume of 50 mM NaOH used, was then added to neutralize the solution before it was used in subsequent experiments

3.2.9 Fluorescent labelling of dimAβ

Maleimide functional groups selectively react with thiol (-SH) groups under physiological conditions, enabling site-specific covalent labelling of cysteine (Cys) containing proteins. For that a cysteine variant of dimAβ was expressed and purified. Cys-dimAβ provides a free thiol that undergoes a Michael addition reaction with maleimide fluorophore, forming a stable thioether linkage. This reaction is typically performed at neutral to slightly basic pH (6.5-7.5), where the thiol remains nucleophilic and maleimide reactivity toward amines is minimized, ensuring specificity for cysteine.

For the fluorescently labelling dimAβ, a variant with a cysteine at position 0 was conjugated with Alexa 488-maleimide by first resuspending in a small volume of 50 mM NaOH before diluting into 1 mM DTT, 300 mM HEPES, pH 7, and adding the same volume of 50 mM HCl. Thereafter, the Alexa 488-maleimide was added and left to react for 30 min at room temperature before purification by RP-HPLC. The fractions that showed coincident signals for both Alexa 488 and the dimAβ were collected and lyophilised (Fig 6.2 A). The lyophilised aliquots were dissolved in buffer as similar to unlabelled dimAβ and were analysed by SDS-PAGE using a pre-stained protein ladder. Prior to loading, the samples were mixed with Laemmli buffer lacking bromophenol blue to avoid interference with fluorescent detection. Following electrophoresis, the gel was imaged directly without Coomassie staining and imaged in both the standard channel and the Alexa 488 fluorescence channel (Fig 6.2 B).

Alexa488 is a green, fluorescent dye with an excitation maximum around 495 nm and an emission maximum near 519 nm. Selection of fluorophores for tau and dimAβ ensured no overlap of excitation and emission maxima of the different fluorophores (Fig 6.3).

3.2.10 Preparation of dimAβ oligomers

DimAβ was initially resuspended in a small volume of 50 mM NaOH, followed by the addition of the appropriate buffer. The pH was then adjusted by titration with an equal volume of 50 mM HCl. The stock solution prepared at higher concentrations (50-60 μM), was subsequently diluted to the desired concentration and incubated at 37 °C for 3-4 h. Oligomerization was confirmed by AFM imaging before experiments.

3.2.11 Turbidity measurements

Turbidity measurements of protein solutions were conducted using UV-Vis spectroscopy on a Spectrophotometer V-650 (Jasco) equipped with QS High Precision Cell cuvettes (Hellma Analytics). Spectra were recorded using 90-100 µL of sample solution over a wavelength range of 450-300 nm, with a scan speed of 200 nm/min and a bandwidth of 1.0 nm in continuous scan mode. A control solution containing all components except the protein was measured first to establish a baseline. The corresponding protein sample was then analysed under identical conditions. Following each measurement, the cuvette was thoroughly rinsed with deionized water, washed with isopropanol and air-dried to prevent cross-contamination.

3.2.12 DLS measurements

DLS was performed on a submicron particle sizer, Nicomp 380 (Particle Sizing Systems Nicomp). Data was analysed with the Nicomp algorithm using the intensity-weighted Gaussian distribution analysis. The sample was measured for 3 repeated cycles, and the average distribution was generated. For samples containing 10% of PEG 6000, a refractive index of 1.33 and viscosity of 2.5 cp was considered. 100-120 µl of each protein sample were prepared for measurement.

3.2.13 DIC microscopy

DIC imaging of condensates and aggregates was performed using a Leica Infinity TIRF microscope operated in DIC mode via Leica LAS AF software. For imaging, 6 µl of each sample was placed onto a 60 × 24 mm glass coverslip and overlaid with a 20 × 20 mm coverslip. Images were acquired using a Leica HCX PL APO 100×/1.47 NA oil immersion objective. Image analysis and processing were carried out using FIJI software (ImageJ, version 1.54f).

3.2.14 Confocal microscopy

Confocal microscopy was performed on a Leica AF6000LX inverted microscope equipped with a Hamamatsu C9100-02-LNK00 EM CCD camera. For imaging, 6 µl of each sample was placed onto a 60 × 24 mm glass coverslip and overlaid with a 20 × 20 mm coverslip. Image analysis and processing were carried out using FIJI software (ImageJ, version 1.54f).

3.2.15 Fluorescence recovery after photobleaching (FRAP)

FRAP experiments were done on *in vitro* droplets formed by tau-Alexa647: tau (mixed in the ratio 1:60) with Alexa 488-Cys0-dimAβ: dimAβ (mixed in the ratio 1:20) using 640 nm and 488 nm laser line, respectively, imaged on an Olympus FV3000 microscope with a 60x UPLSAPO

water immersion objective. To minimize photobleaching during acquisition, low laser transmission settings were used. For every droplet of interest (diameter approx. 3 µm) pre-bleach frames (1 s frame rate, 20 frames) were recorded, followed by bleaching a spot on the droplet (tornado ROI;1s) at 100% transmission in the respective laser lines, and post-bleach images were collected (1 s frame rate, 380 frames). For every experiment all the parameters were conserved and the mean fluorescence intensities of three regions, namely ROI1 = photobleached region inside a droplet, ROI2 = the whole droplet of interest, and ROI3 = background signal outside the droplet, were recorded. The recovery curves were corrected for background and fluorescence loss and normalized with easy FRAP (440), and the resulting data was analysed in Origin (Microcal) following the exponential growth model $A\left(1 - e^{-kx}\right)$.

3.2.16 Electrostatic and hydrophobic screening

To study the contribution of electrostatic interactions, the effect of increasing ionic strength on condensate stability was evaluated by adding sodium chloride (NaCl) at concentrations ranging from 0 to 250 mM. 10 µM tau and 4 µM dimAβOs were co-incubated in the presence or absence of crowding agent with the respective NaCl concentration. The prepared samples were incubated at 37 °C for approximately 5 minutes to reach equilibrium, after which turbidity was measured at 400 nm using a Jasco UV–Visible spectrophotometer. Hydrophobic interactions were probed using 1,6-hexanediol (1,6-HD), an aliphatic alcohol known to disrupt weak hydrophobic contacts. Condensate samples were treated with 1,6-HD at final concentrations ranging from 0 to 5 % (v/v). The sample preparation and turbidity measurements followed the same procedure as with the NaCl screening.

3.2.17 Thioflavin-T (ThT) aggregation kinetics

For ThT assays, ThT, NaN_3, NaCl, and the protein samples were combined in a MOPS/Tris buffer mixture at pH 7.4 to obtain the desired protein concentration along with 20 mM ThT, 0.05% NaN_3, and 150 mM NaCl in a total volume of 100 µL. The measurement was performed in a 96-well low-binding plate (Greiner) in a BMG FluoStar Omega reader at 37°C and under quiescent conditions. Data points were collected every 5 min using the BMG Reader Control software (version 5.40). To calculate the half-time of oligomerization, the time values are placed in one column and the corresponding signal data in the next. The maximum signal is identified, and a half-level value is calculated as 50% of the rise from baseline to the peak. A helper column is then used to find the first point where the signal rises above this half-level. The half-time is obtained by linearly interpolating between the time and signal values just before and just after this crossing with the following formula.

$t_{1/2} = t_1 + y_{1/2} - y_1) (t_2 - t_1)/(y_2 - y_1)$

where:

$t_{½}$ = half-rise signal value

(t_1, y_1) = data point just before crossing half-rise signal value

(t_2, y_2) = data point just after crossing half-rise signal value

3.2.18 Preparation and fluorescent labelling of Aβ42 oligomers

Oligomers from native Aβ42 construct were prepared to study their interaction with tau. 1 mg aliquot of Aβ42 from BACHEM (CAS Number: 107761-42-2) was first dissolved in HFIP, aliquoted and lyophilised. After lyophilisation, each aliquot was first dissolved in 50 µl 50 mM NaOH and sonicated for 30 s in water bath. After dissolution, it was further added with 20 mM NaPi at pH 7.4, followed by 50 µl of HCl. For preparation of oligomers, 40 µM Aβ42 was incubated at 37°C for 2 hours and was used for experiments. For fluorescent labelling, 40 µM Aβ42 was added with Atto 488 Aβ40 in the ratio of 1:20 (labelled: unlabelled). The reaction mix was left for oligomerisation in dark for 2 hours.

3.2.19 Atomic Force Microscopy (AFM)

For observing dimAβ oligomers and fibrils and amorphous aggregates of tau and dimAβ, 3 µl of each respective sample were applied onto freshly cleaved muscovite mica. The samples were left to dry, washed with 500 µl ddH_2O, and dried with a stream of N_2 gas. Imaging was performed in intermittent contact mode (AC mode) in a JPK Nano Wizard 3 atomic force microscope (JPK) using a silicon cantilever with silicon tip (either Olympus OMCL-AC160TS-R3 with a typical tip radius of 9 ± 2 nm, a force constant of 26 N/m and resonance frequency around 250 kHz, or Olympus OMCL-AC240TS with a typical tip radius of 9 ± 2 nm, a force constant of 0.5-4.4 N/m and a resonance frequency around 65 kHz). The choice of tips was made solely for reasons of availability. The images were processed using JPK DP Data Processing Software (version spm-5.0.84). For the presented images, a polynomial fit was subtracted from each scan line first independently and then using limited data range.

3.3 Results

3.3.1 Purification of tau

Recombinant tau protein was successfully expressed in *E.coli* BL21 cells carrying the pET-28a vector. Following cell lysis and removal of debris by centrifugation, the soluble fraction containing tau (~45.7 kDa) was subjected to ammonium sulphate precipitation by the salting-out method. Due to its intrinsically disordered nature and high solubility, tau exhibits a relatively high threshold for precipitation compared to globular proteins. The gradual addition of ammonium sulphate increases the ionic strength of the solution, with salt ions competing for water molecules and thereby reducing solvent availability for maintaining the protein's hydration shell. After overnight incubation, pellet containing precipitated tau was collected by centrifugation, redissolved in water and dialyzed into the appropriate buffer for subsequent purification steps by a combination of chromatographic techniques, including IEC and SEC (Fig 3.1, Fig 3.2)

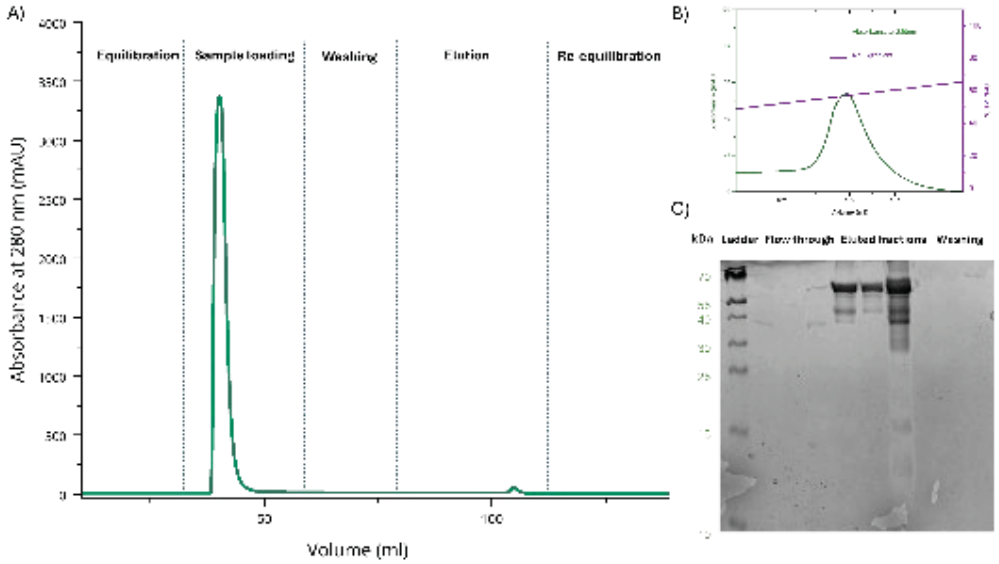

Fig 3.1: IEC purification of tau. A) B) Chromatogram implying IEC purification of tau. **C)** Gel denoting different fractions from IEC

Cation-exchange chromatography was used for tau purification. In cation-exchange chromatography, the resin is negatively charged, allowing proteins with an overall positive charge to bind through electrostatic interactions. At pH 6.5, tau carries a net positive charge and binds strongly to the cation-exchange matrix, while other contaminants with lower or opposite net charge bind weakly or not at all. By applying a NaCl gradient, salt ions compete with the protein for interaction with the resin. This disrupts the electrostatic interactions, causing proteins to elute according to the strength of their charge-based binding. Because tau has characteristic charge properties, it elutes at a defined salt concentration, enabling

its separation from other proteins. Fig 3.1 C shows SDS-PAGE analysis of eluted IEC fractions. The gel showed the protein band of tau (45.7 kDa) against the ladder band between 55 kDa and 70 kDa and this can be attributed to the intrinsic disordered nature of tau as well. IDPs have altered SDS binding and show an extended structure compared to globular proteins, resulting in altered electrophoretic mobility in SDS-PAGE. Additional lower molecular weight bands were also observed on the gel, suggesting presence of truncations. To further improve purity, SEC was performed. The chromatogram showed multiple peaks, with one dominant peak corresponding to tau (Fig 3.2 A). SDS-PAGE gel of these fractions corresponding to the dominant peak confirmed a highly enriched preparation of tau protein (Fig 3.2 B).

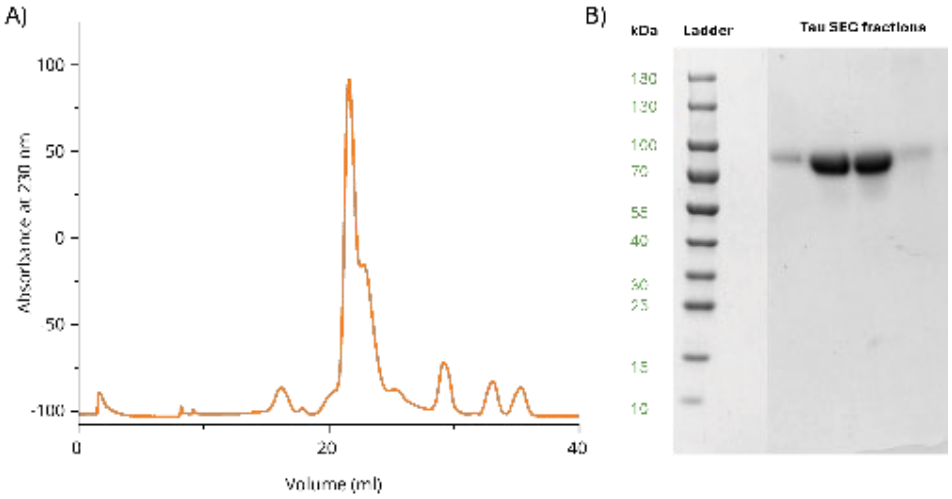

Fig 3.2: SEC purification of tau. A) SEC chromatography for tau purification. **B)** Gel showing the purified tau from SEC

3.3.2 Purification of dimAβ

Recombinant dimAβ was successfully expressed in *E.coli* BL21 cells carrying the pACYCDuet-1 vector. Following cell lysis and removal of debris by centrifugation, the soluble fraction containing dimAβ was subjected for further purification by IMAC.

IMAC exploits the affinity of histidine residues to divalent metal ions immobilized on the resin. The ZAβ3:dimAβ complex contains a His-tag, which enables selective binding to the Ni^{2+}charged HisTrap resin. Unbound and weakly associated proteins are removed during washing, while the target complex is retained through the affinity between histidine side chains and immobilized nickel ions. The ZAβ3:dimAβ bound complex is then eluted by increasing imidazole concentration which competes with histidine residues for Ni^{2+} binding (Fog 3.3 A) sites on the resin. The fractions were collected generously. For the further separation of ZAβ3:dimAβ, the complex was destabilised by TCEP and purification by RP-HPLC was followed. TCEP disrupts disulfide stabilization of the complex and HPLC resolves

ZAβ3:dimAβ into individual proteins of distinct peaks. The dimAβ fractions collected from HPLC were lyophilised for overnight and SDS-gel was formed with the fractions ensuring purity (Fig 3.3 B). Prior to the usage in experiments, to ensure the monomeric state of dimAβ the fractions were dissolved in HFIP and lyophilised again. SEC was performed optionally to confirm the monomeric state.

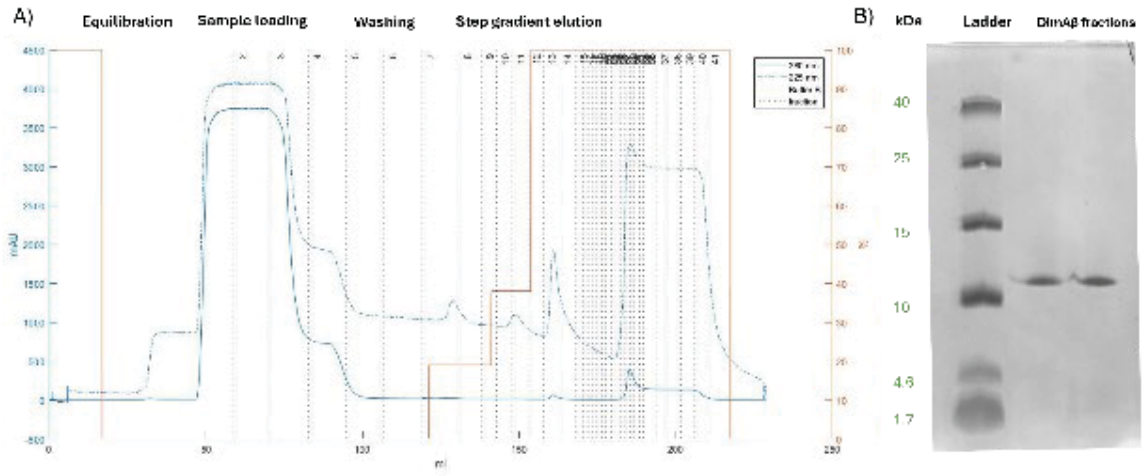

Fig 3.3: Purification of dimAβ. A) IMAC purification of dimAβ. **B)** SDS-PAGE indicating the purified dimAβ

3.3.3 Phase separation of tau

Tau was observed to undergo LLPS under crowding conditions. PEG acts as a crowding agent that mimics dense intracellular environment and lowers the energetic barrier for tau to self-associate into phase-separated droplets. The protein-rich droplets formed via LLPS scatter light, and this can be quantitatively monitored by turbidity measurements. Increase in absorbance, typically measured in the range of 400 nm-600 nm, reflect the extent of droplet formation and provide a simple, indirect and preliminary method to follow phase separation in solution. Upon incubation with increasing PEG, turbidity of 10 μM tau solutions were significantly enhanced (Fig 3.4 A). Microscopic analysis of high-turbid solutions of tau indicated the formation of protein-rich droplets in solution (Fig 3.4 B). These spherical droplets showed flowing like movements and fused upon contact into bigger droplets, supporting their liquid-like properties. The extent of droplet formation increased in response to increasing PEG concentration. Also, for 10 μM tau no droplet formation or turbidity was observed in the absence of PEG.

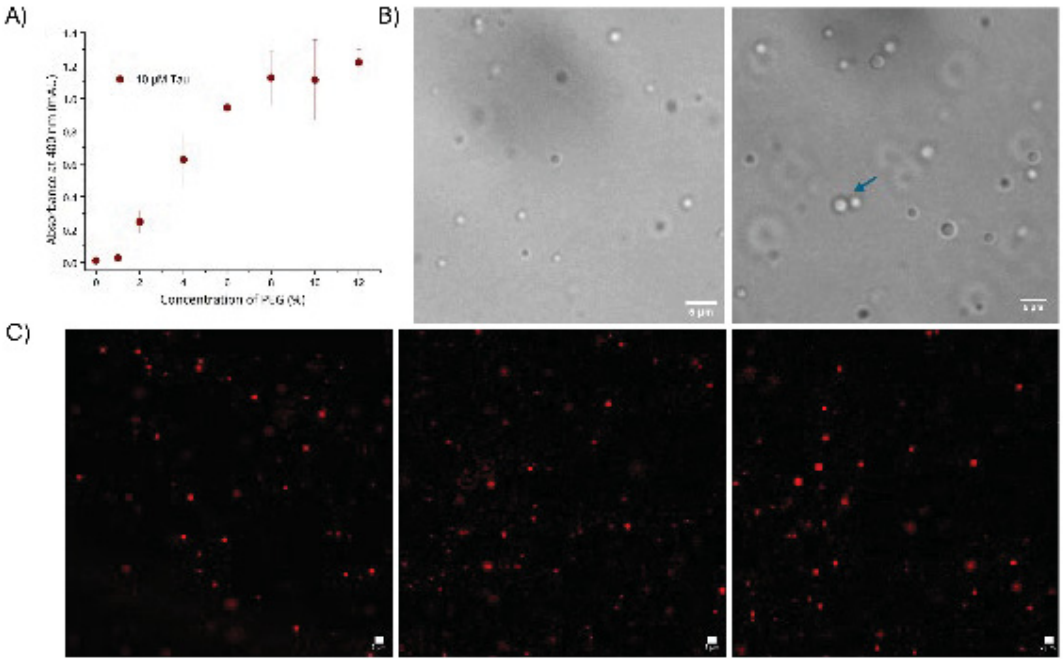

Fig 3.4: LLPS of tau. A) Turbidity of 10 µM tau in response to increasing PEG concentrations. Condensates of 10 µM tau with 10 % PEG, pH 7.4 was visualised in **B)** DIC (Scale bar 5 µm) and **C)** confocal microscopy (Scale bar 2 µm). Arrow mark indicating fusing nature of tau condensates.

Further to demonstrate that these droplets are enriched with tau protein, the PEG experiment was repeated with fluorescently labelled tau. Alexa 647 labelled tau was mixed with non-labelled tau in the ratio of 1:60 and incubated for 1-2 h. Further, the newly labelled tau was incubated with 10 % PEG and were analysed with confocal microscopy. Microscopy showed enrichment of tau in the droplets (Fig 3.4 C). A magnified view of the droplets showed a uniform of tau protein across the droplets, and they vary in their diameters in the range of several micrometres (Fig 3.5 A). These observations aligns with the previous studies that tau can self-associate into dynamic condensates under physiological-like conditions (90). This provides a basis for further investigation to the influence of dimAβ into phase separation behaviour of tau.

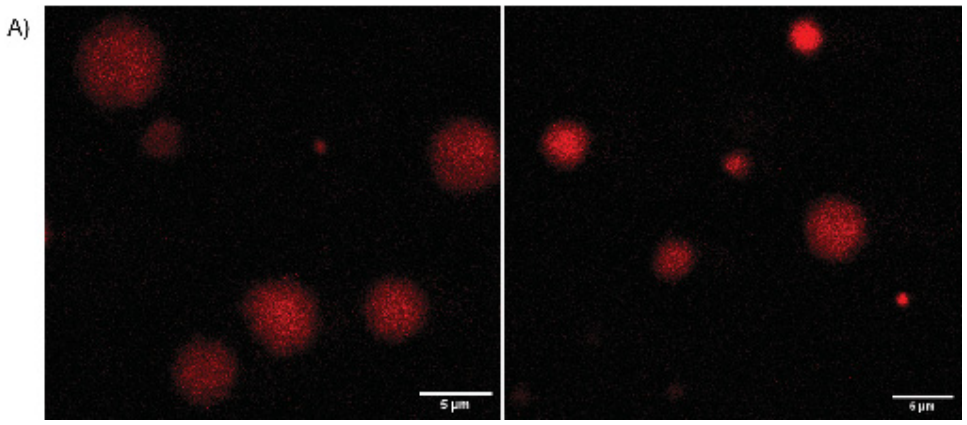

Fig 3.5: Droplets of tau. A) 10 µM tau shows a uniform distribution of protein across the droplet

3.3.4 Oligomers of dimAβ

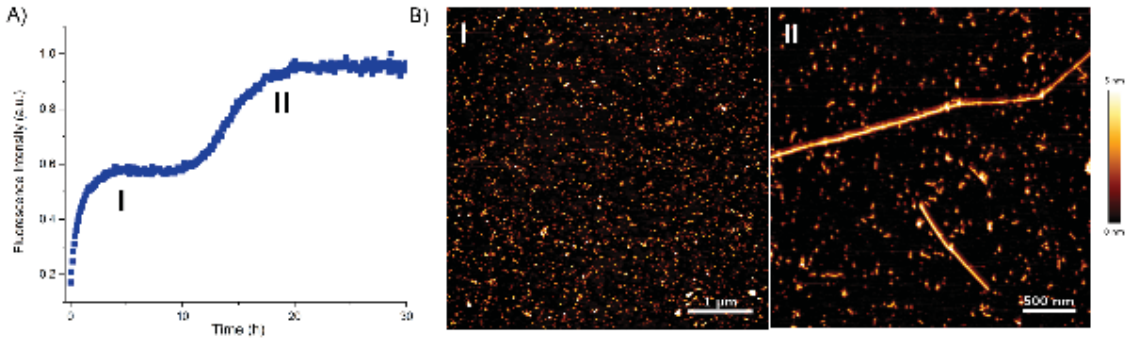

Fig 3.6: DimAβ kinetics and AFM. A) ThT assay depicts the biphasic kinetics of 10 μM dimAβ at pH 7.4 with an oligomer formation phase (I) followed by the replacement of oligomers with fibrils (II). **B)** AFM images corresponding to the two phases.

The characteristic biphasic kinetics of dimAβ was studied using a Thioflavin T (ThT) fluorescence assay (A). ThT is a widely used fluorescent dye for monitoring the aggregation of proteins, particularly in studies of oligomer and fibril formation (441). Upon binding to the β-sheet-rich structures that are characteristic of amyloid aggregates, ThT undergoes a conformational restriction that results in a substantial increase in fluorescence intensity, providing a quantitative and kinetic measure of amyloid formation. This makes ThT an invaluable tool for tracking the kinetics of Aβ oligomerization *in vitro*, enabling the assessment of aggregation rates, the effects of modulatory compounds and the characterization of intermediate species. In the biphasic kinetics of dimAβ, where the initial lag-free oligomeric phase (I) is followed by an amyloid fibril formation phase (II) (Fig 3.6 A). Off-pathway oligomers from dimAβ (hereafter referred to as dimAβOs) were isolated by incubating 10 μM dimAβ at pH 7.4 and 37°C in the absence of any mechanical agitation (e.g., as caused by the movement of a microplate in a fluorescence plate reader), which abrogates the amyloid fibril formation phase (169). The resulting dimAβOs were harvested after 3-4 hours of incubation and imaged by AFM (Fig 3.6 B) prior to their application in tau interaction experiments. In the course of our studies, to investigate the interaction with tau, dimAβ was labelled with Alexa 488 fluorophore. The cys0 variant of tau was labelled with Alexa 488-malemaide and was incubated with fresh unlabelled dimAβ in the ratio of 1:20 and was co-incubated for 1-2 h. ThT assays and AFM imaging of the labelled dimAβ were performed to ensure that the fluorophore did not affect the characteristic kinetics of dimAβ (Fig 3.7 A, B).

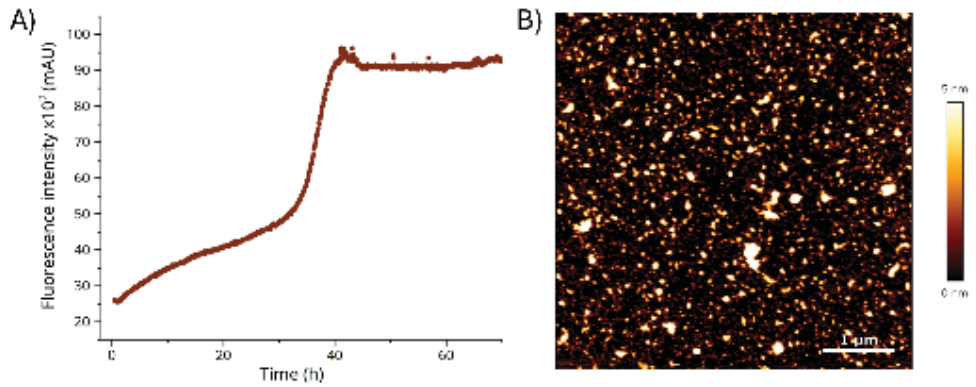

Fig 3.7: Alexa 488 dimAβ. 2 µM of Alexa 488 labelled dimAβ showing the characteristic biphasic **A)** ThT kinetics and the **B)** AFM image of oligomers formed.

3.3.5 Turbidity measurements and DIC imaging of tau-dimAβOs under LLPS conditions

Turbidity serves as a rapid and quantitative method for monitoring condensation in phase-separating systems and is commonly used as a complementary readout to microscopy. To investigate the interaction between tau and dimAβOs, tau was incubated with varying concentrations of dimAβOs and PEG, and the turbidity of the resulting solutions was measured (Fig 3.8 A). The presence of dimAβOs led to a higher turbidity of tau solutions and notably, samples containing the highest concentrations of dimAβOs exhibited the greatest turbidity across nearly all PEG concentrations tested. This observation suggests the presence of droplets in these samples and a potential increase in either the number or the size of condensates. However, further complementary experiments would be required to confirm this interpretation.

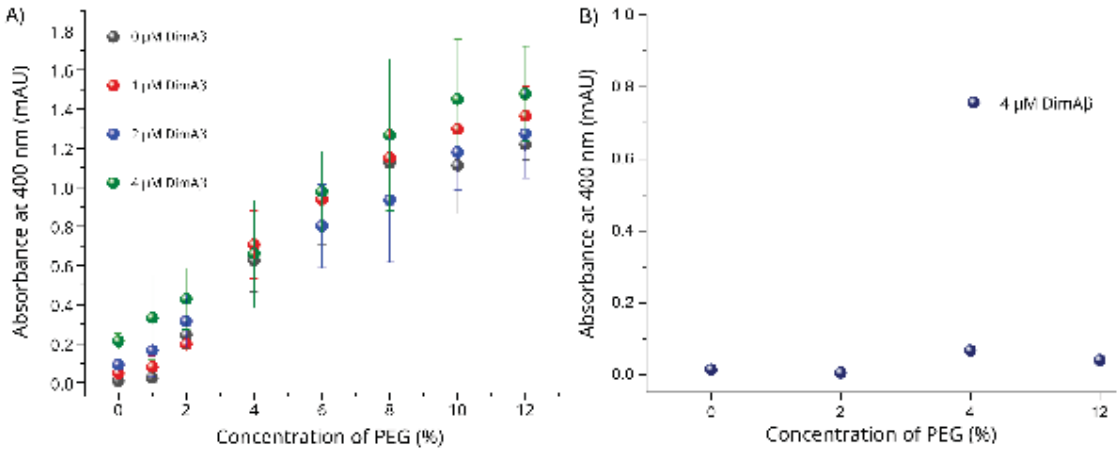

Fig 3.8: Turbidity measurements. A) Turbidity of 10 µM tau titrated with varying concentrations of dimAβOs (0-4 µM) and PEG (0-12%). **B)** Turbidity of 4 µM dimAβ in the presence of different concentrations of PEG.

PEG induced macromolecular crowding did not exert any measurable effect on dimAβOs when tested alone (Fig 3.8 B). The turbidity of dimAβOs-only solutions remained consistently close to the baseline control values with increasing PEG concentrations, indicating an absence of phase separation under these conditions.

Since an increased turbidity can arise not only from phase separation but also from the formation of nonspecific amorphous aggregates, it was important to determine whether the turbidity in tau-dimAβOs-PEG samples resulted from condensate formation. Interestingly, the evaluation of these samples with DIC microscopy showed a clear formation of condensates (Fig 3.9 A, B). These condensates were morphologically similar to those formed by tau alone, raising questions regarding the localization, partitioning behaviour and potential functional influence of dimAβOs within the condensates.

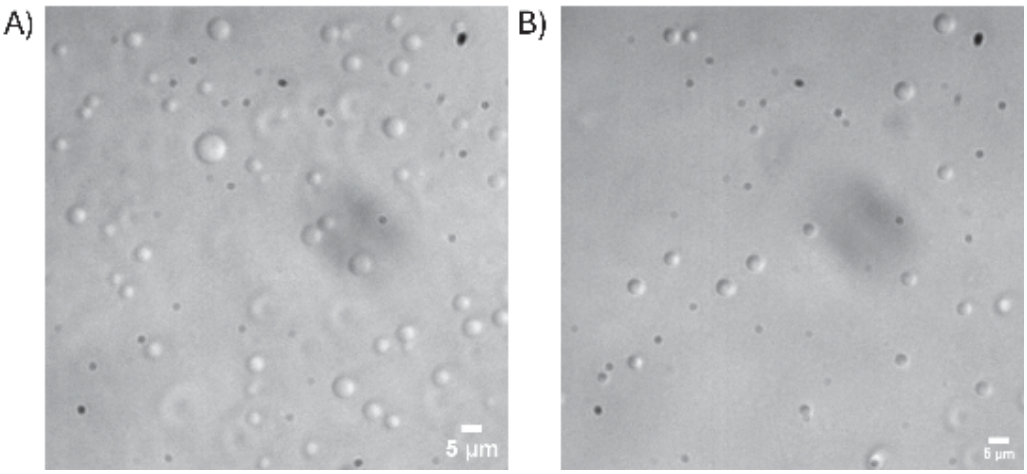

Fig 3.9: Tau-dimAβOs interaction. A) 10 µM tau LLPS **B)** 10 µM tau and 4 µM dimAβOs LLPS.

3.3.6 Co-phase separation of tau and dimAβOs

Following the observation of condensates upon incubation of tau and dimAβOs in the presence of PEG, we investigated the spatial localization of dimAβOs within these assemblies using fluorescently labelled proteins. Tau was labelled with Alexa 647, and dimAβOs were labelled with Alexa 488 to perform specific detection. Fluorescence microscopy revealed that, upon excitation at ~495 nm and ~650 nm for Alexa 488 and Alexa 647 respectively, both fluorescent signals co-localized with the condensates visualized in DIC mode (Fig 3.10 A, B, C, D). DimAβOs were found to preferentially partition into all tau

condensates, indicating a strong molecular association between tau and dimAβOs within these phase-separated assemblies.

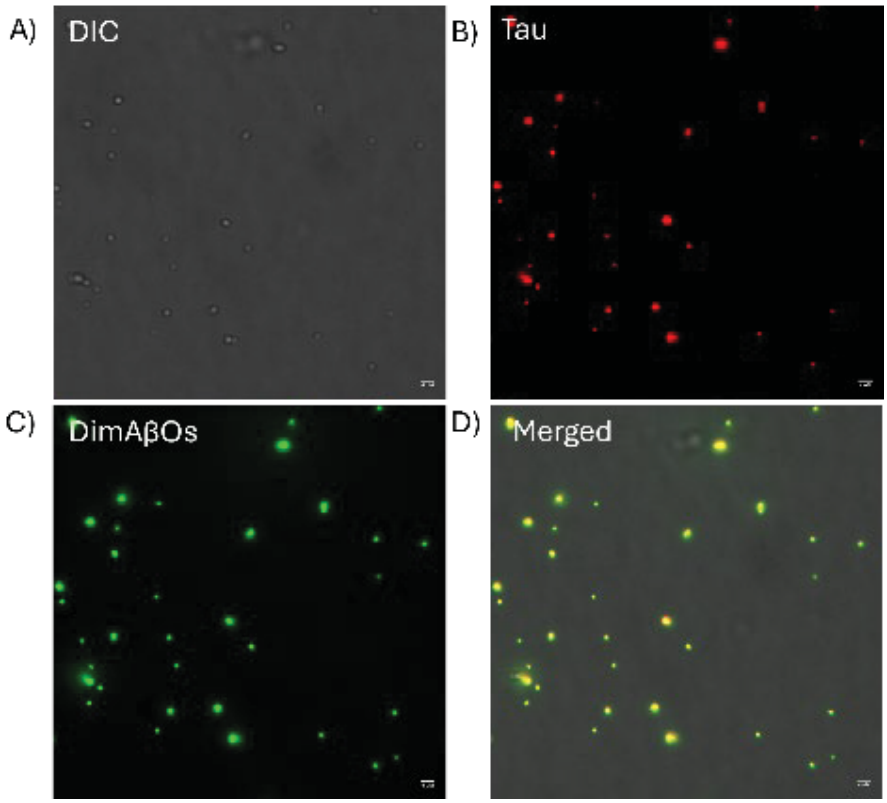

Fig 3.10: Colocalization of tau and dimAβOs. 10 μM tau and 4 μM dimAβOs when mixed under crowding conditions colocalise within the condensates of tau. **A)** DIC microscopy of the co-condensates. **B)** Alexa-644 labelled tau condensates. **C)** Alexa-488 labelled dimAβOs co-localised with tau. D) Overlay of all the channels.

3.3.7 Multiphasic co-condensates of tau and dimAβ

High-resolution confocal imaging of the condensates revealed a striking multiphasic organization of dimAβOs within tau droplets (Fig 3.11). Specifically, dimAβOs displayed a “phase-in-phase” distribution, forming discrete accumulations inside the droplets, while tau remained uniformly distributed throughout the condensates. Interestingly, not all tau condensates contained nests of dimAβOs, and their occurrence appeared heterogeneous in size, shape and number across the droplet population (Fig 3.12).

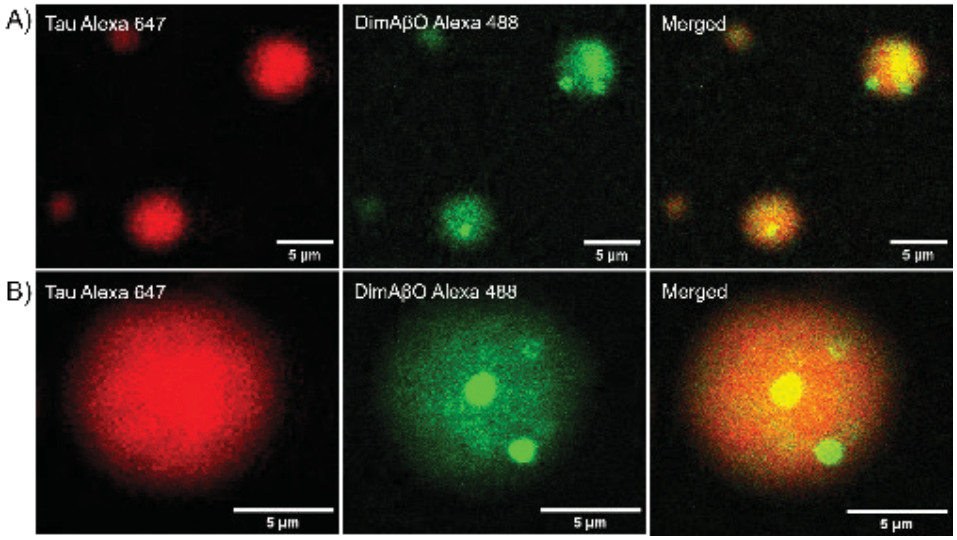

Fig 3.11: Tau-dimAβOs co-condensates. A) Incubation of 10 µM of tau with 4 µM of dimAβOs in presence of 10 % PEG 6000 resulted in formation of colocalized droplets within minutes of mixing. **B)** Magnified view revealing multiphasic organisation within the condensates.

The dimAβOs nests were observed both at the periphery and at the centre of tau condensates (Fig 3.11, Fig 3.12). Most nests exhibited a spherical morphology, resembling smaller condensates within the larger tau droplets, while others displayed irregular or amorphous shapes (Fig. 3.12). Importantly, this multiphasic organization was not observed in homotypic condensates of tau, indicating that the formation of dimAβO nests is a specific feature of tau-dimAβO condensates.

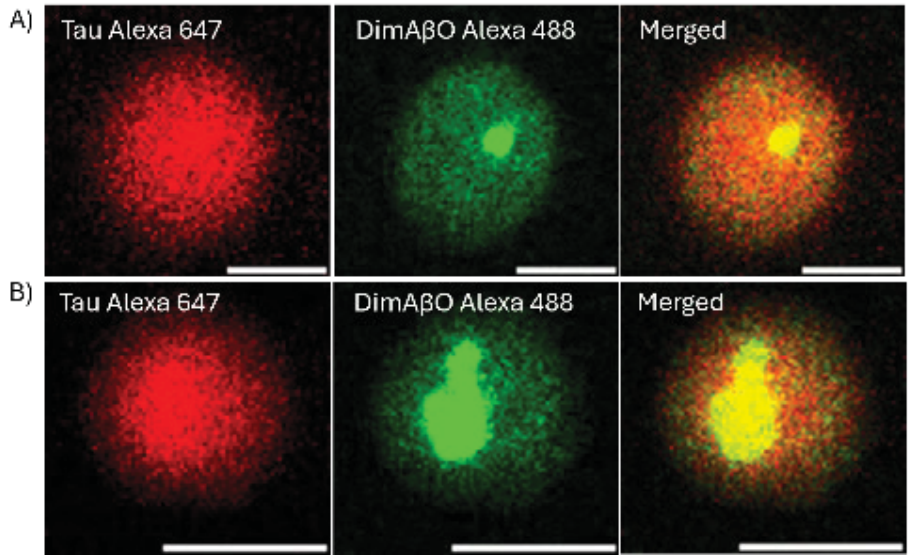

Fig 3.12: Multiphasic organisation of dimAβO. A) B) DimAβOs form distinct concentrated AβO nests in the condensates. The shape and number of dimAβOs nests on tau condensates varied across droplets. Scale bar: 5 µm

3.3.8 Particle size measurement of tau-dimAβOs co-condensates

Further characterization of tau-dimAβOs condensates was performed using DLS. DLS measures fluctuations in scattered light intensity arising from Brownian motion of molecules in the solution, providing insights into the size distribution and heterogeneity among between different protein states. We analysed the particle sizes of tau monomers, dimAβ monomers, dimAβOs, tau condensates and tau-dimAβOs condensates.

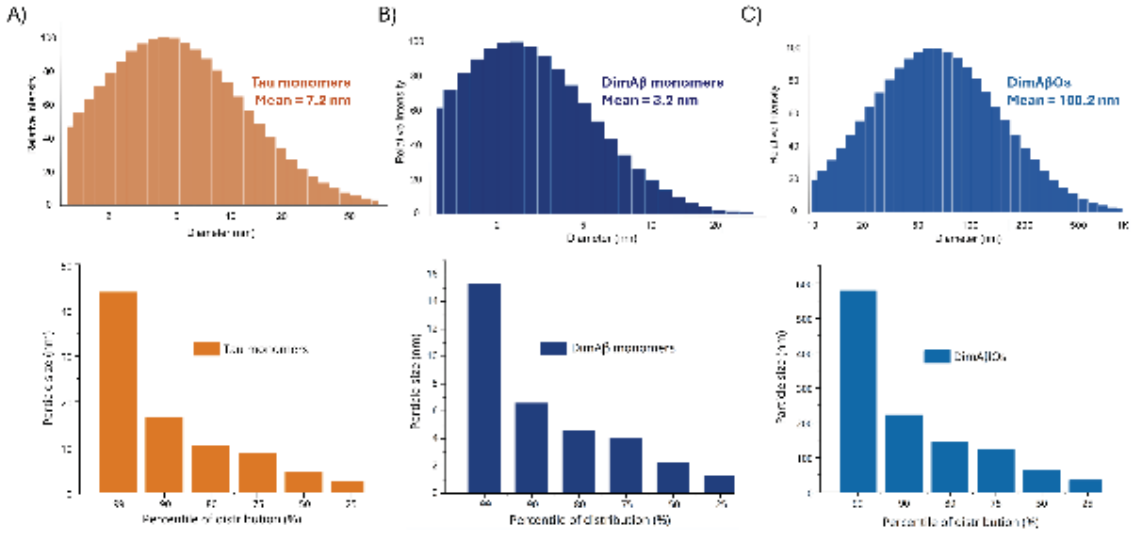

Fig 3.13: Particle size distribution and percentile distribution. DLS measurement of **A)** 10 μM tau, **B)** 4μM dimAβ monomers and **C)** 4μM dimAβ oligomers

Tau monomers showed a particle distribution ranging from 1 nm to 50 nm with a mean diameter of 7.2 nm and 90 % of the tau species occurred within the range of approx. 18 nm (Fig 3.13 A). These values aligns with the theoretical reported values of tau monomers (332). While dimAβ monomers showed a particle distribution in the range of 1 nm to 20 nm, upon oligomerisation the particle size increased to the range of 10 nm to 1 μm (Fig 3.13 B, C). The mean hydrodynamic diameters of dimAβ monomers and dimAβOs were 3.2 nm and 100.2 nm respectively, consistent with AFM images and previous reported values (169). These control experiments also ruled out the presence of larger aggregates in these samples.

We next assessed the size distribution of tau condensates formed via LLPS. Tau droplets displayed a mean diameter of 2.3 μm, with particle sizes spanning from 500 nm to 10 μm (Fig 3.14 A). Percentile distribution show that most of the tau condensates occurred within 3.5 μm, in agreement with microscopic observations. When examining tau-dimAβOs condensates, the mean diameter increased to 3.2 μm, with 90 % of droplets distributed below approx. 5 μm (Fig 3.14 B). This represents approximately a 40 % increase in mean condensate size relative to tau alone. The enlargement of droplets in the presence of

dimAβOs is consistent with their partitioning into tau condensates and correlates with the turbidity increase observed in the tau-dimAβOs samples.

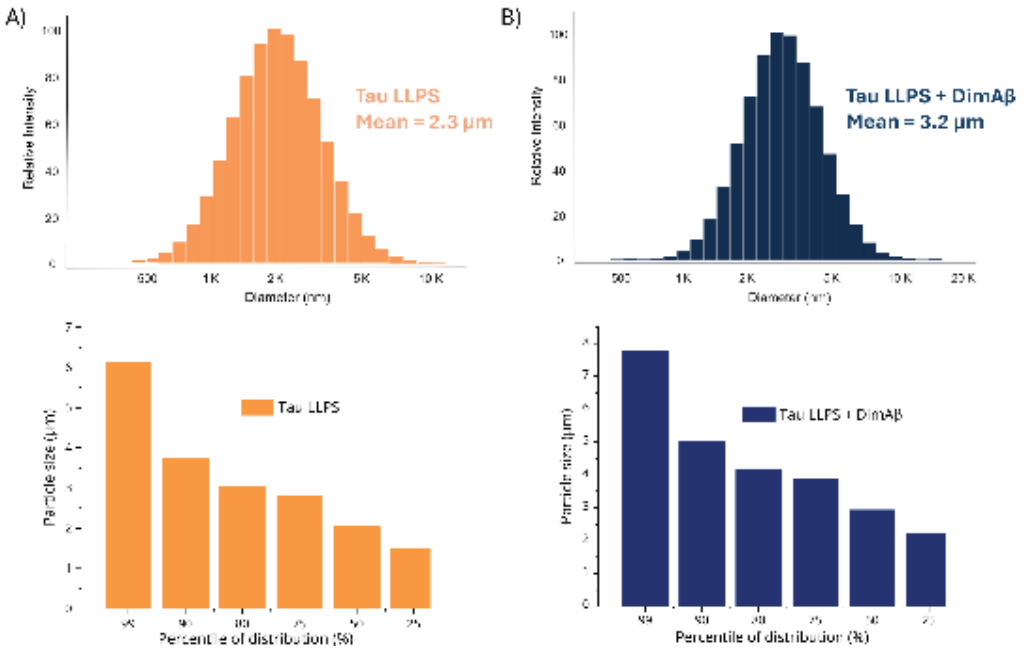

Fig 3.14: Particle size distribution and percentile distribution. DLS measurement of **A)** 10 µM tau + 10 % PEG, **B)**10 µM tau + 10 % PEG + 4µM dimAβOs

3.3.9 Electrostatic and hydrophobic screening of tau-dimAβOs condensates

Phase separation studies widely employ NaCl to study the role of electrostatic interactions in stabilising condensates formed through LLPS (102). NaCl disrupts electrostatic interactions by shielding opposing charges present on protein surfaces, thereby weakening the forces drive condensate formation. As salt concentration increases, Na^+ and Cl^- ions neutralize charged groups, disrupting the salt bridges and other electrostatic interactions, leading to the dissolution of assemblies stabilized by these forces. Like NaCl,1,6-hexanediol (1,6-HD) is also widely used to study the role of hydrophobic interactions (442). 1,6-HD is an amphiphilic alcohol that interferes with weak hydrophobic contacts between proteins. Increasing concentrations of 1,6-HD disrupts the surrounding water molecules stabilising the interactions and break short-ranged hydrophobic associations.

To investigate the roles of electrostatic and hydrophobic interactions, we incubated tau-dimAβOs condensates with increasing concentrations of NaCl and 1,6-HD and monitored the absorbance at 400 nm as the turbidity readout. Initially, the turbidity of tau-dimAβOs condensates did not show any response to 25 mM NaCl but showed a drop at 50 mM NaCl and followed by a gradual decrease until 250 mM NaCl (Fig 3.15 A). In contrast, 1,6-HD treatment caused an initial reduction in turbidity at 1.25% (v/v), but no further decrease was observed at higher concentrations (Fig 3.15 B). These results suggests that tau-dimAβOs condensates are highly sensitive to ionic strength, indicating the importance of electrostatic interactions for their stability. On the other hand, the condensates were only moderately affected by increasing concentration of 1,6-HD, indicating that 1,6-HD can interfere with the weak hydrophobic contacts but does not dissolve the condensates.

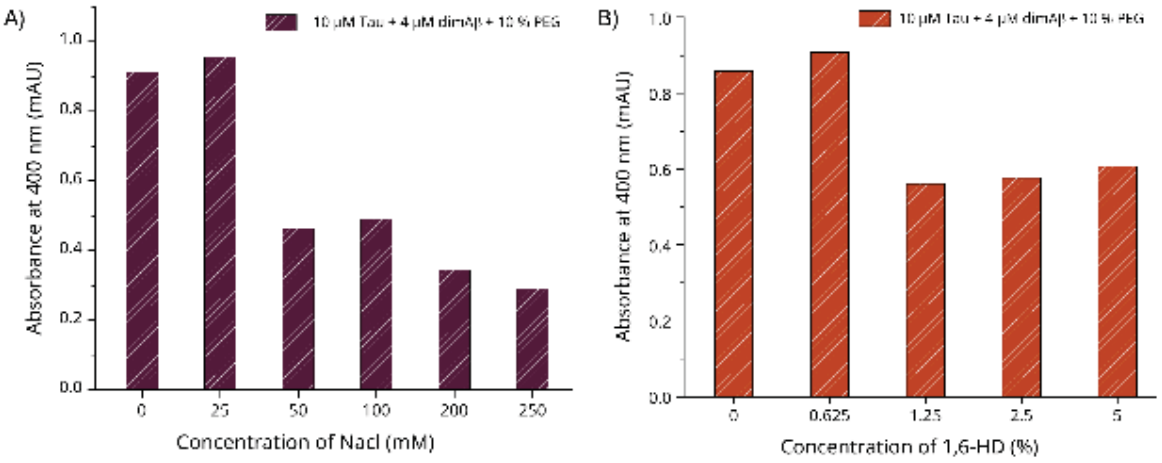

Fig 3.15: Electrostatic and hydrophobic screening of tau-dimAβOs condensates. Turbidity of co-incubated 10 μM tau and 4 μM dimAβOs in the presence of crowding agent and with increasing concentrations of **A)** NaCl and **B)** 1,6 HD.

3.3.10 FRAP assay of the co-localised droplets

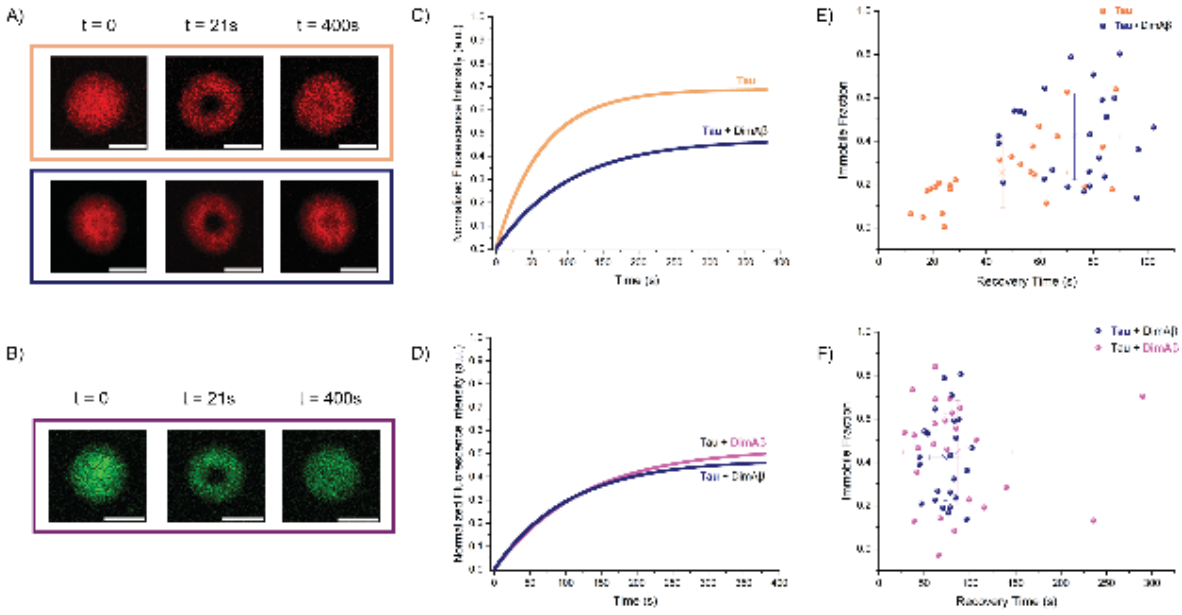

Fig 3.16: FRAP recovery experiment. A), B) Time series of images captured during FRAP experiments using a 640 nm and a 488 nm laser line, visualising tau **(A)** and dimAβOs **(B),** respectively. The experiments were performed at 10 µM tau and 4 µM dimAβOs in the presence of 10 % PEG. To determine the dynamics of the tau in the condensates, individual analysis of 25 independent experiments (n=25) was conducted. In each case, a region of interest (ROI), mostly central to the droplets was photobleached and fluorescence recovery was analysed to assess protein mobility. Scale bar: 5 µm. **C)** Recovery curves of tau in the condensates +/- dimAβOs, depicting the mean values for half time of recovery and mobile fraction of tau in the respective cases. **D)** Recovery curves depicting the mean of recovery of dimAβOs compared with the recovery of tau in the co-condensates. **E), F)** Individual half-recovery times and immobile fractions from each of the independent experiments.

FRAP is widely used to study the dynamic nature and molecular mobility within assemblies like aggregates or condensates (443). In this technique, a region of interest (ROI) is selected and uniformly bleached using a high-intensity laser, after which fluorescence recovery is monitored over time to quantify molecular diffusion or exchange rates. The extent and kinetics of recovery reflect the internal dynamics and degree of molecular mobility within the assembly.

We used FRAP to investigate the impact of dimAβOs on tau dynamics within colocalized condensates (Fig 3.16 A, C, E). FRAP experiments were performed on freshly prepared Alexa 647-labelled tau with 10% PEG, using the 640 nm laser line. 25 tau droplets each in the presence/absence of dimAβOs were measured over a time period of 400 s and were subsequently analysed and compared. The results revealed a wide distribution of recovery times and immobile fractions for tau in the condensates. In the absence of dimAβOs, tau condensates showed a mean recovery half time and immobile fraction of 46 ± 24 s and 0.25

± 0.16 respectively, implying highly mobile, liquid-like dynamics for tau in the condensates. Upon addition of dimAβOs to the tau condensates, tau showed an increase in both the half time of recovery and the immobile fraction in the majority of the droplets. The recovery half time of 73 ± 17 s of tau in co-condensates indicated an increase by 58% to that of tau only droplets. Similarly, the immobile fraction of the condensates increased by 68% reaching 0.42 ± 0.20 with the inclusion of dimAβOs into tau condensates. These results demonstrate that dimAβOs influence the dynamics of tau in the condensates by increasing the half time of recovery and reducing the mobile fraction in the majority of the droplets, suggesting a decrease in the overall fluidity of the condensates. This shift toward a less dynamic state of tau indicates a pronounced effect of dimAβOs on the conformational behaviour of tau.

An attempt was made to explicitly study the mobility of dimAβOs in the condensates, both in the dimAβO-dense puncta and in droplets exhibiting homogeneously distributed dimAβOs. However, bleaching of the puncta was not possible due to their small size relative to the laser focus and due to their over-saturated fluorescence compared to the background. Hence to study the dynamics of dimAβOs, condensates without puncta were selected. Similar to the earlier FRAP experiment, 25 individual recovery curves were analysed separately to determine mean half time of recovery and the mobile dimAβO fraction in the co-droplets (Fig 3.16 B, D, F). This analysis yielded a mean half time of recovery of 86 ± 60 s and an immobile fraction of 0.44 ± 0.24. Compared to tau, the recovery of dimAβOs in the co-localised droplet showed a 18% higher recovery time and a 5% higher immobile fraction for dimAβOs (Fig 3.16 D, F). However, the distribution of dimAβO recovery times extended over a wider range, including high values up to 300 s. This hints at a heterogeneous population of different species and interactions of dimAβOs in the condensates. The individual half time and mobile fraction for each of the photobleaching experiments are listed in 6.5.

3.3.11 Aggregation kinetics of dimAβ within tau droplets

As discussed, dimAβOs, like AβOs, have neurotoxic properties (168,169,444) and given our observation that preformed dimAβOs interact with tau through co-condensation, we next examined whether tau influences the kinetics of monomeric dimAβ. As described earlier, dimAβ displays the characteristic biphasic assembly kinetics at a COC of ~1.5 μM with an initial off-pathway oligomer (dimAβOs) formation phase, followed by a second phase in which these dimAβOs are gradually replaced by amyloid fibrils (Fig 3.6) (169,179).

To assess whether tau affects this process, we monitored the aggregation kinetics of three different concentrations of dimAβ in the presence of tau under crowding conditions (Fig 3.17 A, B, C). Interestingly, the biphasic kinetics of dimAβ was inhibited at all the three

concentrations in the presence of tau, regardless of the crowding conditions. These findings suggest that upon sequestration of dimAβOs within tau condensates, their progression toward fibril formation is inhibited. Thus, dimAβOs remain stabilized as oligomeric species within tau droplets, with tau condensates effectively serving as a reservoir for AβOs. Importantly, PEG alone did not hamper the continued aggregation of dimAβOs, but in the presence of PEG, the half-time for oligomer formation was several hours shorter compared with the combined presence of tau and PEG (Fig 3.17 D). This observation suggests that PEG accelerates dimAβ aggregation into fibrils through macromolecular crowding, whereas tau counteracts this effect by trapping oligomers and preventing their continued kinetics.

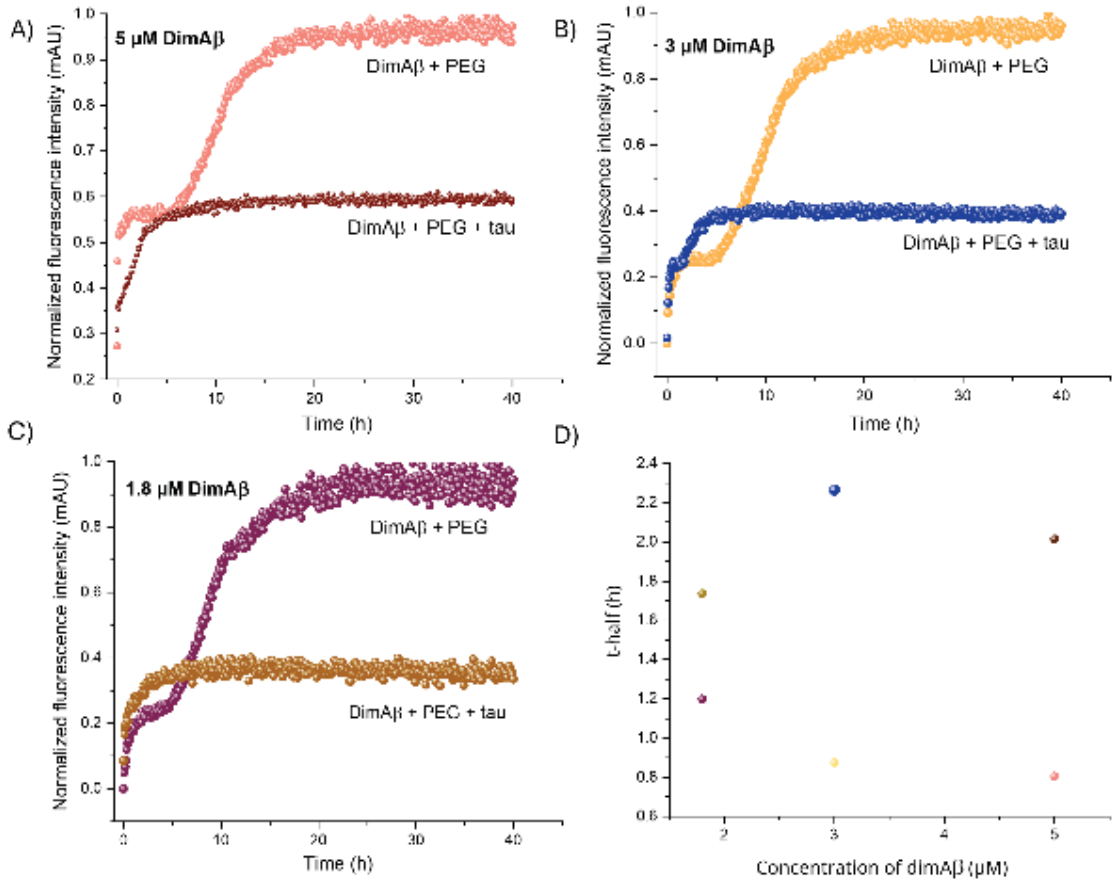

Fig 3.17: Aggregation kinetics of dimAβ in the presence of tau. ThT kinetic profiles of **A)** 5 µM, **B)** 3 µM and **C)** 1.8 µM of dimAβ in the presence and absence of tau under crowding conditions. **D)** Half-time of oligomerisation was calculated for each of the curves.

3.3.12 Interaction of Aβ42 oligomers with tau under crowding conditions

To further validate the results of colocalization of dimAβOs with tau, oligomers derived from native Aβ42 construct was prepared and their interaction with tau was studied. Interestingly, we observed a colocalization of Aβ42Os with tau (Fig 3.18). However, this colocalization under crowding conditions was not only as condensates but also in the form of amorphous aggregates. Although the co-condensates retained dynamic properties, both the size and number of droplets were substantially reduced. Similar to dimAβOs, Aβ42Os displayed an uneven distribution within tau condensates, suggesting a multiphasic internal organization. The co-existence of amorphous aggregates with condensates implies that, unlike dimAβOs, Aβ42Os may exhibit greater conformational heterogeneity, leading to sub-populations in which some species partition into condensates while others misassemble into co-aggregates.

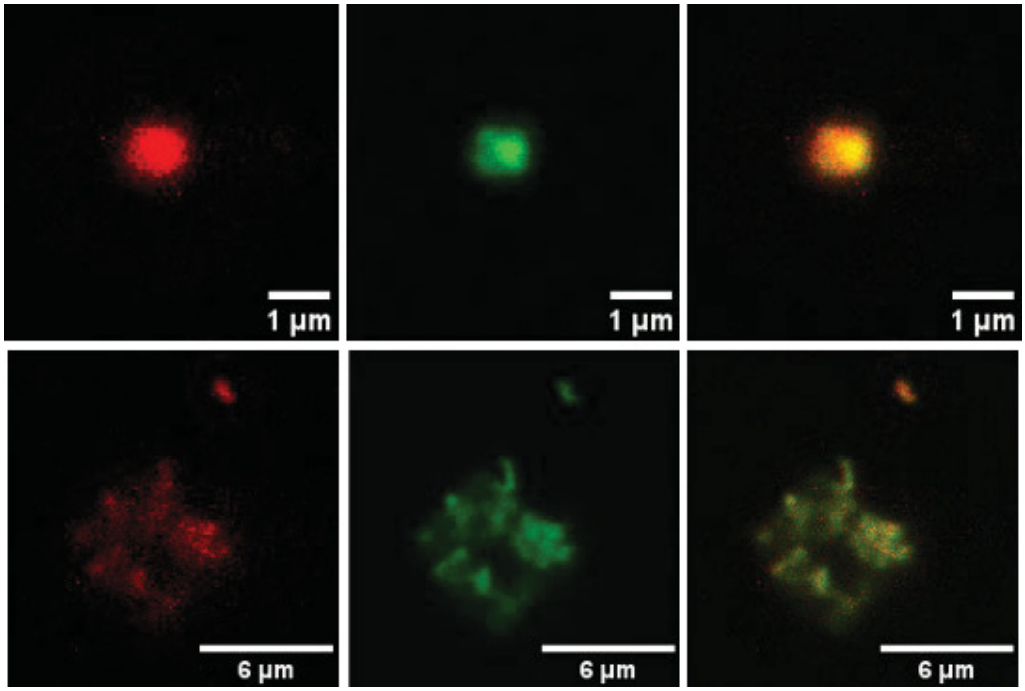

Fig 3.18: Interaction of tau with Aβ42 oligomers. 10 µM tau co-localised with 4 µM Aβ42Os in the presence of 10 % PEG in the form of both condensates and amorphous aggregates.

Chapter 4 : Tau-Aβ interaction under non-LLPS conditions

Manuscript Information

Title: Liquid-liquid phase-separated tau colocalizes with and stabilizes Aβ oligomers
Authors: Tina Jacob, Marie Schützmann and Wolfgang Hoyer

Journal: Nature Communications

Status: Under revision (September 2025)

Contributions: Transformation, expression, purification, FRAP assays, fluorescent labelling, ThT kinetics, TIRF microscopy, DLS, turbidity assays, AFM, cell toxicity assays, preparation of figures, writing and reviewing of the manuscript.

This chapter includes sections from the manuscript that describe the interaction between tau and AβOs under non-LLPS conditions. It has been further expanded to include the interaction of tau with monomeric dimAβ, along with additional experimental data and techniques that were employed to provide a more comprehensive understanding of these interactions under non-LLPS conditions.

4.1 Aim of the study

This chapter study interaction of tau and AβOs under non-LLPS conditions. The non-LLPS condition highlights their association in soluble environments and without crowding agents. The study aims to provide a framework for understanding how these interactions could initiate in physiologically relevant, non-phase-separated contexts and how they could contribute to early aggregation events linked to AD pathology.

4.2 Materials and methods

The materials and methods described in Chapter 3 have been applied here as well, and only additional procedures specific to this chapter are detailed below.

4.2.1 Western blotting

Western blotting is widely used to detect proteins using antibodies and visualising them. It involves separating proteins using gel electrophoresis and transferring them to a membrane and then using specific antibodies to detect the target protein (445). For performing the western blot, the tau-dimAβOs sample was incubated for 10 minutes and were centrifuged. The pellet hence obtained was dissolved in tris-buffer pH 7.4. The pellets and supernatants from each sample were performed on a tris-glycine SDS-PAGE gel. After the completion of the electrophoresis, protein transfer was performed. For that, six sheets of filter paper were pre-equilibrated in Towbin transfer buffer, and a polyvinylidene difluoride (PVDF) membrane of identical size was activated in ethanol for 2-3 minutes. The transfer stack was assembled in the following order: three sheets of moistened filter paper, the gel, the activated PVDF membrane, and three additional sheets of filter paper. Protein transfer was carried out using a standard Bio-Rad wet transfer system for 30 minutes. Following transfer, the membrane was blocked for 1 hour at room temperature in 5% (w/v) non-fat dry milk prepared in Tris-buffered saline containing 0.1% Tween-20 (TBST). The membrane was briefly rinsed in TBST (1-2 times) and then incubated overnight at 4 °C with the 4G8 primary antibody (1:1000 dilution in TBST). The following day, the membrane was washed three times with TBST, 10 minutes per wash, and subsequently incubated with a goat anti-mouse horseradish peroxidase (HRP)-conjugated secondary antibody (1:5000 dilution in TBST) for 1 hour at room temperature. After incubation with the secondary antibody, the membrane was washed three additional times with TBST for 10 minutes each. For signal detection, the HRP substrate solution was prepared by mixing equal volumes of luminol enhancer and peroxide solutions (500 µL each; Thermo Fisher Scientific). The membrane was incubated with the substrate mixture for 3-5 minutes in the dark and chemiluminescent signals were visualized using the ChemiDoc MP Imaging System (Bio-Rad).

4.2.2 LDH assay

LDH assay was performed in SH-SY5Y human neuroblastoma cells that were maintained under standard culture conditions at 37 °C in a humidified incubator with 5% CO_2.

Passage 6 (P6) SH-SY5Y cells were retrieved from −80 °C storage and thawed at the water bath for 2-3 min. The growth medium was prepared by supplementing fresh Dulbecco's Modified Eagle Medium/Nutrient Mixture F-12 (DMEM/F-12) with 10% fetal bovine serum (FBS), 1% non-essential amino acids (NEAA), and 1% Penicillin-Streptomycin. Approximately 10-12 mL of this medium was added to a culture dish, and the thawed cell suspension was gently transferred into the dish. The plate was gently swirled to ensure even distribution of the cells and then placed in the incubator at 37 °C for continued growth.

Once the cells have reached the desired confluency (80-90%), cells were split into desired experimental set-up. For splitting, the old medium was carefully aspirated from the culture dish, and the dish was rinsed with 5 ml of no Ca^{2+}, no Mg^{2+} Dulbecco's phosphate-buffered saline (PBS), to remove any residual FBS that could inhibit trypsin activity. The DPBS is then carefully aspirated. Then 1 ml of trypsin-EDTA (Gibco™ Trypsin-EDTA (0,25%)) is added to the dish and placed the dish back into the incubator for 2-3 minutes. The trypsination leads to the detachment of the cells from the dish surface. Further 5 ml of the growth medium was added and was thoroughly mixed 2-3 by releasing the cells at 90° angle. 500 µl of the cells in the medium was then transferred to cell counter tube and the cells were counted using cell counter. A 96-well plate was used for LDH assay and experiments were performed in a volume of 100 µl. Each well in a 96-well plate has a surface area of ~0.32 cm^2 and 4,200 cells per well were plated for the assay. The plated wells were grown for another 24 hours and then each of the conditions were introduced onto the cells in each well. After 48 h, 50 µl from each of the conditions were transferred into a new 96 well plate. To this, 50 µl of reagent mix was added from CyQUANT™ LDH Cytotoxicity Assay Kit. The preparation of reagent mix involved addition of 11.4 mL of ddH2O to substrate mix, then mixed gently to dissolve. Combined the 600 µl of assay buffer stock solution with the 11.4 mL of substrate stock solution, then mixed gently and protect from light until use. After 30 minutes of incubation with the reagent mix, 50 µl of stop solution was added. The absorbance of each well was measured at 490 nm and 680 nm using Tecan Safire 2 multi-detection plate reader. For analysis of the measured data, each signal from 490 nm was subtracted with the baseline value from 680 nm. Each subtracted signal was then calculated for its fold-increase in comparison with the baseline value.

4.3 Results

4.3.1 Turbidity and DTT measurements

PEG is widely used as a crowding agent due to its water solubility, chemical inertness, and availability across a broad range of molecular weights, allowing control over crowding strength. However, recent studies have shown that PEG may also interact with biomolecules, influencing protein folding, enzymatic activity, and phase behaviour. PEG induced confinement effects, wrapping around protein surfaces, affect DNA replication and also influenced the aging of protein condensates (446–448). Given these negative impacts of using PEG, we investigated the interaction of tau and dimAβOs in the absence of crowding-free conditions

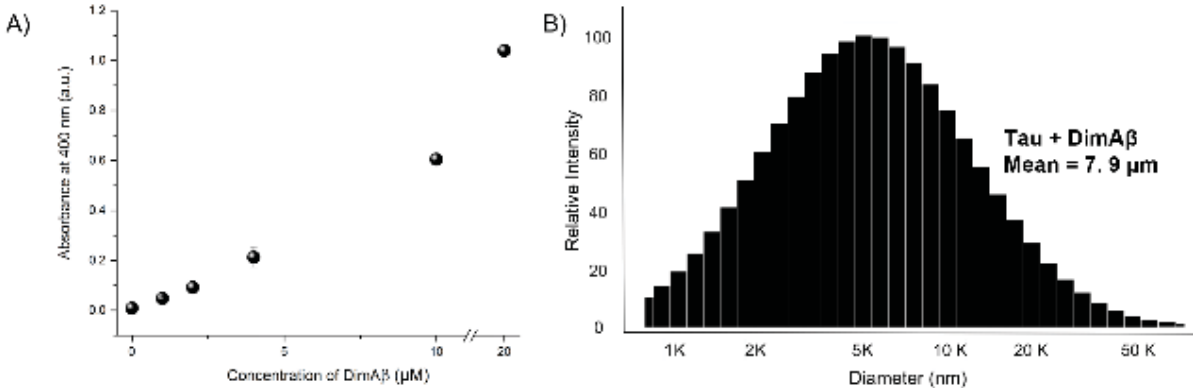

Fig 4.1: Turbidity and DLS measurements under non-LLPS conditions. A) Turbidity of 10 μM tau titrated with increasing dimAβO concentration. **B)** Particle size analysis of the protein mixtures by DLS.

To rapidly assess potential interactions, 10 μM tau was titrated with increasing concentrations of dimAβOs (0-20 μM), and turbidity of these mixtures was recorded. No significant change was observed up to 2 μM dimAβOs, but a gradual increase in turbidity began at 4 μM, reaching high turbidity values at 20 μM dimAβOs (Fig 4.1 A). This increase in turbidity suggests the formation of larger assemblies, likely condensates or aggregates formed by one or both proteins. This observation implies that tau and dimAβOs either promote structural transitions in each other or exhibit strong mutual affinity driving co-assembly. To further characterize these species, we analyzed a mixture containing 10 μM tau and 4 μM dimAβOs using DLS. The measurements revealed a broad range of particle sizes, from 1 μm to 50 μm, with an average diameter of 7.9 μm (Fig 4.1 B). Although typical condensates usually fall within 3-7 μm, the presence of larger particles could suggest fused droplets (449). Since DLS cannot definitively differentiate between condensates and aggregates, additional microscopic analysis was used to determine the nature of these assemblies.

4.3.2 Western blotting and DIC microscopy

A subsequent investigation into whether both tau and dimAβOs are associating together in these high-turbidity samples was performed using western blotting. Western blotting is a widely used technique to detect specific proteins within a complex mixture, allowing both qualitative and semi-quantitative assessment of protein detection and aggregation states. For western blot, proteins are initially separated by electrophoresis based on molecular weight and are transferred onto a membrane, followed by their probing with specific antibodies to visualize target proteins.

We applied the western blotting to examine if molecular-weight distribution of dimAβOs shifted in the presence of tau. Although a similar approach was attempted for tau, tau displayed diffuse and ambiguous detection under the same gel conditions (data not shown). For western blot analysis, 10 μM of tau was incubated with dimAβOs in the ratio 1:1 (10 μM) and 1:2 (20 μM). Higher concentrations of dimAβOs were chosen to ensure confirmed detection with Aβ antibodies. The samples were incubated for 10-15 minutes and centrifuged thereafter. The supernatant was carefully removed from each of the samples and the pellet was dissolved in Tris buffer. Supernatants and the dissolved pellets were run on an 8% tris-glycine SDS-PAGE gel. The gel was then transferred to a PVDF membrane and was followed by detection with primary and secondary antibodies of Aβ. The resultant blot showed the bands for dimAβOs near 10 kDa in the supernatants (Fig 4.2 A). This could be due to the denaturation of higher-order assemblies of dimAβ into lower molecular weights dimers or monomers (450,451). In contrast, pellet fractions displayed Aβ signals at significantly higher molecular weights (Fig 4.2 A). This implies the formation higher order assemblies containing Aβ in the presence of tau and these assemblies were not easily degraded by SDS indicating a higher stability in these samples.

To further characterize these samples, we examined them using light microscopy. A mixture containing 10 μM tau and 4 μM dimAβOs was prepared and imaged using DIC microscopy. We observed the presence of large, irregular amorphous structures in these samples (Fig 4.2 B). These assemblies appeared substantially larger than typical condensates and exhibited undefined, heterogeneous morphologies. But they also showed some spherical structures that would match with condensates co-existing with these aggregates, but this would need a higher magnification imaging to draw definitive conclusions.

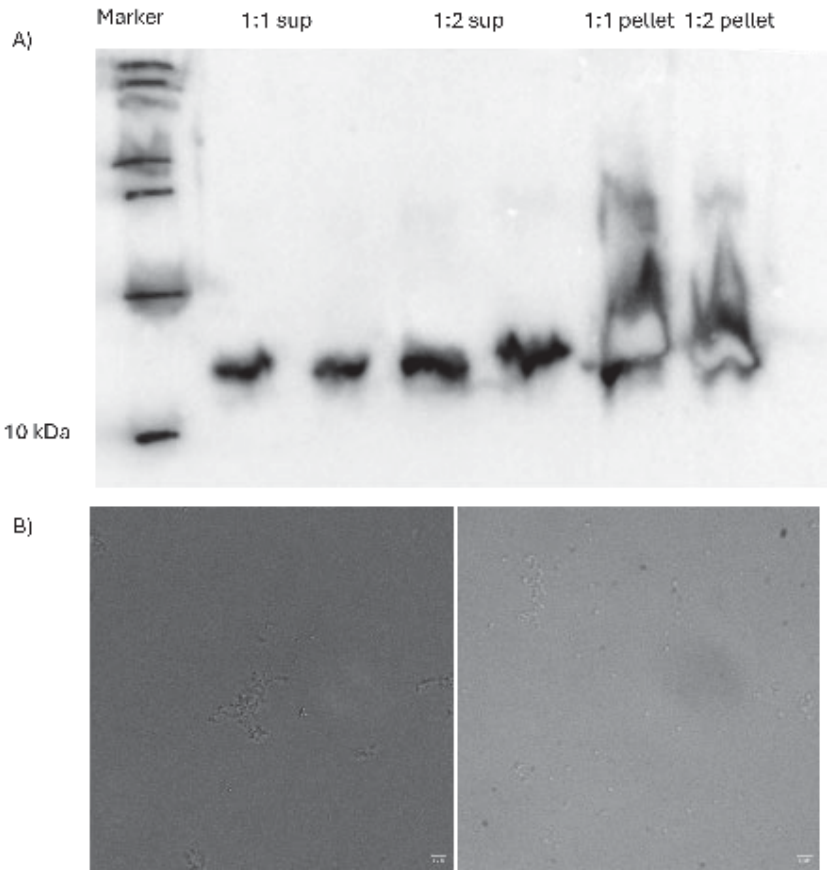

Fig 4.2: Western Blotting and DIC microscopy. A) Western blot depicting the detection with Aβ antibodies in the supernatant and pellet from tau-AβOs under non-LLPS conditions. **B)** DIC microscopy of these high turbidity interactive solutions revealed the presence of amorphous aggregates that highly varied in size and shape. Scale bar: 5 µm

4.3.3 Co-aggregation of tau and dimAβOs

Up to this point, our western blot results indicated the presence of dimAβOs within the high-order assemblies, but the distribution of tau within these samples remained unclear. To address this, we used fluorescently labelled tau and dimAβOs and prepared the samples and observed them under TIRF microscopy. The results revealed a colocalization of tau and dimAβOs within the aggregates, indicating that both proteins are incorporated into these assemblies (Fig 4.3 A, B). Furthermore, the spherical structures observed together with the aggregates also contained both proteins.

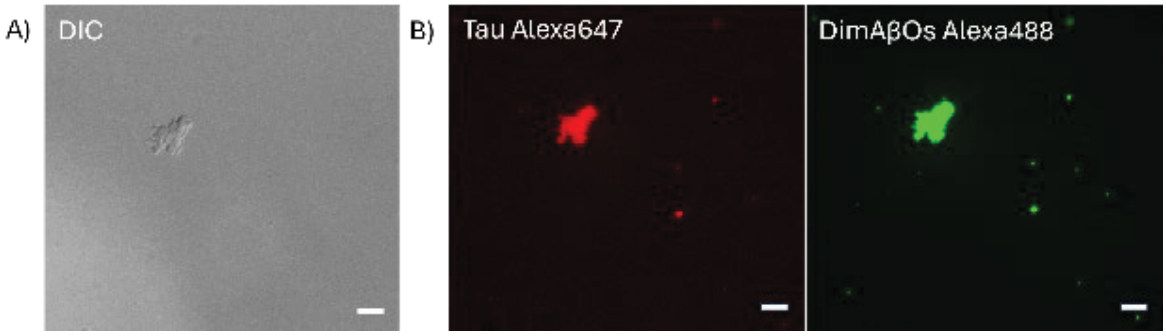

Fig 4.3: Co-localisation tau and dimAβOs in aggregates. A) DIC microscopy showing the aggregates and **B)** fluorescence microscopy with Alexa fluorophore labelled tau and dimAβOs revealed their co-localisation into aggregates under non-LLPS conditions. Scale bar: 5 µm.

Fig 4.4 A presents a magnified view of the aggregates. TIRF imaging reveal that these aggregates are irregular, non-fibrillar and cluster-like in appearance and not canonical long amyloid fibrils. This morphology is consistent with reported intermediate or non-fibrillar aggregation states of tau and Aβ (452,453). We used AFM to further characterize these aggregates (Fig 4.4 B). AFM provides a nanometer-resolution topography, and these aggregates existed as compact, densely packed clusters. Their heterogeneity suggests that the assemblies may be composed of multiple subunits, indicating nucleation and growth rather than fibrillar elongation. Spherical condensate-like structures were not detected by AFM or by magnified imaging. Additional high-resolution will be required to further confirm their presence.

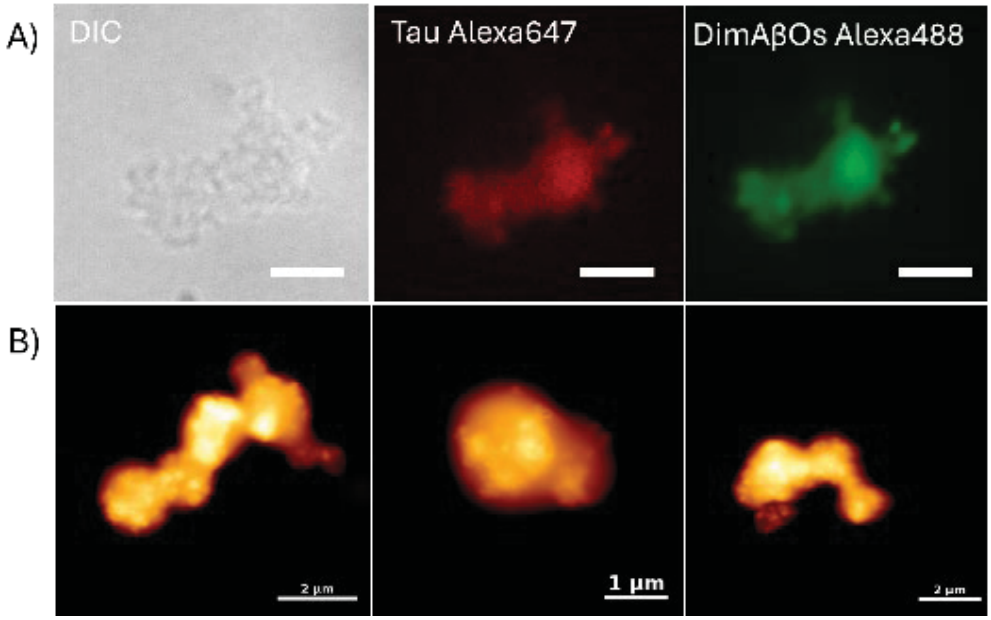

Fig 4.4: Aggregates in fluorescence and AFM microscopy. A) Microscopic images indicating the non-fibrillar nature of the aggregates in DIC mode and in fluorescence microscopy. Scale bar:5 µm**. B)** AFM images of the aggregates.

4.3.4 Interaction of tau with monomeric dimAβ

Intrigued by the presence of amorphous assemblies observed upon co-incubation of tau with dimAβO, we next investigated if dimAβ monomers (dimAβMs) would behave differently upon interaction with tau. We mixed 4 µM dimAβMs with 10 µM tau and incubated it under conditions identical to those used for dimAβOs. Notably, tau incubated with dimAβMs exhibited substantially higher turbidity compared to tau with dimAβOs while dimAβMs or dimAβOs showed no turbidity alone (Fig 4.5 A). DIC microscopy revealed that the tau-dimAβMs samples consistently formed large amorphous aggregates, similar to those previously observed, but with even larger size and higher abundance than observed for the tau-dimAβOs samples (Fig 4.5 B). These aggregates appeared as dense, irregular structures distributed throughout the sample, however unlike as observed with tau-dimAβOs, no spherical condensate-like assemblies were detected.

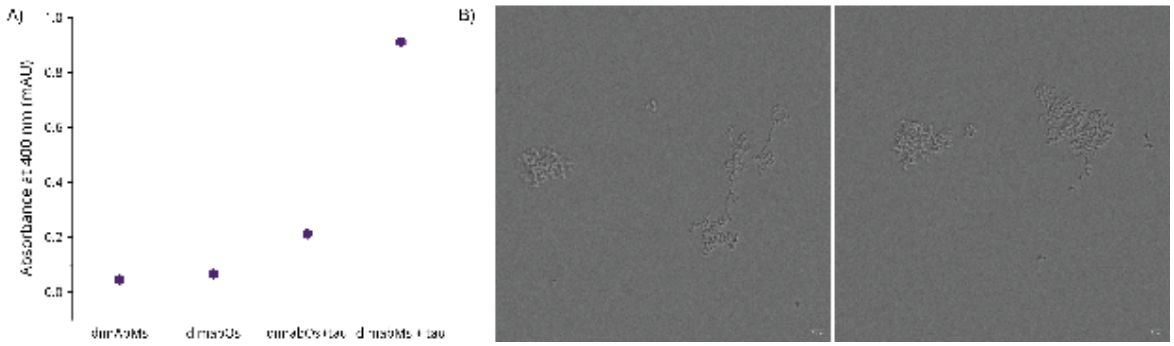

Fig 4.5: Interaction of tau with dimAβ monomers. A) Turbidity measurements of co-incubated 10 µM tau and 4 µM dimAβ monomers compared to that with dimAβOs and other controls. **B)** DIC microscopic images showing the amorphous aggregates formed upon interaction with 10 µM tau and 4 µM dimAβ monomers. Scale bar: 5 µm

This observation is consistent with earlier results (Section 3.3.12) where the oligomeric mixture of Aβ42 led to the formation of large, amorphous aggregates upon interaction with tau, suggesting that structural diversity among Aβ species may modulate co-assembly outcomes with tau.

4.3.5 FRAP assay

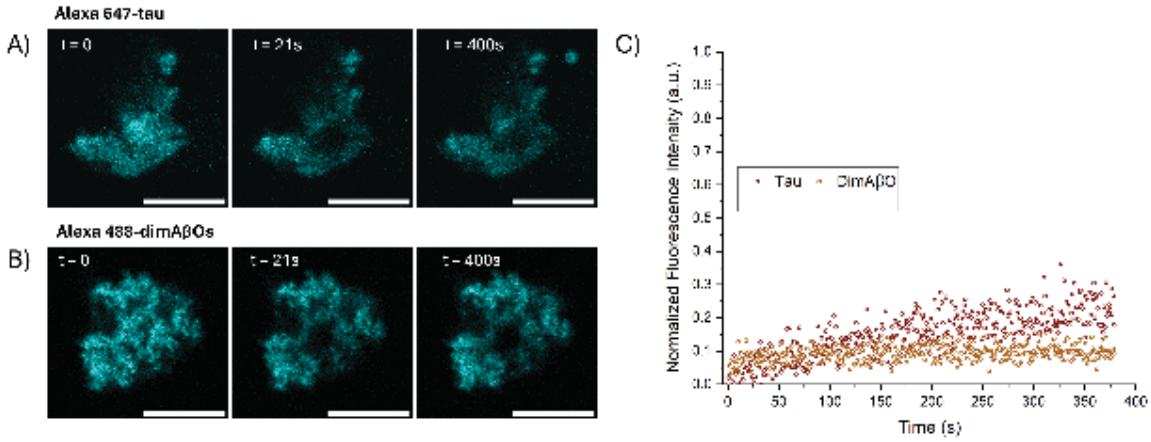

Fig 4.6: FRAP analysis of tau and dimAβ under non-LLPS conditions. Time-series images following the FRAP experiments of **A)** tau and **B)** dimAβOs within the clusters. **C)** Recovery curves for tau and dimAβO. The samples were prepared with 10 μM tau (Alexa-647-labelled tau:tau = 1:60) incubated with 4 μM dimAβO (Alexa-488-labelled dimAβ:dimAβ = 1:20) at pH 7.4.

To further characterize the phase properties and molecular mobility of the tau-dimAβOs co-aggregates, we performed FRAP. The experimental protocol was identical to that used for condensate analysis, and photobleaching was carried out in both the tau and dimAβ fluorescence channels. Unlike the uniformly distributed fluorescence observed in co-condensates for tau, the co-aggregates displayed highly heterogeneous and irregular fluorescence signals for both tau-dimAβOs, making it challenging to define an appropriate ROI. The amorphous morphology further contributed to the difficulty in applying FRAP analysis. Despite these limitations, aggregates that approximately fit within the previously used tornado-shaped ROI were selected and subjected to photobleaching. Tau fluorescence exhibited minimal recovery, resulting in a high immobile fraction of approximately 0.8, consistent with restricted molecular mobility and a solid-like state (Fig 4.6 A, C). Similar to tau, dimAβOs also showed very limited recovery, with an immobile fraction greater than 0.9 (Fig 4.6 B, C). The poor recovery and non-exponential behaviour of the fluorescence recovery prevented the use of standard kinetic fitting models that were applied to the co-condensates. Together, FRAP analysis strongly support that both tau and dimAβOs are rigidly immobilised within the co-aggregates, indicating that they possess solid- or gel-like properties rather than liquid-like dynamics.

4.3.6 Electrostatic and hydrophobic screening of tau-dimAβOs aggregation

Similar to the approach used for tau-dimAβOs condensates, we next examined the roles of electrostatic and hydrophobic interactions in the formation and stability of tau-dimAβOs aggregates. For this, we incubated tau-dimAβOs aggregates with increasing concentrations of NaCl and 1,6 HD. Remarkably, no reduction in turbidity was observed even at the highest levels of either NaCl or 1,6 HD tested (Fig 4.7 A, B). These results indicate that, unlike the condensates, the stability of the co-aggregates is not dependent on electrostatic or weak hydrophobic interactions, suggesting that they are held together by strong, possibly irreversible interactions, consistent with a solid-like, highly stable aggregated state.

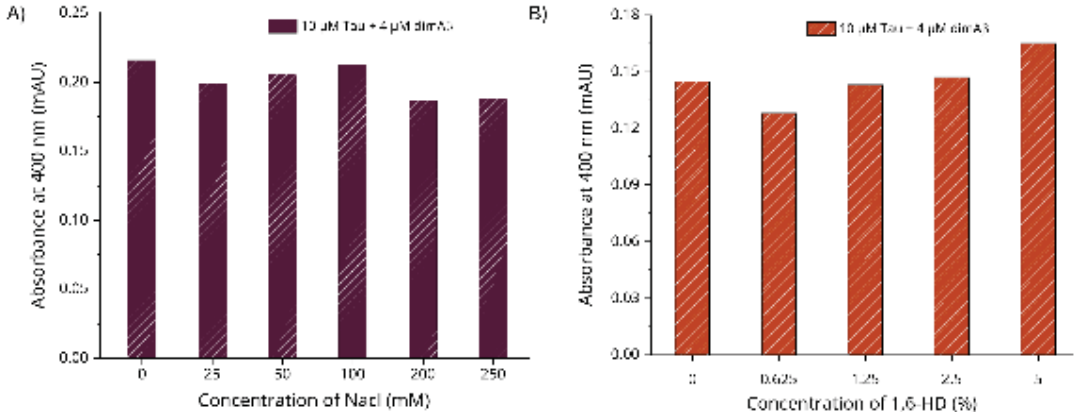

Fig 4.7: Electrostatic and hydrophobic screening of tau-dimAβOs aggregates. Turbidity of co-incubated 10 μM tau and 4 μM dimAβOs with increasing concentrations of **A)** NaCl and **B)** 1,6 HD.

4.3.7 ThT aggregation kinetics

After observing that tau inhibited the progression of dimAβOs toward fibril formation under LLPS conditions, and that tau condensates could act as a reservoir for dimAβOs, we next examined whether a similar effect occurred under non-LLPS conditions. To address this, we monitored the aggregation kinetics of dimAβ at three different concentrations in the presence of 10 μM tau, in the absence of crowding conditions (Fig 4.8 A, B, C) . As expected, dimAβ alone displayed its characteristic biphasic kinetics at all concentrations. However, when incubated with tau, the second phase corresponding to amyloid fibril formation was strongly suppressed across all concentrations tested. These observations suggest that tau prevents the oligomer-to-fibril transition of dimAβ not only within condensates but also in the aggregates. We additionally compared the oligomerization half-times in these samples

and found that tau delayed the oligomerization of dimAβ , however this effect decreased at higher concentrations of dimAβ (Fig 4.8 D).

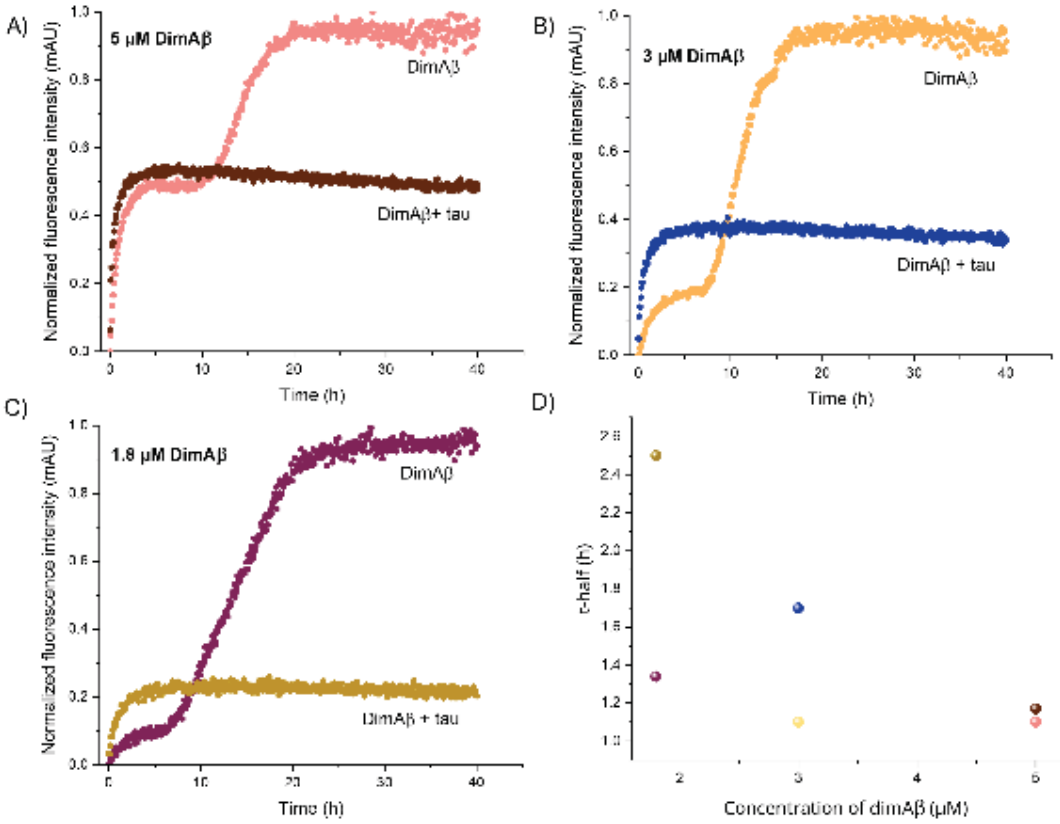

Fig 4.8: ThT kinetics of dimAβ in the presence of tau under non-LLPS conditions. ThT kinetic profiles of **A)** 5 µM, **B)** 3 µM and **C)** 1.8 µM of dimAβ in the presence and absence of tau. This was investigated on the absence of crowding conditions. D) Half-time of oligomerisation was calculated for each of the curves.

4.3.8 LDH toxicity assay

The next aim of the project was to determine whether the tau-dimAβ co-aggregates exerted cellular toxicity. For this, we employed an LDH cytotoxicity assay using the SH-SY5Y neuroblastoma cell line. The LDH assay is a reliable and widely used method to assess the cytotoxicity induced by protein aggregates in cell culture systems (454). It quantitatively measures LDH enzyme activity released into the culture medium when the plasma membrane integrity is compromised by toxic aggregates. The assay specifically detects the conversion of lactate to pyruvate, which produces a measurable fluorometric signal proportional to the amount of LDH released, reflecting cell membrane damage and cell death. The fluorometric signal has a peak maximum at 490 nm. However, raw absorbance readings can include background noise and nonspecific absorbance from the plate, culture media, or other assay components. To correct this, absorbance measured at 680 nm, a reference wavelength, is subtracted from the 490 nm value. This removes the background

signal and improves accuracy by isolating the true LDH-dependent signal, ensuring that the data reflect actual cell membrane damage rather than instrument or plate artifacts. This dual-wavelength measurement enhances the reliability and reproducibility of cytotoxicity quantification to measure toxicity of tau-dimAβOs aggregates.

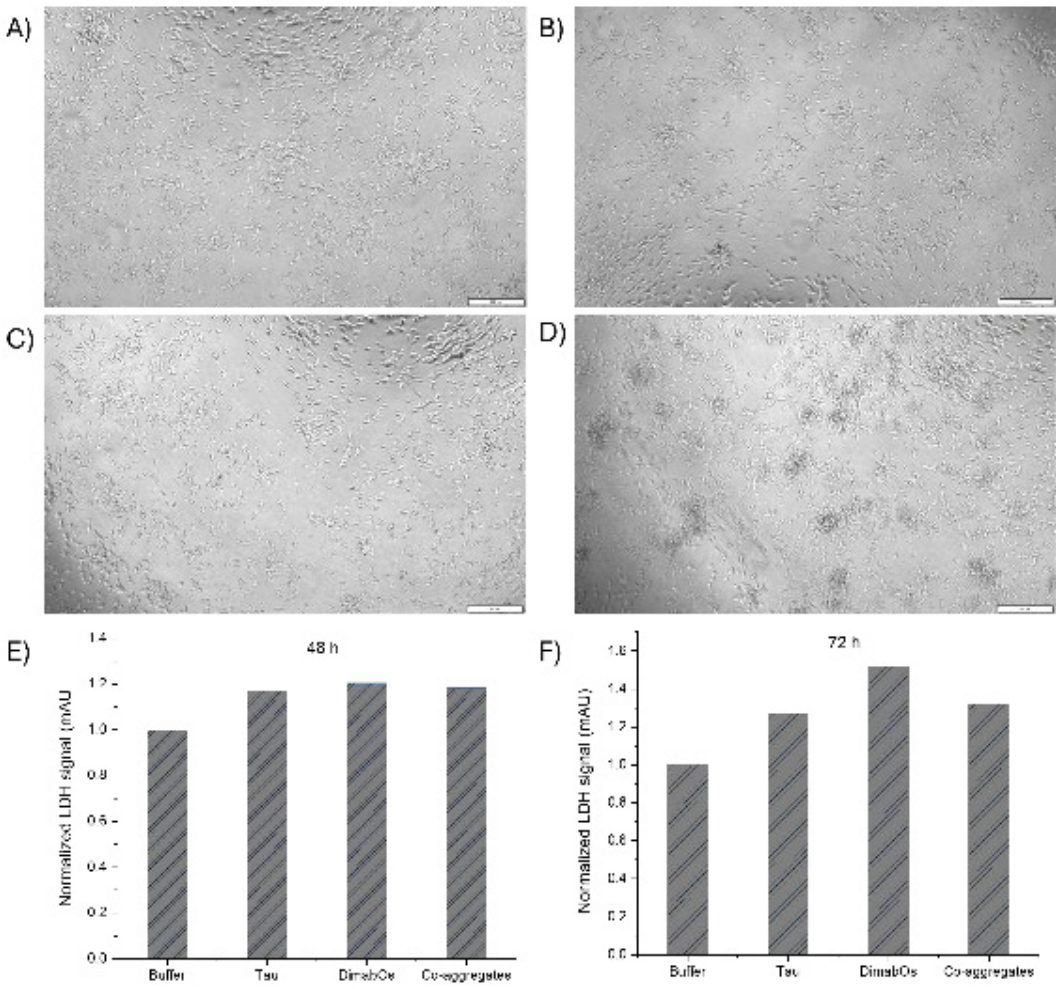

Fig 4.9: Cell imaging and LDH assay. Phase-contrast images of SH-SY5Y neuroblastoma cells after 48 h following their incubation with **A)** buffer, **B)** tau monomers, **C)** dimAβOs and **D)** tau-dimAβOs aggregates. **E) F)** LDH signals of each condition measured after 48 h and 72 h.

We cultured SH-S55Y neuroblastoma cells in nutrient medium until desired confluency is reached. Further, each well was treated with one of the four conditions including buffer (30 mM Tris at pH 7.4), 10 μM tau, 4 μM dimAβOs and tau-dimAβOs co-aggregates. Each condition was performed as standard triple replicates and phase-contrast microscopy was used to assess cell morphology. Cells in the buffer, tau and dimAβO-only conditions appeared morphologically comparable, although slight cell clustering was observed for tau and dimAβOs (Fig 4.9 A). In contrast, wells treated with co-aggregates displayed irregular patch-like regions where cells appeared stressed or morphologically altered, although cell

growth was still evident surrounding these areas. The LDH signal in each condition was recorded after 48 h and 72 h to check any effects (Fig 4.9 B). Surprisingly, none of these conditions showed an increased toxicity when compared to the buffer control. This could point out that the aggregate has some effect on the cells, however this effect is not detectable using LDH signal and would need additional assays to validate this

Chapter 5: Discussion & Conclusion

This thesis investigates the interactions between tau and AβOs with a focus on the LLPS conditions. The crosstalk between tau and Aβ represents a critical nexus in AD pathogenesis, yet the precise molecular mechanisms underlying their interplay remains elusive. This study provides new mechanical insights into how these proteins influence each other's phase behaviour and aggregation, aiming to provide insights that advance our understanding of neurodegenerative processes.

LLPS has recently emerged as a fundamental biological principle in cellular biochemistry (101), where it enables dynamic compartmentalization of proteins and nucleic acids without membrane boundaries unlike the conventional organelles. LLPS also impacted severely on neurodegenerative diseases where it acts as a transition state that locally concentrates proteins above their critical threshold for aggregation (455). Previous studies have shown that tau can form liquid-like condensates that may mature into fibrillar aggregates resembling neurofibrillary tangles (92). Similarly, Aβ peptides can undergo LLPS, which modulates their aggregation pathways and toxicity (171,172). Based on these observations, we sought to determine whether these condensate phases could serve as interactive hubs for tau and Aβ, and how such interactions might contribute to pathological processes.

In this study, we examined the molecular interplay between tau and AβOs, focusing on how LLPS influences their heterotypic interactions, aggregation kinetics and potential pathological consequences.

5.1 DimAβ as a relevant oligomeric model of Aβ

We employed the dimeric Aβ40 construct, dimAβ, for studying the interaction of AβOs with tau. DimAβ consisting of two covalently-linked Aβ units, increases the local peptide concentration of Aβ, reducing its critical thresholds of aggregation and promoting the accumulation into oligomers (169,179,180). Notably, dimAβ exhibits biphasic kinetics above a COC of ~ 1.5 μM where the first phase corresponds to the formation of oligomers and then a second phase that corresponds to the fibril formation. In this way, the AβOs can be extracted solely without interference from monomers or fibrils. The similar *in vivo* toxicity between dimAβ-derived oligomers and Aβ42 oligomers further supports the relevance of dimAβ construct. We used dimAβOs in the experiments and these off-pathway oligomers of dimAβ will be addressed as AβOs from now on.

5.2 Condensates as an interactive milieu for tau and AβOs

Our first intriguing finding in this study was the observation that tau and AβOs can undergo heterotypic LLPS. Several proteins involved in NDs have been studied for their ability to co-phase separate with diverse molecular partners and Chapter 2 gives summary of current research on heterotypic LLPS of tau and αS. Upon studying different heterotypic partners of tau, we found that different partners induce distinct effects on the phase separation behaviour and aggregation propensity of tau. Importantly, all amyloidogenic partners were reported to enhance the aggregation of both tau and αS. These observations led to our hypothesis that, due to the amyloidogenic nature of Aβ, heterotypic phase separation with tau could allow Aβ oligomers to modulate condensate properties and promote tau aggregation.

Indeed, tau and AβOs were found to co-localise within condensates under macromolecular crowding conditions. In our studies, PEG was used for inducing crowding conditions (456). PEG acts as a macromolecular crowding agent that mimics the dense intracellular environment, promoting phase separation by effectively increasing the local protein concentration. PEG is widely used in LLPS studies due to its minimal impact on the intrinsic properties of proteins (457).

Tau readily underwent homotypic LLPS in the presence of PEG and heterotypic LLPS when both PEG and AβOs were present. Initially, with DIC microscopy, we observed that AβOs did not affect the condensates of tau. This observation was also supported by turbidity and particle sizing experiments. Turbidity measurements showed no significant difference between tau condensates formed with and without AβOs. DLS measurements was then used to determine the particle size distributions. The particle size ranges of tau monomers and AβOs alone eliminated the presence of any higher-order assemblies in these control samples. Homotypic tau condensates exhibited diameters consistent with previous reports (335). In the presence of AβOs, tau-AβOs heterotypic condensates showed a 39 % increase in mean particle size. Although this indicates that AβOs influence tau condensates, these measurements could not distinguish whether the changes arose from a co-localisation or from other structural alterations. This limitation necessitated the use of fluorescence microscopy to resolve the spatial distribution of each protein. To achieve this, tau and Aβ were fluorescently labelled using NHS ester chemistry for tau and maleimide coupling for a cysteine-containing dimAβ variant. All fluorescently labelled proteins were purified using chromatographic methods as described in Chapter 3.

Fluorescent labelled tau was first confirmed to undergo condensate formation in the presence of PEG. Similarly, labelled dimAβ was verified to retain biphasic aggregation

kinetics and oligomer formation as assessed by ThT fluorescence and AFM imaging respectively. Fluorescently labelled tau and AβOs were then co-incubated under crowding conditions. By exciting each fluorophore separately, we observed clear co-localisation of tau and AβOs within the same condensates. Interestingly, AβOs did not distribute uniformly throughout the droplets. Instead, they formed microdomains dense puncta resembling nest-like structures, generating multiphasic condensates. Within these condensates, while AβOs segregated into these distinct internal compartments, tau remained evenly distributed. Previous studies have shown that several amyloidogenic proteins including αS, TIA1 and PrP can associate with tau as heterotypic condensate partners (137,138,265). Our findings extend this list by demonstrating that AβOs can also engage in heterotypic LLPS with tau, highlighting a potential basis for synergistic toxicity in NDs.

5.3 Multiphasic condensates of tau and AβOs

We observed an interesting "phase within phase" organisation within the tau-AβO coacervates, forming a multiphasic condensate. Multiphasic condensates exhibit a complex internal organization and composition. While simple condensate forms the single-phase liquid droplets, multiphasic condensates undergo internal demixing that leads to the formation of two or more coexisting immiscible liquid phases with distinct molecular compositions. These multiphasic compositions are implied to be critical for cellular environment as it facilitates multiple biochemical reactions within the same compartment (458). This hierarchical structuring has been previously observed in several functional systems including nucleoli (204,459), stress granules (460), and anisosomes (292). This type of internal layering helps in efficient biochemical compartmentalization and functioning within membraneless organelles. Tau has been previously associated with amyloidogenic proteins like TIA 1 (138) and PrP (137) to form different kinds of multiphasic condensates. Micropolarity and interfacial tension have been shown to play critical role in the structuring of multiphasic condensates (461,462). Typically, such an organization arises when the coexisting components differ in their micropolarity, with the hydrophilic partner forming the shell and the hydrophobic components localizing to the core. Here, comparatively hydrophobic AβOs preferentially adsorb onto the tau-rich matrix and form nested droplet-like sub-domains of AβOs probably due to their higher interfacial tension with the surrounding solvent. The nests of AβOs minimize surface exposure to the solvent and hence also highly favour the homotypic AβOs interaction (461,463,464).

The multiphasic condensates formed by tau and AβOs show an evenly distribution of both proteins throughout the condensate and AβOs additionally form nested droplet-like microdomains. This differs from the classic "nested droplet" structure observed in tau-PrP condensates (137). Like PrP, AβOs concentrate into nests, but unlike PrP, they remain evenly

distributed within the overall condensate. Also, the nests of AβOs highly varied in their size, shapes and numbers across the condensates indicating the existence of heterogenous AβOs population in the condensates. This multiphasic architecture with AβOs nests likely arises from a complex network of heterotypic and homotypic interactions, creating a milieu that may promote further aggregation of tau and Aβ.

5.4 AβOs modulate tau dynamics inside the condensates

Heterotypic LLPS partners often modulate the condensate properties of the scaffold protein (465). To assess whether AβOs alter tau dynamics, we employed FRAP to measure the mobility of tau within the co-condensates. We compared the dynamics of tau in their homotypic condensates and in the heterotypic condensates with AβOs. The recovery time of tau was increased from 46 s to 73 s in the presence of AβOs. Further, the total immobile fraction of tau in these condensates also increased from 0.25 to 0.42. These changes indicate that the otherwise highly dynamic tau condensates become significantly less dynamic upon co-condensation with AβOs. This reduction in dynamics may arise from two non-mutually exclusive mechanisms: (i) heterotypic interactions between tau and AβOs could generate a more extensively interconnected tau-AβO network, or (ii) co-condensation with AβOs could trigger tau aggregation, driving its transition into higher-order assemblies. Even in the first scenario, increased local concentration of tau would be expected to ultimately promote aggregation.

We next examined the dynamics of AβOs within the heterotypic condensates. Previous studies have shown that although oligomers can exhibit dynamic and transient behaviour, their molecular diffusion is substantially slower than that of phase-separated condensates (466). Consistent with this, AβOs showed a recovery time of 86 s, implying an 87% increase relative to the recovery time observed for tau in its homotypic condensates. Their immobile fraction was also markedly higher, representing a 76% increase compared with tau in homotypic condensates. When compared directly to tau within the same heterotypic condensates, AβOs exhibited an 18% higher recovery time and a 5% higher immobile fraction.

Interestingly, the recovery times of AβOs spanned a broad range (40 s to 120 s), suggesting the presence of multiple AβO populations within these assemblies. Although we aimed to specifically assess the dynamics of the AβO “nests,” their very small size and highly saturated fluorescence prevented reliable FRAP measurements.

Overall, these results indicate that AβOs do undergo limited molecular diffusion within the heterotypic condensates, but their mobility is substantially lower than that of tau in homotypic condensates. In addition, the formation of nest-like AβO microdomains and the

wide distribution of recovery times suggest that AβOs experience structural transitions inside the condensates and exist as a heterogeneous population.

5.5 AβOs show affinity to tau monomers

Intrigued by the co-localisation of tau with AβOs in condensates, we next tested whether AβOs interact with tau under non-LLPS conditions. Although PEG is widely used as a crowding agent, several studies have highlighted limitations to its use. PEG can directly interact with target proteins and its physicochemical properties differ from endogenous macromolecules (467,468). Therefore, we examined tau-AβO interactions in the absence of LLPS-promoting crowding agents.

Upon co-incubation of tau with AβOs we observed pronounced turbidity that increased with AβO concentration. Particle sizing showed that this turbidity arose from assemblies ranging from 1 μm to 50 μm. To determine whether these assemblies contained both tau and Aβ species, samples were centrifuged and pellet and supernatant were analysed by western blot. The supernatant contained a single AβO band, whereas the pellet contained Aβ species of higher apparent molecular weight. Attempts to probe the same samples with tau antibodies were unsuccessful owing to technical problems with tau detection by western blot.

DIC microscopy confirmed that tau-AβOs samples comprised of aggregates of several micrometres in diameter together with numerous smaller accumulations. Fluorescent labelling of tau and AβOs demonstrated a clear co-localisation of both proteins within these assemblies, indicating an affinity of AβOs for tau monomers under non-LLPS conditions.

The tau-AβO aggregate assemblies varied widely in size and morphology, consistent with an amorphous character. Amorphous aggregates are protein assemblies that lack an ordered, high-resolution structure (469). For several years, these aggregates were commonly regarded as non-specific translational byproducts and were rarely studied or characterized in the context of pathological processes (470). However, accumulating evidence indicated that these amorphous aggregates could serve as potential precursors for amyloid fibrils. Studies have shown that tau can accumulate into toxic amorphous aggregates (471) can form amorphous co-aggregates with other amyloidogenic proteins such as PrP (137).

We next investigated the dynamics of these co-aggregates using FRAP, applying the same settings used for condensate dynamics. Both tau and AβOs exhibited very low fluorescence recovery and a large immobile fraction after photobleaching, consistent with a solid-like, stable and persistent state. These observations suggest the modulation caused by AβOs from highly dynamic tau in homotypic condensates to less dynamic heterotypic tau

condensates formed under LLPS conditions, and to solid-like heterotypic tau aggregates formed under non-LLPS conditions (Fig 5.1).

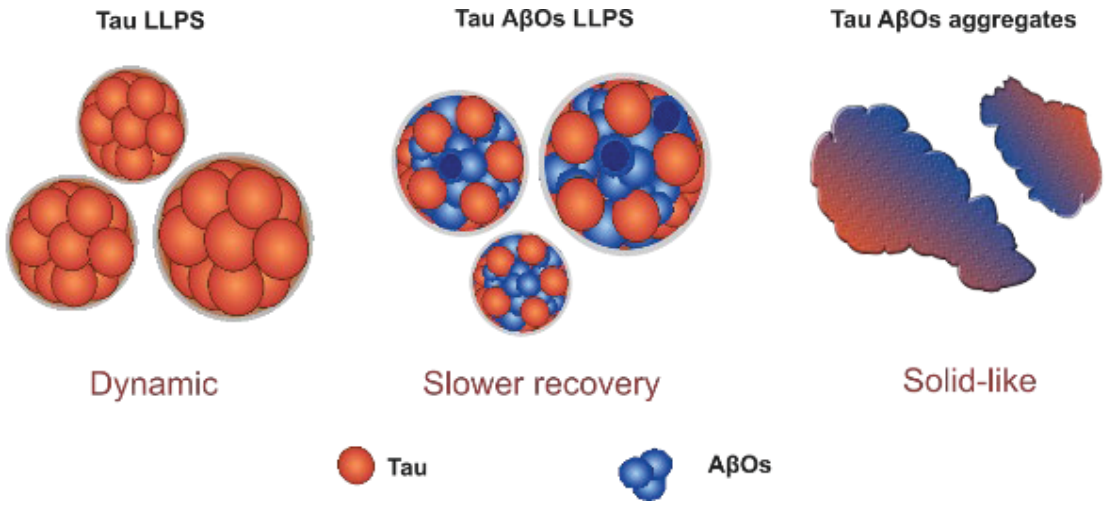

Fig 5.1: Mobility of tau in different assemblies. Dynamic tau shows slower recovery upon heterotypic condensation and solid-like nature upon heterotypic aggregation with AβOs.

To test whether tau binds only AβOs or also Aβ monomers, we prepared dimAβ monomers and avoided incubation at physiological temperature, so that they remained monomeric. Co-incubation of tau with dimAβ monomers produced markedly increased turbidity when compared to tau co-incubated with dimAβOs. Microscopy revealed amorphous aggregates in these samples as well; however, aggregates formed with dimAβ monomers were larger, denser and more numerous than those formed with dimAβOs. These observations indicate a strong affinity between Aβ monomers and tau and suggest formation of stabilised hetero-assemblies This is consistent with previous reports that fragments of tau and Aβ can interact to form hetero-oligomers or granular aggregates (472), and supports the relevance of dimAβ construct.

Finally, we assessed the cytotoxicity of these co-aggregates using an LDH release assay. Neuroblastoma cells were incubated with aggregates or controls and monitored at 48 h and 72 h. LDH signals from cells treated with aggregates did not differ appreciably from buffer controls; tau monomers and AβOs alone likewise showed no significant toxicity in this assay. However, microscopy revealed patch-like material associated with cells exposed to aggregates, suggesting a tendency for aggregates to adhere to cell surfaces. Confirming this observation will require fluorescently labelled proteins and high-resolution fluorescence imaging. While being widely used to monitor neuronal damage following exposure to toxic agents or aggregated proteins (473), it is also important to note limitations of the LDH assays. LDH measurements can suffer from lack of specificity and other confounds that

complicate interpretation of toxicity in neurodegenerative disease contexts. Thus, although our LDH data do not indicate acute toxicity for these aggregates relative to buffer controls, more sensitive functional assays and *in vivo* or advanced model systems are required to evaluate their pathogenic potential.

Previous *in vitro* studies reveal that tau monomers exhibit a high affinity for AβOs, progressing towards granular aggregates and larger oligomeric assemblies when complexed with Aβ (472,474). Crucially, tau regions containing the aggregation-prone VQIINK and VQIVYK motifs appear central to this process. These findings indicate that tau-Aβ interaction can be driven by defined sequence motifs that facilitate nucleation and accelerate pathological co-assembly.

5.6 The role of electrostatics and hydrophobics forces in tau-Aβ interaction

Electrostatic and hydrophobic interactions are two principal non-covalent forces mediating protein-protein interactions (475). Electrostatic interactions arise from attractive or repulsive forces between oppositely charged amino acid residues (476) and are highly sensitive to the ionic strength of the environment. Hydrophobic interactions are driven by the tendency of non-polar side chains to avoid exposure to aqueous environments, promoting interfacial burial of hydrophobic surfaces (477). In this study, we examined the contribution of these interaction types to the stability of tau-AβOs assemblies formed under LLPS and non-LLPS conditions.

Under LLPS conditions, tau and AβOs formed heterotypic condensates whose stability decreased with increasing ionic strength and, to a lesser extent, with hydrophobic perturbation. Turbidity progressively decreased between 50 mM and 250 mM NaCl, indicating that condensate formation is strongly dependent on electrostatic interactions. At physiological pH (7.4), tau carries an overall positive charge, whereas Aβ is negatively charged. Hence, electrostatic attraction likely mediates their initial association and increasing salt concentration screens these charged interactions, promoting condensate dissolution. Previous studies have shown that tau homotypic condensates are predominantly driven by electrostatic interactions with a minimal contribution from hydrophobic forces (478). Consistent with this, our results suggest that although electrostatic interactions remain central, both homotypic (tau–tau) and heterotypic (tau–AβO) electrostatic interactions may contribute to stabilizing tau-AβO condensates. The hydrophobic perturbant 1,6-hexanediol (1,6-HD) caused only a moderate reduction in turbidity, with a measurable effect at 1.25% (v/v), but no further dissolution at higher concentrations. This implies that weak hydrophobic contacts contribute to condensate

stability but are not the dominant force and they appear to play a secondary, supportive role in maintaining the condensate network.

In contrast, tau-AβOs assemblies formed under non-LLPS conditions remained highly turbid and resistant to even the highest concentrations of NaCl and 1,6-HD. This behaviour suggests that once tau and AβOs transition into solid-like aggregates, they are stabilised by strong, irreversible interactions that are no longer susceptible to ionic screening or disruption of weak hydrophobic contacts.

Together, our results suggest a model in which electrostatic interactions predominantly drive the assembly and stability of tau-AβOs condensates, while hydrophobicity contributes only partially to condensate integrity. However, under non-LLPS conditions tau and dimAβOs form hetero aggregates that are stabilized by strong, irreversible interactions and are no longer sensitive to ionic or hydrophobic perturbations (Fig 5.2).

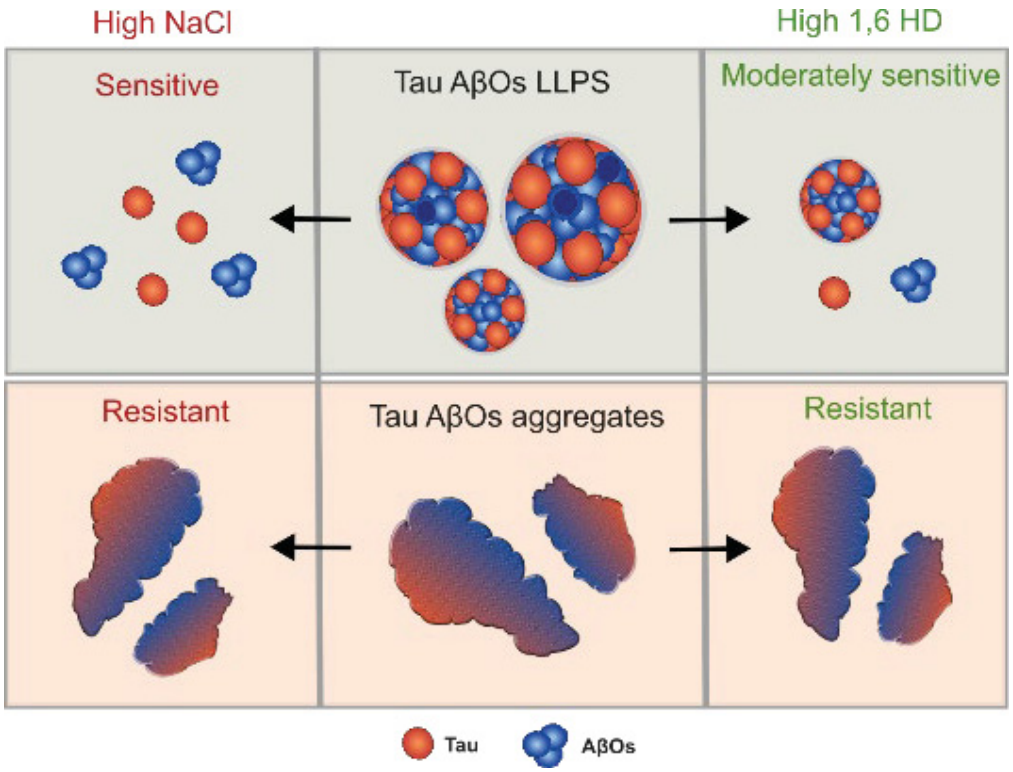

Fig 5.2: Role of electrostatics and hydrophobicity in tau-AβOs interaction. Tau-AβOs LLPS were sensitive to high salt and moderately sensitive to hydrophobic perturbations. Tau-AβOs aggregates were resistant to both high salt and high 1,6-HD.

5.7 Tau inhibits continued kinetics of AβOs

After characterizing the effect of AβOs on tau, we next examined the reciprocal influence of tau on the aggregation kinetics of Aβ. To do so, we monitored ThT fluorescence of Aβ monomers in the presence of tau under both LLPS and non-LLPS conditions, using the dimAβ model to specifically assess its characteristic biphasic aggregation profile. Remarkably, tau markedly suppressed the biphasic kinetics of dimAβ and arrested Aβ in its oligomeric state. Control experiments performed either without tau or in the presence of a crowding agent showed no alteration in the biphasic behaviour, indicating that the observed effect was exclusively mediated by tau. These findings suggest that, within co-condensates and co-aggregates, Aβ is stabilised in an oligomeric form, thereby functioning as a reservoir for tau-rich assemblies.

Studies have demonstrated that non-phosphorylated tau can slow the elongation phase of Aβ42 fibril formation by binding to AβOs and shielding hydrophobic surfaces, suggesting that tau may exert a neuroprotective effect by limiting amyloid fibril maturation (479). Consistent with this, recent work shows that full-length tau can solubilize Aβ40 peptides and prevent its transition into fibrillar structures (480). Tau delays Aβ40 fibrillation even at sub-stoichiometric ratios and displays differential binding affinities toward distinct aggregation states of Aβ, implying a selective interaction mechanism. Collectively, these findings suggest that tau can modulate Aβ aggregation pathways by stabilizing oligomeric species and preventing their fibrillar maturation, providing insights into a possible mechanistic basis for a bidirectional Aβ-tau interaction in NDs.

5.8 Tau interacts with oligomeric population of native Aβ42

To determine whether the observed affinity of AβOs for tau could also be reproduced using native Aβ42 constructs, we repeated the experiments with an Aβ42. A key limitation was that biphasic aggregation kinetics of Aβ42 require substantially higher peptide concentrations compared with dimAβ. Therefore, Aβ42 was incubated at 40 μM for 2-3 hours before co-incubation with tau, according to a pre-defined protocol. Fluorescently labelled proteins were used to visualize the potential co-localisation. Under LLPS conditions, oligomeric Aβ42 clearly co-localized with tau within condensates. Additionally, we observed the presence of heterotypic aggregates, similar to those detected in tau-dimAβO samples. This behaviour is consistent with the previous reports highlighting the difficulty of isolating pure oligomeric species from native Aβ40 or Aβ42 constructs due to their inherent tendency to form heterogeneous mixtures comprising monomers, oligomers, and higher-order assemblies. Such heterogeneity likely contributes to ambiguity in tau-Aβ42Os interactions and complicates mechanistic interpretation.

These findings therefore further validate the use of dimAβ as a controlled, off-pathway oligomeric model system, enabling experiments that specifically probe Aβ oligomer behaviour without interference from heterogeneous higher-order Aβ species.

5.9 Conclusion

This thesis provides novel insights into the molecular interplay of tau and AβOs, studying how LLPS conditions modulate tau-AβOs interactions, dynamics, and assembly states. Fig 5.3 denotes the key findings made in this thesis. By employing the dimeric Aβ model, dimAβ, we demonstrated that tau and AβOs undergo heterotypic LLPS to form multiphasic condensates where AβOs form nested microdomains in a tau-rich phase. These condensates are primarily stabilized by electrostatic interactions while hydrophobic forces provide a weak supportive role. Notably, tau in tau-dimAβOs condensates showed reduced dynamics when compared to tau in homotypic condensates, reflecting the complex interprotein interactions formed during co-condensation. This suggests that the heterotypic condensates provide a microenvironment promoting cross-interactions that may lead to accelerated aggregation, offering new mechanistic insights into the synergistic nature of tau-Aβ pathology. Also, we emphasize the importance of electrostatic interactions in driving pathological tau-AβOs heterotypic condensates and how these interactions affect the properties of the condensates.

In contrast, tau and AβOs form stable, solid-like amorphous aggregates under non-LLPS conditions. These aggregates were resistant to perturbation by salt or hydrotropes, indicating that irreversible intermolecular interactions dominate their stabilization than the transient electrostatic or hydrophobic interactions. Similar aggregate formation was observed upon interaction of tau with dimAβ monomers as well as monomers derived from the native Aβ construct. The emergence of these amorphous aggregates indicates a strong intrinsic affinity of tau for both AβOs and Aβ monomers, raising the possibility that tau may act as a nucleation platform that facilitates Aβ aggregation.

Moreover, tau modulates Aβ aggregation kinetics by arresting dimAβ in its oligomeric states, suggesting that tau-Aβ assemblies act as reservoirs of AβOs. These reservoirs increase the lifetime of the oligomers and may lead to their enhanced toxicity in a cellular context. While LDH cytotoxicity assays did not show acute toxicity for these aggregates, preliminary microscopy observations show their adherence to the neuroblastoma cells underscoring the need for further investigation using advanced neuronal models.

Together, our findings provide a framework for understanding tau-AβOs interaction primarily on the context of phase separation. We also indicate that their ability to form different aggregative assemblies based on the environment. Understanding these differential

molecular mechanisms advances our knowledge in understanding AD pathogenesis and highlights LLPS as both an interactive milieu and a potential precursor state for pathological aggregation.

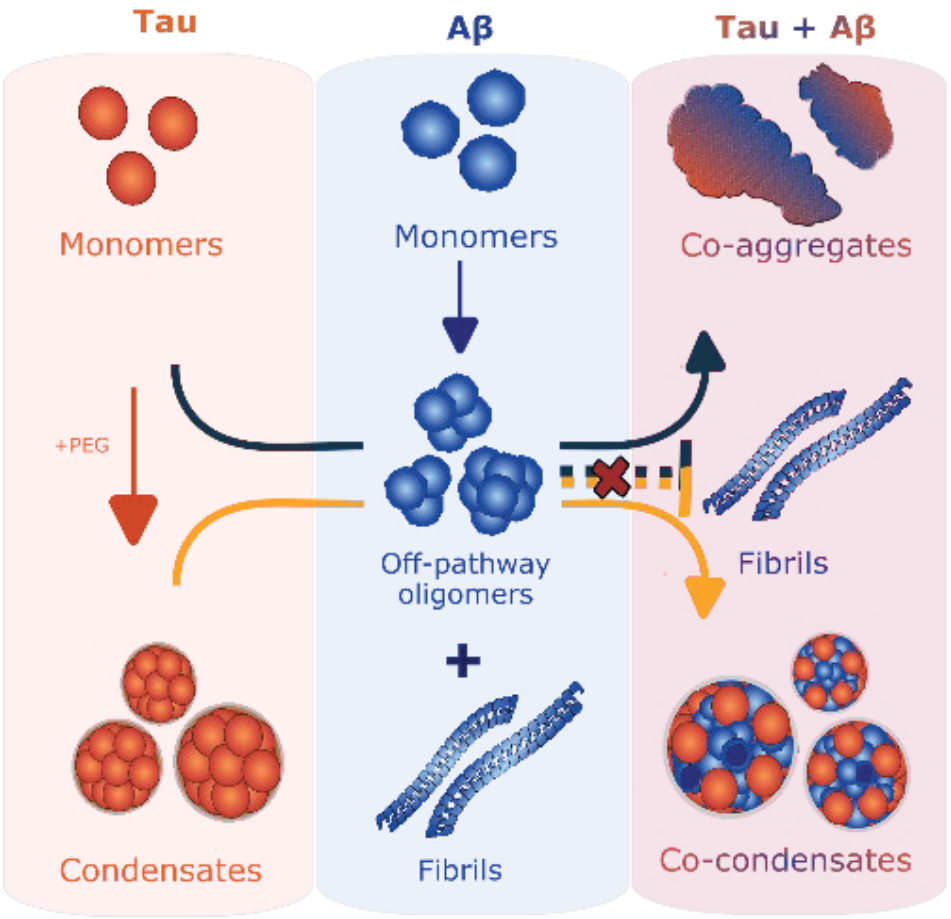

Fig 5.3: Interaction of tau and AβOs. Tau interacts with AβOs under LLPS and non-LLPS conditions leading to the formation of co-condensates and co-aggregates respectively. Tau inhibited the transition of these AβOs into fibril formation indicating that these assemblies act as a reservoir for AβOs.

Chapter 6. APPENDIX

6.1 Tau amino acid sequence

MAEPRQEFEVMEDHAGTYGLGDRKDQGGYTMHQDQEGDTDAGLKESPLQTPTEDGSEEPGSETSDAKSTPTAEDVTAPLVDEGAPG
KQAAAQPHTEIPEGTTAEEAGIGDTPSLEDEAAGHVTQARMVSKSKDGTGSDDKKAKGADGKTKIATPRGAAPPGQKGQANATRIPAKT
PPAPKTPPSSGEPPKSGDRSGYSSPGSPGTPGSRSRTPSLPTPPTREPKKAVVRTPPKSPSSAKSRLQTAPVPMPDLKNVKSKIGSTENL
KHQPGGGKVQIINKKLDLSNVQSKCGSKDNIKHVPGGGSVQIVYKPVDLSKVTSKCGSLGNIHHKPGGGQVEVKSEKLDFKDRVQSK
IGSLDNITHVPGGGNKKIETHKLTFRENAKAKTDHGAEIVYKSPVVSGDTSPRHLSNVSSTGSIDMVDSPQLATLADEVSASLAKQGL

6.2 DimAβ amino acid sequence

MDAEFRHDSGYEVHHQKLVFFAEDVGSNKGAIIGLMVGGVVGGGGSGGGGSGGGGSGGGGSDAEFRHDSGYEVHHQKLVFFAE
DVGSNKGAIIGLMVGGVV

6.3 Fluorescent labelling of tau

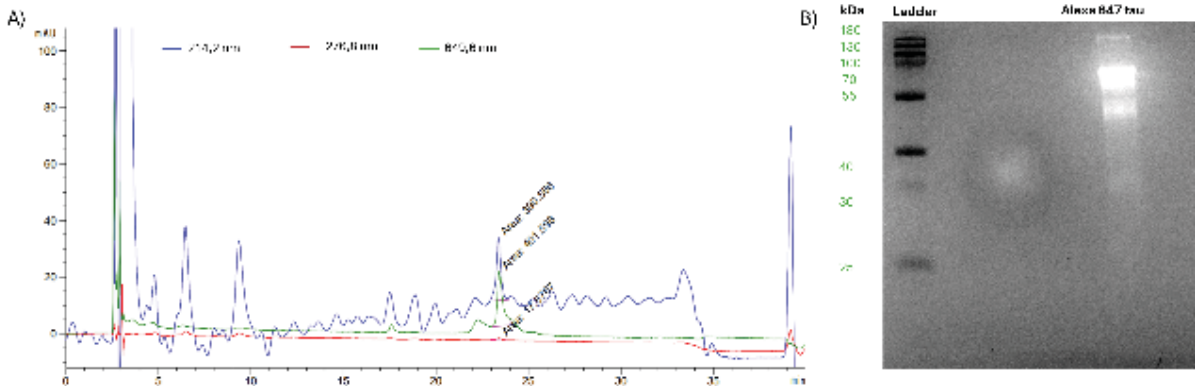

Fig 6.1: Fluorescent labelling of tau. A) HPLC chromatogram of Alexa 647 labelling of tau. **B)** SDS-gel of labelled tau.

6.4 Fluorescent labelling of dimAβ

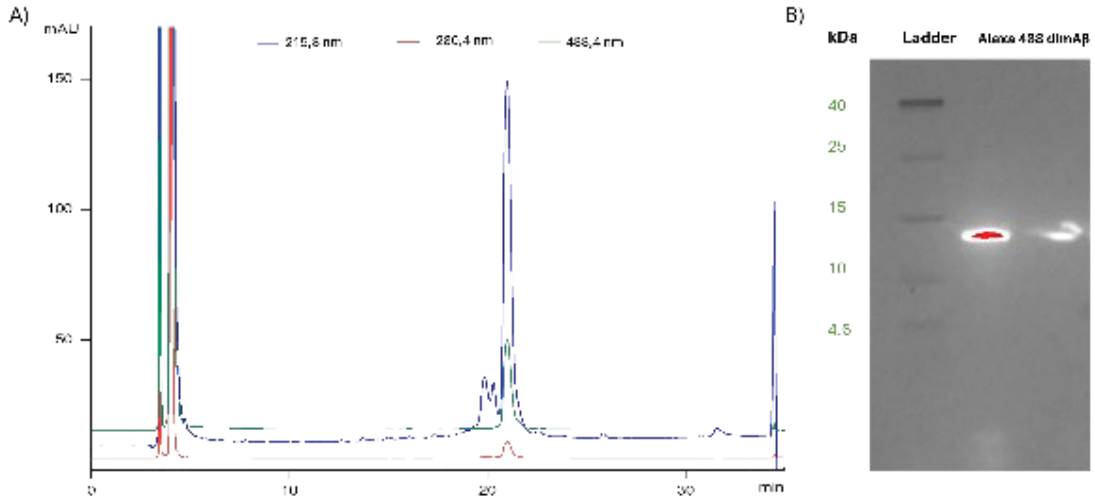

Fig 6.2: Fluorescent labelling of dimAβ. A) HPLC chromatogram of Alexa 488 labelling of dimAβ. **B)** SDS-gel of labelled dimAβ.

6.5 FRAP half-times of recovery (t-half) and immobile fractions

Table 6.1**:** T-half and immobile fraction of tau in the homotypic condensates from 25 FRAP experiments.

t-half	Immobile fraction
17.99	0.17012
24.41	0.003837
28.54	0.220734
20.8	0.184762
11.89	0.06396
23.64	0.065693
26.65	0.178153
16.5	0.04697
22.35	0.206352
26.33	0.198425
19.22	0.17976
45.17	0.313961
56.6	0.256547
83.4	0.373361
70.2	0.627304
88.3	0.639615
59.8	0.468873
86.9	0.176671
66.5	0.422595
62.37	0.112805
57.9	0.245036
49.43	0.327705
57.22	0.375389
52.82	0.292816
76.8	0.189355

Table 6.2**:** T-half and immobile fraction of tau in the heterotypic condensates from 25 FRAP experiments.

t-half	Immobile fraction
46.47	0.20892
44.6	0.423722
64.7	0.266338
61.65	0.224797
44.65	0.389491
54.22	0.530966
52.5	0.537935
61.88	0.64464
84.82	0.511459
78.66	0.430665
70.4	0.188979
83.2	0.590939

50.29	0.540852
84	0.235508
76.5	0.166689
78.3	0.260482
78.66	0.191703
96.65	0.361407
87.83	0.598222
96.25	0.13753
82.2	0.322933
89.88	0.803178
102.36	0.463262
71.73	0.787331
79.8	0.706913
46.47	0.20892

Table 6.3**:** T-half and immobile fraction of dimAβ in in the heterotypic condensates from 25 FRAP experiments.

t-half	Immobile fraction
75	0.459482
38.5	0.523222
62.04	0.689677
61.8	0.8392
89.4	0.648433
60.26	0.481904
28.3	0.53597
41.9	0.354611
38.5	0.128871
65.37	-0.02786
37.05	0.733675
83	0.083095
43.1	0.464923
78.12	0.693732
80.4	0.625892
140	0.283583
115.7	0.191377
235.7	0.131118
99.3	0.227209
73.1	0.591386
289.9	0.703275
67.3	0.139984
61.3	0.576639
106.8	0.502982
85	0.555854

6.6 Comparison of Alexa 647 and Alexa 488 fluorophores

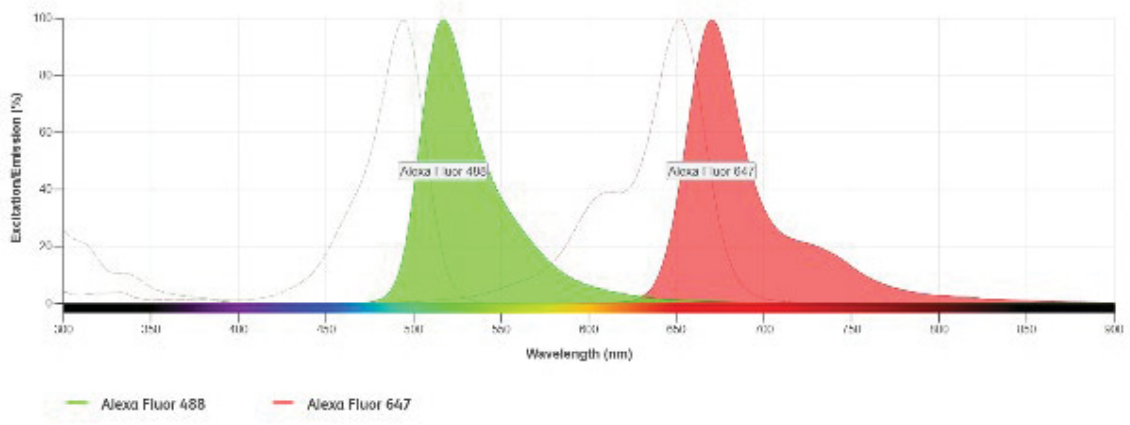

Fig 6.3: Emission and excitation maxima of Alexa 488 and Alexa 647. Created using bdbiosciences.com

6.7 Buffers

10X PBS (pH 7.4)	1.37 M NaCl 100 mM Na2HPO4 18 mM KH2PO4 27 mM KCl
4X Laemmli Buffer	1.37 M NaCl 100 mM Na2HPO4 18 mM KH2PO4 27 mM KCl
Coomassie blue staining	0.02% Coomassie brilliant blue 5% aluminium sulfate 10% ethanol 2% orthophosphoric acid
10X TGS (pH 8.8)	250 mM Tris 1.92 M Glycine 1% SDS

10X Tris-tricine SDS-Page kathode buffer	1 M tricine 1% SDS 1 M Tris
10X Tris-tricine SDS-Page anode buffer (pH 8.9)	2 M Tris
10X M9 salt	33.7 mM Na_2HPO_4 22 mM KH_2PO_4 8.55 mM NaCl
1X TBST (pH 7.5)	20 mM Tris 150 mM NaCl 0.1% Tween-20

References

1. Dugger BN, Dickson DW. Pathology of Neurodegenerative Diseases. Cold Spring Harb Perspect Biol. 2017 Jan 7;9(7):a028035.

2. Van Schependom J, D'haeseleer M. Advances in Neurodegenerative Diseases. J Clin Med. 2023 Jan;12(5):1709.

3. Gogia N, Tare M, Kannan R, Singh A. Editorial: Protein misfolding, altered mechanisms and neurodegeneration. Front Mol Neurosci. 2023 Feb 1;16:1134855.

4. Kovacs GG. Chapter 21 - Concepts and classification of neurodegenerative diseases. In: Kovacs GG, Alafuzoff I, editors. Handbook of Clinical Neurology [Internet]. Elsevier; 2018 [cited 2025 July 31]. p. 301–7. (Neuropathology; vol. 145). Available from: https://www.sciencedirect.com/science/article/pii/B9780128023952000213

5. Kovacs GG. Molecular Pathological Classification of Neurodegenerative Diseases: Turning towards Precision Medicine. Int J Mol Sci. 2016 Feb;17(2):189.

6. Piaceri I, Nacmias B, Sorbi S. Genetics of familial and sporadic Alzheimer's disease. Front Biosci Elite Ed. 2013 Jan 1;5(1):167–77.

7. Dorszewska J, Prendecki M, Oczkowska A, Dezor M, Kozubski W. Molecular Basis of Familial and Sporadic Alzheimer's Disease. Curr Alzheimer Res. 2016;13(9):952–63.

8. Papapetropoulos S, Adi N, Ellul J, Argyriou AA, Chroni E. A prospective study of familial versus sporadic Parkinson's disease. Neurodegener Dis. 2007;4(6):424–7.

9. Bertram L, Tanzi RE. The genetic epidemiology of neurodegenerative disease. J Clin Invest. 2005 June 1;115(6):1449–57.

10. Mitsui J, Tsuji S. Genomic aspects of sporadic neurodegenerative diseases. Biochem Biophys Res Commun. 2014 Sept 19;452(2):221–5.

11. Rajendran K, Krishnan UM. Biomarkers in Alzheimer's disease. Clin Chim Acta. 2024 Aug 15;562:119857.

12. Shin JH. Dementia Epidemiology Fact Sheet 2022. Ann Rehabil Med. 2022 Apr;46(2):53–9.

13. Trojsi F, Christidi F, Migliaccio R, Santamaría-García H, Santangelo G. Behavioural and Cognitive Changes in Neurodegenerative Diseases and Brain Injury. Behav Neurol. 2018 July 25;2018:4935915.

14. Pandya VA, Patani R. Region-specific vulnerability in neurodegeneration: lessons from normal ageing. Ageing Res Rev. 2021 May;67:101311.

15. DeTure MA, Dickson DW. The neuropathological diagnosis of Alzheimer's disease. Mol Neurodegener. 2019 Aug 2;14(1):32.

16. Guatteo E, Berretta N, Monda V, Ledonne A, Mercuri NB. Pathophysiological Features of Nigral Dopaminergic Neurons in Animal Models of Parkinson's Disease. Int J Mol Sci. 2022 Apr 19;23(9):4508.

17. Blumenstock S, Dudanova I. Cortical and Striatal Circuits in Huntington's Disease. Front Neurosci [Internet]. 2020 Feb 6 [cited 2025 Nov 2];14. Available from: https://www.frontiersin.org/journals/neuroscience/articles/10.3389/fnins.2020.00082/full

18. Mey GM, Mahajan KR, DeSilva TM. Neurodegeneration in multiple sclerosis. WIREs Mech Dis. 2023;15(1):e1583.

19. Wilson DM, Cookson MR, Van Den Bosch L, Zetterberg H, Holtzman DM, Dewachter I. Hallmarks of neurodegenerative diseases. Cell. 2023 Feb 16;186(4):693–714.

20. Gadhave DG, Sugandhi VV, Jha SK, Nangare SN, Gupta G, Singh SK, et al. Neurodegenerative disorders: Mechanisms of degeneration and therapeutic approaches with their clinical relevance. Ageing Res Rev. 2024 Aug 1;99:102357.

21. Hou Y, Dan X, Babbar M, Wei Y, Hasselbalch SG, Croteau DL, et al. Ageing as a risk factor for neurodegenerative disease. Nat Rev Neurol. 2019 Oct;15(10):565–81.

22. Bertram L, Tanzi RE. The genetic epidemiology of neurodegenerative disease. J Clin Invest. 2005 June 1;115(6):1449–57.

23. Cannon JR, Greenamyre JT. The Role of Environmental Exposures in Neurodegeneration and Neurodegenerative Diseases. Toxicol Sci. 2011 Dec;124(2):225–50.

24. Corney KB, Stuart AL, Mohebbi M, Pasco JA, Kavanagh BE, Sui SX, et al. Modifiable Lifestyle Factors and Cognitive Function: A Population-Based Study Amongst Nondemented Men. Acta Neurol Scand. 2024;2024(1):1935091.

25. Cummings JL. Alzheimer's Disease. N Engl J Med. 2004 July 1;351(1):56–67.

26. Goedert M, Ghetti B. Alois Alzheimer: His Life and Times. Brain Pathol. 2007 Feb 26;17(1):57–62.

27. 2024 Alzheimer's disease facts and figures. Alzheimers Dement. 2024;20(5):3708–821.

28. Soria Lopez JA, González HM, Léger GC. Chapter 13 - Alzheimer's disease. In: Dekosky ST, Asthana S, editors. Handbook of Clinical Neurology [Internet]. Elsevier; 2019 [cited 2025 Sept 24]. p. 231–55. (Geriatric Neurology; vol. 167). Available from: https://www.sciencedirect.com/science/article/pii/B9780128047668000133

29. Crews L, Masliah E. Molecular mechanisms of neurodegeneration in Alzheimer's disease. Hum Mol Genet. 2010 Apr 15;19(R1):R12–20.

30. DeTure MA, Dickson DW. The neuropathological diagnosis of Alzheimer's disease. Mol Neurodegener. 2019 Aug 2;14(1):32.

31. Passeri E, Elkhoury K, Morsink M, Broersen K, Linder M, Tamayol A, et al. Alzheimer's Disease: Treatment Strategies and Their Limitations. Int J Mol Sci. 2022 Nov 12;23(22):13954.

32. Lautenschlager NT, Anstey KJ, Kurz AF. Non-pharmacological strategies to delay cognitive decline. Maturitas. 2014 Oct;79(2):170–3.

33. Pharmacological Management of Neurodegenerative Disorders Current and Future Approaches [Internet]. [cited 2025 Nov 2]. Available from: https://www.ijsrtjournal.com/article/Pharmacological+Management+of+Neurodegenerative+Disorders+Current+and+Future+Approaches

34. Villain N, Planche V, Lilamand M, Cordonnier C, Soto-Martin M, Mollion H, et al. Lecanemab for early Alzheimer's disease: Appropriate use recommendations from the French federation of memory clinics. J Prev Alzheimers Dis. 2025 Apr 1;12(4):100094.

35. van Dyck CH, Swanson CJ, Aisen P, Bateman RJ, Chen C, Gee M, et al. Lecanemab in Early Alzheimer's Disease. N Engl J Med. 2023 Jan 5;388(1):9–21.

36. Xing X, Zhang X, Wang K, Wang Z, Feng Y, Li X, et al. Post-marketing safety concerns with lecanemab: a pharmacovigilance study based on the FDA Adverse Event Reporting System database. Alzheimers Res Ther. 2025 Jan 8;17:15.

37. Abdelazim K, Allam AA, Afifi B, Abdulazeem H, Elbehiry AI. The efficacy and safety of lecanemab 10 mg/kg biweekly compared to a placebo in patients with Alzheimer's disease: a systematic review and meta-analysis of randomized controlled trials. Neurol Sci. 2024 Aug 1;45(8):3583–97.

38. Chong FP, Ng KY, Koh RY, Chye SM. Tau Proteins and Tauopathies in Alzheimer's Disease. Cell Mol Neurobiol. 2018 Jan 3;38(5):965–80.

39. Boutajangout A, Sigurdsson EM, Krishnamurthy PK. Tau as a Therapeutic Target for Alzheimer's Disease. Curr Alzheimer Res. 2011 Sept;8(6):666–77.

40. Weingarten MD, Lockwood AH, Hwo SY, Kirschner MW. A protein factor essential for microtubule assembly. Proc Natl Acad Sci. 1975 May;72(5):1858–62.

41. Parra Bravo C, Naguib SA, Gan L. Cellular and pathological functions of tau. Nat Rev Mol Cell Biol. 2024 Nov;25(11):845–64.

42. Luo Y, Ma B, Nussinov R, Wei G. Structural Insight into Tau Protein's Paradox of Intrinsically Disordered Behavior, Self-Acetylation Activity, and Aggregation. J Phys Chem Lett. 2014 Sept 4;5(17):3026–31.

43. Skrabana R, Skrabanova M, Csokova N, Sevcik J, Novak M. Intrinsically disordered tau protein in Alzheimer's tangles: a coincidence or a rule? Bratisl Lek Listy. 2006;107(9–10):354–8.

44. Chen Y, Yu Y. Tau and neuroinflammation in Alzheimer's disease: interplay mechanisms and clinical translation. J Neuroinflammation. 2023 July 14;20(1):165.

45. Barbier P, Zejneli O, Martinho M, Lasorsa A, Belle V, Smet-Nocca C, et al. Role of Tau as a Microtubule-Associated Protein: Structural and Functional Aspects. Front Aging Neurosci. 2019 Aug 7;11:204.

46. Buchholz S, Zempel H. The six brain-specific TAU isoforms and their role in Alzheimer's disease and related neurodegenerative dementia syndromes. Alzheimers Dement. 2024 Mar 31;20(5):3606–28.

47. Zeng Y, Yang J, Zhang B, Gao M, Su Z, Huang Y. The structure and phase of tau: from monomer to amyloid filament. Cell Mol Life Sci CMLS. 2020 Oct 19;78(5):1873–86.

48. Wang Y, Mandelkow E. Tau in physiology and pathology. Nat Rev Neurosci. 2016 Jan;17(1):22–35.

49. Chen Y, Yu Y. Tau and neuroinflammation in Alzheimer's disease: interplay mechanisms and clinical translation. J Neuroinflammation. 2023 July 14;20(1):165.

50. Goedert M. Tau gene mutations and their effects. Mov Disord. 2005;20(S12):S45–52.

51. Hutton M, Lendon CL, Rizzu P, Baker M, Froelich S, Houlden H, et al. Association of missense and 5'-splice-site mutations in tau with the inherited dementia FTDP-17. Nature. 1998 June;393(6686):702–5.

52. Alquezar C, Arya S, Kao AW. Tau Post-translational Modifications: Dynamic Transformers of Tau Function, Degradation, and Aggregation. Front Neurol. 2021 Jan 7;11:595532.

53. Zhong Q, Xiao X, Qiu Y, Xu Z, Chen C, Chong B, et al. Protein posttranslational modifications in health and diseases: Functions, regulatory mechanisms, and therapeutic implications. MedComm. 2023 May 2;4(3):e261.

54. Lee JM, Hammarén HM, Savitski MM, Baek SH. Control of protein stability by post-translational modifications. Nat Commun. 2023 Jan 13;14(1):201.

55. Wesseling H, Mair W, Kumar M, Schlaffner CN, Tang S, Beerepoot P, et al. Tau PTM Profiles Identify Patient Heterogeneity and Stages of Alzheimer's Disease. Cell. 2020 Dec 10;183(6):1699-1713.e13.

56. Johnson GVW, Stoothoff WH. Tau phosphorylation in neuronal cell function and dysfunction. J Cell Sci. 2004 Nov 15;117(24):5721–9.

57. Köpke E, Tung YC, Shaikh S, Alonso AC, Iqbal K, Grundke-Iqbal I. Microtubule-associated protein tau. Abnormal phosphorylation of a non-paired helical filament pool in Alzheimer disease. J Biol Chem. 1993 Nov 15;268(32):24374–84.

58. Liu E, Zhang Y, Wang JZ. Updates in Alzheimer's disease: from basic research to diagnosis and therapies. Transl Neurodegener. 2024 Sept 4;13(1):45.

59. Rawat P, Sehar U, Bisht J, Selman A, Culberson J, Reddy PH. Phosphorylated Tau in Alzheimer's Disease and Other Tauopathies. Int J Mol Sci. 2022 Oct 25;23(21):12841.

60. Abasi LS, Elathram N, Movva M, Deep A, Corbett KD, Debelouchina GT. Phosphorylation regulates tau's phase separation behavior and interactions with chromatin. Commun Biol. 2024 Mar 1;7(1):251.

61. Alonso A del C, Zaidi T, Novak M, Grundke-Iqbal I, Iqbal K. Hyperphosphorylation induces self-assembly of τ into tangles of paired helical filaments/straight filaments. Proc Natl Acad Sci U S A. 2001 June 5;98(12):6923–8.

62. Alonso ADC, Grundke-Iqbal I, Iqbal K. Alzheimer's disease hyperphosphorylated tau sequesters normal tau into tangles of filaments and disassembles microtubules. Nat Med. 1996 July;2(7):783–7.

63. Shin YRO& MK. Decoding tau acetylation in Alzheimer's disease and tauopathies: from site-specific mechanisms to therapeutic horizons. BMB Rep. 2025 Aug 31;58(8):325–39.

64. Chakraborty P, Rivière G, Hebestreit A, de Opakua AI, Vorberg IM, Andreas LB, et al. Acetylation discriminates disease-specific tau deposition. Nat Commun. 2023 Sept 22;14(1):5919.

65. Reynolds MR, Reyes JF, Fu Y, Bigio EH, Guillozet-Bongaarts AL, Berry RW, et al. Tau nitration occurs at tyrosine 29 in the fibrillar lesions of Alzheimer's disease and other tauopathies. J Neurosci Off J Soc Neurosci. 2006 Oct 18;26(42):10636–45.

66. Reyes JF, Reynolds MR, Horowitz PM, Fu Y, Guillozet-Bongaarts AL, Berry R, et al. A possible link between astrocyte activation and tau nitration in Alzheimer's disease. Neurobiol Dis. 2008 Aug 1;31(2):198–208.

67. Balmik AA, Chinnathambi S. Methylation as a key regulator of Tau aggregation and neuronal health in Alzheimer's disease. Cell Commun Signal CCS. 2021 May 7;19:51.

68. Li L, Jiang Y, Wang JZ, Liu R, Wang X. Tau Ubiquitination in Alzheimer's Disease. Front Neurol [Internet]. 2022 Feb 8 [cited 2025 Oct 8];12. Available from: https://www.frontiersin.org/journals/neurology/articles/10.3389/fneur.2021.786353/full

69. Schweers O, Mandelkow EM, Biernat J, Mandelkow E. Oxidation of cysteine-322 in the repeat domain of microtubule-associated protein tau controls the in vitro assembly of paired helical filaments. Proc Natl Acad Sci U S A. 1995 Aug 29;92(18):8463–7.

70. Alquezar C, Arya S, Kao AW. Tau Post-translational Modifications: Dynamic Transformers of Tau Function, Degradation, and Aggregation. Front Neurol. 2021 Jan 7;11:595532.

71. Strang KH, Golde TE, Giasson BI. MAPT mutations, tauopathy, and mechanisms of neurodegeneration. Lab Investig J Tech Methods Pathol. 2019 July;99(7):912–28.

72. Creekmore BC, Watanabe R, Lee EB. Neurodegenerative Disease Tauopathies. Annu Rev Pathol. 2024 Jan 24;19:345–70.

73. Zheng H, Sun H, Cai Q, Tai HC. The Enigma of Tau Protein Aggregation: Mechanistic Insights and Future Challenges. Int J Mol Sci. 2024 May 2;25(9):4969.

74. Lo CH, Lim CKW, Ding Z, Wickramasinghe SP, Braun AR, Ashe KH, et al. Targeting the ensemble of heterogeneous tau oligomers in cells: A novel small molecule screening platform for tauopathies. Alzheimers Dement J Alzheimers Assoc. 2019 Nov;15(11):1489–502.

75. Ghag G, Bhatt N, Cantu DV, Guerrero-Munoz MJ, Ellsworth A, Sengupta U, et al. Soluble tau aggregates, not large fibrils, are the toxic species that display seeding and cross-seeding behavior. Protein Sci. 2018;27(11):1901–9.

76. Patterson KR, Remmers C, Fu Y, Brooker S, Kanaan NM, Vana L, et al. Characterization of Prefibrillar Tau Oligomers *in Vitro* and in Alzheimer Disease*. J Biol Chem. 2011 July 1;286(26):23063–76.

77. Berger Z, Roder H, Hanna A, Carlson A, Rangachari V, Yue M, et al. Accumulation of Pathological Tau Species and Memory Loss in a Conditional Model of Tauopathy. J Neurosci. 2007 Apr 4;27(14):3650–62.

78. Castillo-Carranza DL, Gerson JE, Sengupta U, Guerrero-Muñoz MJ, Lasagna-Reeves CA, Kayed R. Specific Targeting of Tau Oligomers in Htau Mice Prevents Cognitive Impairment and Tau Toxicity Following Injection with Brain-Derived Tau Oligomeric Seeds. J Alzheimer's Dis. 2014 May 27;40(s1):S97–111.

79. Niewiadomska G, Niewiadomski W, Steczkowska M, Gasiorowska A. Tau Oligomers Neurotoxicity. Life Basel Switz. 2021 Jan 6;11(1):28.

80. Lasagna-Reeves CA, Castillo-Carranza DL, Sengupta U, Clos AL, Jackson GR, Kayed R. Tau oligomers impair memory and induce synaptic and mitochondrial dysfunction in wild-type mice. Mol Neurodegener. 2011 June 6;6(1):39.

81. Al-Hilaly YK, Foster BE, Biasetti L, Lutter L, Pollack SJ, Rickard JE, et al. Tau (297-391) forms filaments that structurally mimic the core of paired helical filaments in Alzheimer's disease brain. FEBS Lett. 2020;594(5):944–50.

82. Lövestam S, Koh FA, van Knippenberg B, Kotecha A, Murzin AG, Goedert M, et al. Assembly of recombinant tau into filaments identical to those of Alzheimer's disease and chronic traumatic encephalopathy. Egelman EH, Chin J, Egelman EH, Wang F, Serpell LC, editors. eLife. 2022 Mar 4;11:e76494.

83. Guzman-Martinez L, Farias GA, Maccioni RB. Tau Oligomers as Potential Targets for Alzheimer's Diagnosis and Novel Drugs. Front Neurol [Internet]. 2013 Oct 28 [cited 2025 Oct 9];4. Available from: https://www.frontiersin.org/journals/neurology/articles/10.3389/fneur.2013.00167/full

84. Ono K, Yamada M. Low-n oligomers as therapeutic targets of Alzheimer's disease. J Neurochem. 2011;117(1):19–28.

85. Gerson JE, Castillo-Carranza DL, Kayed R. Advances in Therapeutics for Neurodegenerative Tauopathies: Moving toward the Specific Targeting of the Most Toxic Tau Species. ACS Chem Neurosci. 2014 Sept 17;5(9):752–69.

86. Ingham DJ, Hillyer KM, McGuire MJ, Gamblin TC. In vitro Tau Aggregation Inducer Molecules Influence the Effects of MAPT Mutations on Aggregation Dynamics. Biochemistry. 2022 July 5;61(13):1243–59.

87. Tetz G, Pinho M, Pritzkow S, Mendez N, Soto C, Tetz V. Bacterial DNA promotes Tau aggregation. Sci Rep. 2020 Feb 11;10(1):2369.

88. Zwierzchowski-Zarate AN, Mendoza-Oliva A, Kashmer OM, Collazo-Lopez JE, White CL, Diamond MI. RNA induces unique tau strains and stabilizes Alzheimer's disease seeds. J Biol Chem. 2022 June 11;298(8):102132.

89. Goedert M, Jakes R, Spillantini MG, Hasegawa M, Smith MJ, Crowther RA. Assembly of microtubule-associated protein tau into Alzheimer-like filaments induced by sulphated glycosaminoglycans. Nature. 1996 Oct;383(6600):550–3.

90. Ambadipudi S, Biernat J, Riedel D, Mandelkow E, Zweckstetter M. Liquid–liquid phase separation of the microtubule-binding repeats of the Alzheimer-related protein Tau. Nat Commun. 2017 Aug 17;8(1):275.

91. Kanaan NM, Hamel C, Grabinski T, Combs B. Liquid-liquid phase separation induces pathogenic tau conformations in vitro. Nat Commun. 2020 June 4;11(1):2809.

92. Wegmann S, Eftekharzadeh B, Tepper K, Zoltowska KM, Bennett RE, Dujardin S, et al. Tau protein liquid–liquid phase separation can initiate tau aggregation. EMBO J. 2018 Apr 3;37(7):e98049.

93. Alyenbaawi H, Allison WT, Mok SA. Prion-Like Propagation Mechanisms in Tauopathies and Traumatic Brain Injury: Challenges and Prospects. Biomolecules. 2020 Oct 27;10(11):1487.

94. Narasimhan S, Guo JL, Changolkar L, Stieber A, McBride JD, Silva LV, et al. Pathological Tau Strains from Human Brains Recapitulate the Diversity of Tauopathies in Nontransgenic Mouse Brain. J Neurosci. 2017 Nov 22;37(47):11406–23.

95. Clavaguera F, Akatsu H, Fraser G, Crowther RA, Frank S, Hench J, et al. Brain homogenates from human tauopathies induce tau inclusions in mouse brain. Proc Natl Acad Sci U S A. 2013 June 4;110(23):9535–40.

96. Li Y, Liu Y, Yu XY, Xu Y, Pan X, Sun Y, et al. Membraneless organelles in health and disease: exploring the molecular basis, physiological roles and pathological implications. Signal Transduct Target Ther. 2024 Nov 18;9(1):305.

97. Zhao YG, Zhang H. Phase Separation in Membrane Biology: The Interplay between Membrane-Bound Organelles and Membraneless Condensates. Dev Cell. 2020 Oct 12;55(1):30–44.

98. Li Y, Liu Y, Yu XY, Xu Y, Pan X, Sun Y, et al. Membraneless organelles in health and disease: exploring the molecular basis, physiological roles and pathological implications. Signal Transduct Target Ther. 2024 Nov 18;9(1):305.

99. Tong X, Tang R, Xu J, Wang W, Zhao Y, Yu X, et al. Liquid–liquid phase separation in tumor biology. Signal Transduct Target Ther. 2022 July 8;7(1):221.

100. Lu X, Lu J, Li S, Feng S, Wang Y, Cui L. The Role of Liquid-Liquid Phase Separation in the Accumulation of Pathological Proteins: New Perspectives on the Mechanism of Neurodegenerative Diseases. Aging Dis. 2024 Apr 20;16(2):769–86.

101. Peng PH, Hsu KW, Wu KJ. Liquid-liquid phase separation (LLPS) in cellular physiology and tumor biology. Am J Cancer Res. 2021 Aug 15;11(8):3766–76.

102. Krainer G, Welsh TJ, Joseph JA, Espinosa JR, Wittmann S, de Csilléry E, et al. Reentrant liquid condensate phase of proteins is stabilized by hydrophobic and non-ionic interactions. Nat Commun. 2021 Feb 17;12(1):1085.

103. Niu X, Zhang L, Wu Y, Zong Z, Wang B, Liu J, et al. Biomolecular condensates: Formation mechanisms, biological functions, and therapeutic targets. MedComm. 2023 Feb 28;4(2):e223.

104. Lu X, Lu J, Li S, Feng S, Wang Y, Cui L. The Role of Liquid-Liquid Phase Separation in the Accumulation of Pathological Proteins: New Perspectives on the Mechanism of Neurodegenerative Diseases. Aging Dis. 2024 Apr 20;16(2):769–86.

105. Luo YY, Wu JJ, Li YM. Regulation of liquid–liquid phase separation with focus on post-translational modifications. Chem Commun. 2021 Dec 9;57(98):13275–87.

106. Zbinden A, Pérez-Berlanga M, De Rossi P, Polymenidou M. Phase Separation and Neurodegenerative Diseases: A Disturbance in the Force. Dev Cell. 2020 Oct 12;55(1):45–68.

107. Li YR, King OD, Shorter J, Gitler AD. Stress granules as crucibles of ALS pathogenesis. J Cell Biol. 2013 Apr 29;201(3):361–72.

108. Gracia P, Polanco D, Tarancón-Díez J, Serra I, Bracci M, Oroz J, et al. Molecular mechanism for the synchronized electrostatic coacervation and co-aggregation of alpha-synuclein and tau. Nat Commun. 2022 Aug 6;13(1):4586.

109. Xu Z, Wang W, Cao Y, Xue B. Liquid-liquid phase separation: Fundamental physical principles, biological implications, and applications in supramolecular materials engineering. Supramol Mater. 2023 Dec 1;2:100049.

110. Poudyal M, Patel K, Gadhe L, Sawner AS, Kadu P, Datta D, et al. Intermolecular interactions underlie protein/peptide phase separation irrespective of sequence and structure at crowded milieu. Nat Commun. 2023 Oct 4;14(1):6199.

111. Flory PJ. Thermodynamics of High Polymer Solutions. J Chem Phys. 1942 Jan 1;10(1):51–61.

112. Qian D, Michaels TCT, Knowles TPJ. Analytical Solution to the Flory–Huggins Model. J Phys Chem Lett. 2022 Aug 25;13(33):7853–60.

113. Mao S, Kuldinow D, Haataja MP, Košmrlj A. Phase behavior and morphology of multicomponent liquid mixtures. Soft Matter. 2019 Feb 6;15(6):1297–311.

114. Zhou HX, Nguemaha V, Mazarakos K, Qin S. Why do disordered and structured proteins behave differently in phase separation? Trends Biochem Sci. 2018 July;43(7):499–516.

115. Lin Y, McCarty J, Rauch JN, Delaney KT, Kosik KS, Fredrickson GH, et al. Narrow equilibrium window for complex coacervation of tau and RNA under cellular conditions. Shan Y, Barkai N, Castaneda C, editors. eLife. 2019 Apr 5;8:e42571.

116. Li L ge, Hou Z. Theoretical modelling of liquid–liquid phase separation: from particle-based to field-based simulation. Biophys Rep. 2022 Apr 30;8(2):55–67.

117. Shin Y. Rich Phase Separation Behavior of Biomolecules. Mol Cells. 2022 Jan 1;45(1):6–15.

118. Emenecker RJ, Holehouse AS, Strader LC. Biological Phase Separation and Biomolecular Condensates in Plants. Annu Rev Plant Biol. 2021 June 17;72:17–46.

119. Crowe CD, Keating CD. Liquid–liquid phase separation in artificial cells. Interface Focus. 2018 Aug 17;8(5):20180032.

120. Abbas M, P. Lipiński W, Wang J, Spruijt E. Peptide-based coacervates as biomimetic protocells. Chem Soc Rev. 2021;50(6):3690–705.

121. Naz M, Zhang L, Chen C, Yang S, Dou H, Mann S, et al. Self-assembly of stabilized droplets from liquid–liquid phase separation for higher-order structures and functions. Commun Chem. 2024 Apr 9;7(1):1–14.

122. Naz M, Zhang L, Chen C, Yang S, Dou H, Mann S, et al. Self-assembly of stabilized droplets from liquid–liquid phase separation for higher-order structures and functions. Commun Chem. 2024 Apr 9;7(1):79.

123. Intrinsically disordered proteins in cellular signalling and regulation | Nature Reviews Molecular Cell Biology [Internet]. [cited 2025 June 8]. Available from: https://www.nature.com/articles/nrm3920

124. Witus SR, Tuttle LM, Li W, Zelter A, Wang M, Kermoade KE, et al. BRCA1/BARD1 intrinsically disordered regions facilitate chromatin recruitment and ubiquitylation. EMBO J. 2023 Aug;42(15):e113565.

125. Intrinsic disorder is an essential characteristic of components in the conserved circadian circuit | Cell Communication and Signaling [Internet]. [cited 2025 June 8]. Available from: https://link.springer.com/article/10.1186/s12964-020-00658-y

126. Tompa P, Csermely P. The role of structural disorder in the function of RNA and protein chaperones. FASEB J. 2004;18(11):1169–75.

127. Holehouse AS, Kragelund BB. The molecular basis for cellular function of intrinsically disordered protein regions. Nat Rev Mol Cell Biol. 2024 Mar;25(3):187–211.

128. Kastano K, Mier P, Andrade-Navarro MA. The Role of Low Complexity Regions in Protein Interaction Modes: An Illustration in Huntingtin. Int J Mol Sci. 2021 Feb 9;22(4):1727.

129. Nordenskiöld L, Shi X, Korolev N, Zhao L, Zhai Z, Lindman B. Liquid-liquid phase separation (LLPS) in DNA and chromatin systems from the perspective of colloid physical chemistry. Adv Colloid Interface Sci. 2024 Apr 1;326:103133.

130. Wang Q, Chen T, Yan S, Li Y, Qi B. Segregative phase separation of protein/polysaccharide mixed systems: Phase separation mechanisms, characterization technologies, influencing factors, and food applications—a review. Food Res Int. 2025 May 1;208:116240.

131. Islam M, Shen F, Regmi D, Petersen K, Karim MRU, Du D. Tau liquid–liquid phase separation: At the crossroads of tau physiology and tauopathy. J Cell Physiol. 2024;239(6):e30853.

132. Hernández-Vega A, Braun M, Scharrel L, Jahnel M, Wegmann S, Hyman BT, et al. Local Nucleation of Microtubule Bundles through Tubulin Concentration into a Condensed Tau Phase. Cell Rep. 2017 Sept;20(10):2304–12.

133. Elbaum-Garfinkle S. Matter over mind: Liquid phase separation and neurodegeneration. J Biol Chem. 2019 May 1;294(18):7160–8.

134. Boyko S, Surewicz K, Surewicz WK. Regulatory mechanisms of tau protein fibrillation under the conditions of liquid–liquid phase separation. Proc Natl Acad Sci. 2020 Dec 15;117(50):31882–90.

135. Savastano A, Flores D, Kadavath H, Biernat J, Mandelkow E, Zweckstetter M. Disease-Associated Tau Phosphorylation Hinders Tubulin Assembly within Tau Condensates. Angew Chem Int Ed. 2021;60(2):726–30.

136. Cohen TJ, Guo JL, Hurtado DE, Kwong LK, Mills IP, Trojanowski JQ, et al. The acetylation of tau inhibits its function and promotes pathological tau aggregation. Nat Commun. 2011 Mar 22;2(1):252.

137. Rai SK, Khanna R, Avni A, Mukhopadhyay S. Heterotypic electrostatic interactions control complex phase separation of tau and prion into multiphasic condensates and co-aggregates. Proc Natl Acad Sci. 2023 Jan 10;120(2):e2216338120.

138. Ash PEA, Lei S, Shattuck J, Boudeau S, Carlomagno Y, Medalla M, et al. TIA1 potentiates tau phase separation and promotes generation of toxic oligomeric tau. Proc Natl Acad Sci. 2021 Mar 2;118(9):e2014188118.

139. Lin Y, Fichou Y, Zeng Z, Hu NY, Han S. Electrostatically Driven Complex Coacervation and Amyloid Aggregation of Tau Are Independent Processes with Overlapping Conditions. ACS Chem Neurosci. 2020 Feb 19;11(4):615–27.

140. Bloom GS. Amyloid-β and tau: the trigger and bullet in Alzheimer disease pathogenesis. JAMA Neurol. 2014 Apr;71(4):505–8.

141. Chen G fang, Xu T hai, Yan Y, Zhou Y ren, Jiang Y, Melcher K, et al. Amyloid beta: structure, biology and structure-based therapeutic development. Acta Pharmacol Sin. 2017 Sept;38(9):1205–35.

142. Hampel H, Hardy J, Blennow K, Chen C, Perry G, Kim SH, et al. The Amyloid-β Pathway in Alzheimer's Disease. Mol Psychiatry. 2021;26(10):5481–503.

143. Ovsepian SV, O'Leary VB, Zaborszky L, Ntziachristos V, Dolly JO. Amyloid Plaques of Alzheimer's Disease as Hotspots of Glutamatergic Activity. Neurosci Rev J Bringing Neurobiol Neurol Psychiatry. 2019 Aug;25(4):288–97.

144. Pfundstein G, Nikonenko AG, Sytnyk V. Amyloid precursor protein (APP) and amyloid β (Aβ) interact with cell adhesion molecules: Implications in Alzheimer's disease and normal physiology. Front Cell Dev Biol [Internet]. 2022 July 26 [cited 2025 Oct 30];10. Available from: https://www.frontiersin.org/journals/cell-and-developmental-biology/articles/10.3389/fcell.2022.969547/full

145. Chow VW, Mattson MP, Wong PC, Gleichmann M. An Overview of APP Processing Enzymes and Products. Neuromolecular Med. 2010 Mar;12(1):1–12.

146. Turner AJ, Fisk L, Nalivaeva NN. Targeting amyloid-degrading enzymes as therapeutic strategies in neurodegeneration. Ann N Y Acad Sci. 2004 Dec;1035:1–20.

147. Yoon SS, Jo SA. Mechanisms of Amyloid-β Peptide Clearance: Potential Therapeutic Targets for Alzheimer's Disease. Biomol Ther. 2012 May;20(3):245–55.

148. Jansen WJ, Ossenkoppele R, Knol DL, Tijms BM, Scheltens P, Verhey FRJ, et al. Prevalence of Cerebral Amyloid Pathology in Persons Without Dementia. JAMA. 2015 May 19;313(19):1924–38.

149. Haass C, Schlossmacher MG, Hung A, Vigo-Pelfreyt C, Mellon A, Ostaszewski BL, et al. Amyloid p-peptide is produced by cultured cells during normal metabolism. 1992;359.

150. Jan A, Gokce O, Luthi-Carter R, Lashuel HA. The Ratio of Monomeric to Aggregated Forms of Aβ40 and Aβ42 Is an Important Determinant of Amyloid-β Aggregation, Fibrillogenesis, and Toxicity*. J Biol Chem. 2008 Oct 17;283(42):28176–89.

151. Cai W, Li L, Sang S, Pan X, Zhong C. Physiological Roles of β-amyloid in Regulating Synaptic Function: Implications for AD Pathophysiology. Neurosci Bull. 2022 Nov 28;39(8):1289–308.

152. Bishop GM, Robinson SR. Physiological roles of amyloid-beta and implications for its removal in Alzheimer's disease. Drugs Aging. 2004;21(10):621–30.

153. Hardy JA, Higgins GA. Alzheimer's Disease: The Amyloid Cascade Hypothesis. Science. 1992 Apr 10;256(5054):184–5.

154. Hardy J, Selkoe DJ. The Amyloid Hypothesis of Alzheimer's Disease: Progress and Problems on the Road to Therapeutics. Science. 2002 July 19;297(5580):353–6.

155. Saidlitz P, Voisin T, Vellas B, Payoux P, Gabelle A, Formaglio M, et al. Amyloid imaging in Alzheimer's disease: A literature review. J Nutr Health Aging. 2014 Aug 1;18(7):723–40.

156. DaRocha-Souto B, Scotton TC, Coma M, Serrano-Pozo A, Hashimoto T, Serenó L, et al. Brain Oligomeric β-Amyloid but Not Total Amyloid Plaque Burden Correlates With Neuronal Loss and Astrocyte Inflammatory Response in Amyloid Precursor Protein/Tau Transgenic Mice. J Neuropathol Exp Neurol. 2011 May;70(5):360–76.

157. Sgourakis NG, Yan Y, McCallum S, Wang C, Garcia AE. The Alzheimer's peptides Aβ40 and 42 adopt distinct conformations in water: A combined MD / NMR study. J Mol Biol. 2007 May 18;368(5):1448–57.

158. Jeong H, Shin H, Hong S, Kim Y. Physiological Roles of Monomeric Amyloid-β and Implications for Alzheimer's Disease Therapeutics. Exp Neurobiol. 2022 Apr 30;31(2):65–88.

159. Azargoonjahromi A. The duality of amyloid-β: its role in normal and Alzheimer's disease states. Mol Brain. 2024 July 17;17(1):44.

160. Niu Z, Gui X, Feng S, Reif B. Aggregation Mechanisms and Molecular Structures of Amyloid-β in Alzheimer's Disease. Chem – Eur J. 2024;30(48):e202400277.

161. Viola KL, Klein WL. Amyloid β oligomers in Alzheimer's disease pathogenesis, treatment, and diagnosis. Acta Neuropathol (Berl). 2015 Feb;129(2):183–206.

162. Cline EN, Bicca MA, Viola KL, Klein WL. The Amyloid-β Oligomer Hypothesis: Beginning of the Third Decade. J Alzheimers Dis JAD. 2018;64(s1):S567–610.

163. Sengupta U, Nilson AN, Kayed R. The Role of Amyloid-β Oligomers in Toxicity, Propagation, and Immunotherapy. EBioMedicine. 2016 Apr 5;6:42–9.

164. Alberdi E, Sánchez-Gómez MV, Cavaliere F, Pérez-Samartín A, Zugaza JL, Trullas R, et al. Amyloid beta oligomers induce Ca2+ dysregulation and neuronal death through activation of ionotropic glutamate receptors. Cell Calcium. 2010 Mar;47(3):264–72.

165. Resende R, Ferreiro E, Pereira C, Resende de Oliveira C. Neurotoxic effect of oligomeric and fibrillar species of amyloid-beta peptide 1-42: involvement of endoplasmic reticulum calcium release in oligomer-induced cell death. Neuroscience. 2008 Aug 26;155(3):725–37.

166. Muschol M, Hoyer W. Amyloid oligomers as on-pathway precursors or off-pathway competitors of fibrils. Front Mol Biosci. 2023 Feb 9;10:1120416.

167. Dear AJ, Meisl G, Šarić A, Michaels TCT, Kjaergaard M, Linse S, et al. Identification of on- and off-pathway oligomers in amyloid fibril formation. Chem Sci. 2020 June 24;11(24):6236–47.

168. Viola KL, Klein WL. Amyloid β oligomers in Alzheimer's disease pathogenesis, treatment, and diagnosis. Acta Neuropathol (Berl). 2015 Feb;129(2):183–206.

169. Schützmann MP, Hasecke F, Bachmann S, Zielinski M, Hänsch S, Schröder GF, et al. Endo-lysosomal Aβ concentration and pH trigger formation of Aβ oligomers that potently induce Tau missorting. Nat Commun. 2021 July 30;12(1):4634.

170. Michaels TCT, Šarić A, Curk S, Bernfur K, Arosio P, Meisl G, et al. Dynamics of oligomer populations formed during the aggregation of Alzheimer's Aβ42 peptide. Nat Chem. 2020 May;12(5):445–51.

171. Kobayashi R, Nabika H. Liquid–liquid phase separation induced by crowding condition affects amyloid-β aggregation mechanism. Soft Matter. 2024 July 10;20(27):5331–42.

172. Sudhakar S, Manohar A, Mani E. Liquid–Liquid Phase Separation (LLPS)-Driven Fibrilization of Amyloid-β Protein. ACS Chem Neurosci. 2023 Oct 4;14(19):3655–64.

173. Rahman MM, Lendel C. Extracellular protein components of amyloid plaques and their roles in Alzheimer's disease pathology. Mol Neurodegener. 2021 Aug 28;16(1):59.

174. Baek Y, Lee M. Exploring the complexity of amyloid-beta fibrils: structural polymorphisms and molecular interactions. Biochem Soc Trans. 2024 July 19;52(4):1631–46.

175. Paul TJ, Hoffmann Z, Wang C, Shanmugasundaram M, DeJoannis J, Shekhtman A, et al. Structural and Mechanical Properties of Amyloid Beta Fibrils: A Combined Experimental and Theoretical Approach. J Phys Chem Lett. 2016 July 21;7(14):2758–64.

176. Matveyenka M, Sholukh M, Kurouski D. Cytotoxicity of Amyloid β1–42 Fibrils to Brain Immune Cells. ACS Chem Neurosci. 2025 Mar 8;16(6):1144–9.

177. Ma YW, Lin TY, Tsai MY. Fibril Surface-Dependent Amyloid Precursors Revealed by Coarse-Grained Molecular Dynamics Simulation. Front Mol Biosci. 2021 Aug 6;8:719320.

178. Ruttenberg SM, Nowick JS. A Turn for the Worse: Aβ β-Hairpins in Alzheimer's Disease. Bioorg Med Chem. 2024 May 1;105:117715.

179. Hasecke F, Niyangoda C, Borjas G, Pan J, Matthews G, Muschol M, et al. Protofibril-Fibril Interactions Inhibit Amyloid Fibril Assembly by Obstructing Secondary Nucleation. Angew Chem Int Ed Engl. 2021 Feb 8;60(6):3016–21.

180. Hasecke F, Miti T, Perez C, Barton J, Schölzel D, Gremer L, et al. Origin of metastable oligomers and their effects on amyloid fibril self-assembly. Chem Sci. 2018 July 11;9(27):5937–48.

181. Nguyen HL, Linh HQ, Krupa P, La Penna G, Li MS. Amyloid β Dodecamer Disrupts the Neuronal Membrane More Strongly than the Mature Fibril: Understanding the Role of Oligomers in Neurotoxicity. J Phys Chem B. 2022 May 26;126(20):3659–72.

182. Zempel H, Mandelkow E. Lost after translation: missorting of Tau protein and consequences for Alzheimer disease. Trends Neurosci. 2014 Dec 1;37(12):721–32.

183. Qiao O, Ji H, Zhang Y, Zhang X, Zhang X, Liu N, et al. New insights in drug development for Alzheimer's disease based on microglia function. Biomed Pharmacother. 2021 Aug 1;140:111703.

184. Li X, Lei P, Tuo Q, Ayton S, Li QX, Moon S, et al. Enduring Elevations of Hippocampal Amyloid Precursor Protein and Iron Are Features of β-Amyloid Toxicity and Are Mediated by Tau. Neurotherapeutics. 2015 Oct 1;12(4):862–73.

185. Ng B, Vowles J, Bertherat F, Abey A, Kilfeather P, Beccano-Kelly D, et al. Tau depletion in human neurons mitigates Aβ-driven toxicity. Mol Psychiatry. 2024 July;29(7):2009–20.

186. Vossel KA, Xu JC, Fomenko V, Miyamoto T, Suberbielle E, Knox JA, et al. Tau reduction prevents Aβ-induced axonal transport deficits by blocking activation of GSK3β. J Cell Biol. 2015 May 11;209(3):419–33.

187. Tokutake T, Kasuga K, Yajima R, Sekine Y, Tezuka T, Nishizawa M, et al. Hyperphosphorylation of Tau Induced by Naturally Secreted Amyloid-β at Nanomolar Concentrations Is Modulated by Insulin-dependent Akt-GSK3β Signaling Pathway*. J Biol Chem. 2012 Oct 12;287(42):35222–33.

188. Terwel D, Muyllaert D, Dewachter I, Borghgraef P, Croes S, Devijver H, et al. Amyloid Activates GSK-3β to Aggravate Neuronal Tauopathy in Bigenic Mice. Am J Pathol. 2008 Mar 1;172(3):786–98.

189. Rhein V, Song X, Wiesner A, Ittner LM, Baysang G, Meier F, et al. Amyloid-β and tau synergistically impair the oxidative phosphorylation system in triple transgenic Alzheimer's disease mice. Proc Natl Acad Sci U S A. 2009 Nov 24;106(47):20057–62.

190. Eckert A, Schulz KL, Rhein V, Götz J. Convergence of Amyloid-β and Tau Pathologies on Mitochondria In Vivo. Mol Neurobiol. 2010 June 1;41(2):107–14.

191. Tripathi T, Khan H. Direct Interaction between the β-Amyloid Core and Tau Facilitates Cross-Seeding: A Novel Target for Therapeutic Intervention. Biochemistry. 2020 Feb 4;59(4):341–2.

192. Shoff TA, Derbez-Morin M, Cai P, Julian RR. The microtubule nexus linking amyloid beta and tau: A simple and unifying theory for the underlying cause of Alzheimer's Disease [Internet]. bioRxiv; 2025 [cited 2025 Nov 17]. p. 2025.09.16.676664. Available from: https://www.biorxiv.org/content/10.1101/2025.09.16.676664v1

193. Benbow SJ, Strovas TJ, Darvas M, Saxton A, Kraemer BC. Synergistic toxicity between tau and amyloid drives neuronal dysfunction and neurodegeneration in transgenic C. elegans. Hum Mol Genet. 2020 Feb 1;29(3):495–505.

194. Gallego-Rudolf J, Wiesman AI, Pichet Binette A, Villeneuve S, Baillet S. Synergistic association of Aβ and tau pathology with cortical neurophysiology and cognitive decline in asymptomatic older adults. Nat Neurosci. 2024 Nov;27(11):2130–7.

195. Morales R, Callegari K, Soto C. Prion-like features of misfolded Aβ and tau aggregates. Virus Res. 2015 Sept 2;207:106–12.

196. Kadamangudi S, Marcatti M, Zhang WR, Fracassi A, Kayed R, Limon A, et al. Amyloid-β oligomers increase the binding and internalization of tau oligomers in human synapses. Acta Neuropathol (Berl). 2024 Dec 17;149(1):2.

197. Manczak M, Reddy PH. Abnormal interaction of oligomeric amyloid-β with phosphorylated tau: implications to synaptic dysfunction and neuronal damage. J Alzheimers Dis JAD. 2013 Jan 1;36(2):285–95.

198. Wang B, Zhang L, Dai T, Qin Z, Lu H, Zhang L, et al. Liquid–liquid phase separation in human health and diseases. Signal Transduct Target Ther. 2021 Aug 2;6(1):1–16.

199. Alberti S, Gladfelter A, Mittag T. Considerations and Challenges in Studying Liquid-Liquid Phase Separation and Biomolecular Condensates. Cell. 2019 Jan 24;176(3):419–34.

200. Shin Y, Brangwynne CP. Liquid phase condensation in cell physiology and disease. Science. 2017 Sept 22;357(6357):eaaf4382.

201. Bergmann AM, Bauermann J, Bartolucci G, Donau C, Stasi M, Holtmannspötter AL, et al. Liquid spherical shells are a non-equilibrium steady state of active droplets. Nat Commun. 2023 Oct 17;14(1):6552.

202. Banani SF, Lee HO, Hyman AA, Rosen MK. Biomolecular condensates: Organizers of cellular biochemistry. Nat Rev Mol Cell Biol. 2017 May;18(5):285–98.

203. Strome S, Wood WB. Generation of asymmetry and segregation of germ-line granules in early C. elegans embryos. Cell. 1983 Nov;35(1):15–25.

204. Lafontaine DLJ, Riback JA, Bascetin R, Brangwynne CP. The nucleolus as a multiphase liquid condensate. Nat Rev Mol Cell Biol. 2021 Mar;22(3):165–82.

205. Staněk D, Fox AH. Nuclear bodies: news insights into structure and function. Curr Opin Cell Biol. 2017 June 1;46:94–101.

206. Hofmann S, Kedersha N, Anderson P, Ivanov P. Molecular mechanisms of stress granule assembly and disassembly. Biochim Biophys Acta BBA - Mol Cell Res. 2021 Jan 1;1868(1):118876.

207. Alberti S. Phase separation in biology. Curr Biol. 2017 Oct 23;27(20):R1097–102.

208. Xu WX, Qu Q, Zhuang HH, Teng XQ, Wei YW, Luo J, et al. The Burgeoning Significance of Liquid-Liquid Phase Separation in the Pathogenesis and Therapeutics of Cancers. Int J Biol Sci. 2024 Feb 12;20(5):1652–68.

209. Tong X, Tang R, Xu J, Wang W, Zhao Y, Yu X, et al. Liquid–liquid phase separation in tumor biology. Signal Transduct Target Ther. 2022 July 8;7(1):1–22.

210. Klein IA, Boija A, Afeyan LK, Hawken SW, Fan M, Dall'Agnese A, et al. Partitioning of cancer therapeutics in nuclear condensates. Science. 2020 June 19;368(6497):1386–92.

211. Ren J, Zhang Z, Zong Z, Zhang L, Zhou F. Emerging Implications of Phase Separation in Cancer. Adv Sci. 2022;9(31):2202855.

212. Luo YY, Wu JJ, Li YM. Regulation of liquid–liquid phase separation with focus on post-translational modifications. Chem Commun. 2021 Dec 9;57(98):13275–87.

213. Ajmal MR. Protein Misfolding and Aggregation in Proteinopathies: Causes, Mechanism and Cellular Response. Diseases. 2023 Feb 9;11(1):30.

214. Fassler JS, Skuodas S, Weeks DL, Phillips BT. Protein Aggregation and Disaggregation in Cells and Development. J Mol Biol. 2021 Oct 15;433(21):167215.

215. Cox D, Raeburn C, Sui X, Hatters DM. Protein aggregation in cell biology: An aggregomics perspective of health and disease. Semin Cell Dev Biol. 2020 Mar 1;99:40–54.

216. Babinchak WM, Surewicz WK. Liquid–Liquid Phase Separation and Its Mechanistic Role in Pathological Protein Aggregation. J Mol Biol. 2020 Mar 27;432(7):1910–25.

217. Li M, Fan Y, Li Q, Wang X, Zhao L, Zhu M. Liquid-Liquid Phase Separation Promotes Protein Aggregation and Its Implications in Ferroptosis in Parkinson's Disease Dementia. Oxid Med Cell Longev. 2022 Oct 6;2022:7165387.

218. Chakraborty P, Zweckstetter M. Role of aberrant phase separation in pathological protein aggregation. Curr Opin Struct Biol. 2023 Oct 1;82:102678.

219. Martin EW, Holehouse AS. Intrinsically disordered protein regions and phase separation: sequence determinants of assembly or lack thereof. Emerg Top Life Sci. 2020 Oct 20;4(3):307–29.

220. Harmon TS, Holehouse AS, Rosen MK, Pappu RV. Intrinsically disordered linkers determine the interplay between phase separation and gelation in multivalent proteins. Hyman AA, editor. eLife. 2017 Nov 1;6:e30294.

221. Zbinden A, Pérez-Berlanga M, De Rossi P, Polymenidou M. Phase Separation and Neurodegenerative Diseases: A Disturbance in the Force. Dev Cell. 2020 Oct 12;55(1):45–68.

222. Naskar A, Nayak A, Salaikumaran MR, Vishal SS, Gopal PP. Phase separation and pathologic transitions of RNP condensates in neurons: implications for amyotrophic lateral sclerosis, frontotemporal dementia and other neurodegenerative disorders. Front Mol Neurosci. 2023;16:1242925.

223. Banani SF, Rice AM, Peeples WB, Lin Y, Jain S, Parker R, et al. Compositional Control of Phase-Separated Cellular Bodies. Cell. 2016 July 28;166(3):651–63.

224. Tom JKA, Deniz AA. Complex dynamics of multicomponent biological coacervates. Curr Opin Colloid Interface Sci. 2021 Dec 1;56:101488.

225. Sołtys K, Tarczewska A, Bystranowska D. Modulation of biomolecular phase behavior by metal ions. Biochim Biophys Acta BBA - Mol Cell Res. 2023 Dec 1;1870(8):119567.

226. Dignon GL, Best RB, Mittal J. Biomolecular Phase Separation: From Molecular Driving Forces to Macroscopic Properties. Annu Rev Phys Chem. 2020 Apr 20;71(Volume 71, 2020):53–75.

227. Rodríguez LC, Foressi NN, Celej MS. Liquid-liquid phase separation of tau and α-synuclein: A new pathway of overlapping neuropathologies. Biochem Biophys Res Commun. 2024 Dec 31;741:151053.

228. Najafi S, Lin Y, Longhini AP, Zhang X, Delaney KT, Kosik KS, et al. Liquid–liquid phase separation of Tau by self and complex coacervation. Protein Sci. 2021;30(7):1393–407.

229. Franzmeier N, Roemer-Cassiano SN, Bernhardt AM, Dehsarvi A, Dewenter A, Steward A, et al. Alpha synuclein co-pathology is associated with accelerated amyloid-driven tau accumulation in Alzheimer's disease. Mol Neurodegener. 2025 Mar 18;20:31.

230. Yan X, Uronen RL, Huttunen HJ. The interaction of α-synuclein and Tau: A molecular conspiracy in neurodegeneration? Semin Cell Dev Biol. 2020 Mar 1;99:55–64.

231. Badiola N, de Oliveira RM, Herrera F, Guardia-Laguarta C, Gonçalves SA, Pera M, et al. Tau enhances α-synuclein aggregation and toxicity in cellular models of synucleinopathy. PloS One. 2011;6(10):e26609.

232. Guo JL, Covell DJ, Daniels JP, Iba M, Stieber A, Zhang B, et al. Distinct α-synuclein strains differentially promote tau inclusions in neurons. Cell. 2013 July 3;154(1):103–17.

233. Roy B, Jackson GR. Interactions between Tau and α-synuclein augment neurotoxicity in a Drosophila model of Parkinson's disease. Hum Mol Genet. 2014 June 1;23(11):3008–23.

234. Bhasne K, Sebastian S, Jain N, Mukhopadhyay S. Synergistic Amyloid Switch Triggered by Early Heterotypic Oligomerization of Intrinsically Disordered α-Synuclein and Tau. J Mol Biol. 2018 Aug 3;430(16):2508–20.

235. Moussaud S, Jones DR, Moussaud-Lamodière EL, Delenclos M, Ross OA, McLean PJ. Alpha-synuclein and tau: teammates in neurodegeneration? Mol Neurodegener. 2014 Oct 29;9(1):43.

236. Boeynaems S, Holehouse AS, Weinhardt V, Kovacs D, Van Lindt J, Larabell C, et al. Spontaneous driving forces give rise to protein−RNA condensates with coexisting phases and complex material properties. Proc Natl Acad Sci. 2019 Apr 16;116(16):7889–98.

237. Ditlev JA, Case LB, Rosen MK. Who's In and Who's Out—Compositional Control of Biomolecular Condensates. J Mol Biol. 2018 Nov 2;430(23):4666–84.

238. Espinosa JR, Joseph JA, Sanchez-Burgos I, Garaizar A, Frenkel D, Collepardo-Guevara R. Liquid network connectivity regulates the stability and composition of biomolecular condensates with many components. Proc Natl Acad Sci U S A. 2020 June 16;117(24):13238–47.

239. Sanchez-Burgos I, Joseph JA, Collepardo-Guevara R, Espinosa JR. Size conservation emerges spontaneously in biomolecular condensates formed by scaffolds and surfactant clients. Sci Rep. 2021 July 27;11(1):15241.

240. Onuchic PL, Milin AN, Alshareedah I, Deniz AA, Banerjee PR. Divalent cations can control a switch-like behavior in heterotypic and homotypic RNA coacervates. Sci Rep. 2019 Aug 21;9(1):12161.

241. C BK, Nii T, Mori T, Katayama Y, Kishimura A. Dynamic frustrated charge hotspots created by charge density modulation sequester globular proteins into complex coacervates. Chem Sci. 2023 June 21;14(24):6608–20.

242. Dehmelt L, Halpain S. The MAP2/Tau family of microtubule-associated proteins. Genome Biol. 2004 Dec 23;6(1):204.

243. Mukrasch MD, Bibow S, Korukottu J, Jeganathan S, Biernat J, Griesinger C, et al. Structural Polymorphism of 441-Residue Tau at Single Residue Resolution. PLOS Biol. 2009 Feb 17;7(2):e1000034.

244. Brunello CA, Merezhko M, Uronen RL, Huttunen HJ. Mechanisms of secretion and spreading of pathological tau protein. Cell Mol Life Sci. 2020 May 1;77(9):1721–44.

245. Zheng H, Sun H, Cai Q, Tai HC. The Enigma of Tau Protein Aggregation: Mechanistic Insights and Future Challenges. Int J Mol Sci. 2024 May 2;25(9):4969.

246. Lasagna-Reeves CA, Castillo-Carranza DL, Sengupta U, Guerrero-Munoz MJ, Kiritoshi T, Neugebauer V, et al. Alzheimer brain-derived tau oligomers propagate pathology from endogenous tau. Sci Rep. 2012 Oct 3;2(1):700.

247. Rocher AB, Crimins JL, Amatrudo JM, Kinson MS, Todd-Brown MA, Lewis J, et al. Structural and functional changes in tau mutant mice neurons are not linked to the presence of NFTs. Exp Neurol. 2010 June 1;223(2):385–93.

248. Santacruz K, Lewis J, Spires T, Paulson J, Kotilinek L, Ingelsson M, et al. Tau suppression in a neurodegenerative mouse model improves memory function. Science. 2005 July 15;309(5733):476–81.

249. Yoshiyama Y, Higuchi M, Zhang B, Huang SM, Iwata N, Saido TC, et al. Synapse Loss and Microglial Activation Precede Tangles in a P301S Tauopathy Mouse Model. Neuron. 2007 Feb 1;53(3):337–51.

250. Jiang L, Ash PEA, Maziuk BF, Ballance HI, Boudeau S, Abdullatif AA, et al. TIA1 regulates the generation and response to toxic tau oligomers. Acta Neuropathol (Berl). 2019 Feb 1;137(2):259–77.

251. Kanaan NM, Hamel C, Grabinski T, Combs B. Liquid-liquid phase separation induces pathogenic tau conformations in vitro. Nat Commun. 2020 June 4;11:2809.

252. Zhang X, Lin Y, Eschmann NA, Zhou H, Rauch JN, Hernandez I, et al. RNA stores tau reversibly in complex coacervates. PLOS Biol. 2017 July 6;15(7):e2002183.

253. Ukmar-Godec T, Hutten S, Grieshop MP, Rezaei-Ghaleh N, Cima-Omori MS, Biernat J, et al. Lysine/RNA-interactions drive and regulate biomolecular condensation. Nat Commun. 2019 July 2;10(1):2909.

254. Ainani H, Bouchmaa N, Ben Mrid R, El Fatimy R. Liquid-liquid phase separation of protein tau: An emerging process in Alzheimer's disease pathogenesis. Neurobiol Dis. 2023 Mar 1;178:106011.

255. Sinsky J, Pichlerova K, Hanes J. Tau Protein Interaction Partners and Their Roles in Alzheimer's Disease and Other Tauopathies. Int J Mol Sci. 2021 Jan;22(17):9207.

256. Lin Y, Fichou Y, Zeng Z, Hu NY, Han S. Electrostatically Driven Complex Coacervation and Amyloid Aggregation of Tau Are Independent Processes with Overlapping Conditions. ACS Chem Neurosci. 2020 Feb 19;11(4):615–27.

257. Han Y, Ye H, Li P, Zeng Y, Yang J, Gao M, et al. In vitro characterization and molecular dynamics simulation reveal mechanism of 14-3-3ζ regulated phase separation of the tau protein. Int J Biol Macromol. 2022 May 31;208:1072–81.

258. Lin Y, Fichou Y, Longhini AP, Llanes LC, Yin P, Bazan GC, et al. Liquid-Liquid Phase Separation of Tau Driven by Hydrophobic Interaction Facilitates Fibrillization of Tau. J Mol Biol. 2021 Jan 22;433(2):166731.

259. Hochmair J, Exner C, Franck M, Dominguez-Baquero A, Diez L, Brognaro H, et al. Molecular crowding and RNA synergize to promote phase separation, microtubule interaction, and seeding of Tau condensates. EMBO J. 2022 June;41(11):e108882.

260. Allahyartorkaman M, Chan TH, Chen EHL, Ng ST, Chen YA, Wen JK, et al. Phosphorylation-Induced Self-Coacervation versus RNA-Assisted Complex Coacervation of Tau Proteins. J Am Chem Soc. 2025 Mar 26;147(12):10172–87.

261. Buée L, Troquier L, Burnouf S, Belarbi K, Van der Jeugd A, Ahmed T, et al. From tau phosphorylation to tau aggregation: what about neuronal death? Biochem Soc Trans. 2010 July 26;38(4):967–72.

262. Rawat P, Sehar U, Bisht J, Selman A, Culberson J, Reddy PH. Phosphorylated Tau in Alzheimer's Disease and Other Tauopathies. Int J Mol Sci. 2022 Oct 25;23(21):12841.

263. Rodríguez LC, Foressi NN, Celej MS. Modulation of α-synuclein phase separation by biomolecules. Biochim Biophys Acta BBA - Proteins Proteomics. 2023 Feb 1;1871(2):140885.

264. Foressi NN, Rodríguez LC, Celej MS. Heterotypic liquid-liquid phase separation of tau and α-synuclein: Implications for overlapping neuropathologies. Biochim Biophys Acta Proteins Proteomics. 2023 Nov 1;1871(6):140950.

265. Siegert A, Rankovic M, Favretto F, Ukmar-Godec T, Strohäker T, Becker S, et al. Interplay between tau and α-synuclein liquid–liquid phase separation. Protein Sci Publ Protein Soc. 2021 July;30(7):1326–36.

266. Ishizawa T, Mattila P, Davies P, Wang D, Dickson DW. Colocalization of tau and alpha-synuclein epitopes in Lewy bodies. J Neuropathol Exp Neurol. 2003 Apr;62(4):389–97.

267. Twohig D, Nielsen HM. α-synuclein in the pathophysiology of Alzheimer's disease. Mol Neurodegener. 2019 June 11;14(1):23.

268. Foressi NN, Rodríguez LC, Celej MS. Heterotypic liquid-liquid phase separation of tau and α-synuclein: Implications for overlapping neuropathologies. Biochim Biophys Acta BBA - Proteins Proteomics. 2023 Nov 1;1871(6):140950.

269. Miranzadeh Mahabadi H, Taghibiglou C. Cellular Prion Protein (PrPc): Putative Interacting Partners and Consequences of the Interaction. Int J Mol Sci. 2020 Sept 25;21(19):7058.

270. Gomes LA, Hipp SA, Rijal Upadhaya A, Balakrishnan K, Ospitalieri S, Koper MJ, et al. Aβ-induced acceleration of Alzheimer-related τ-pathology spreading and its association with prion protein. Acta Neuropathol (Berl). 2019 Dec 1;138(6):913–41.

271. Laurén J, Gimbel DA, Nygaard HB, Gilbert JW, Strittmatter SM. Cellular prion protein mediates impairment of synaptic plasticity by amyloid-β oligomers. Nature. 2009 Feb;457(7233):1128–32.

272. Hu NW, Corbett GT, Moore S, Klyubin I, O'Malley TT, Walsh DM, et al. Extracellular Forms of Aβ and Tau from iPSC Models of Alzheimer's Disease Disrupt Synaptic Plasticity. Cell Rep. 2018 May 15;23(7):1932–8.

273. Rai SK, Khanna R, Avni A, Mukhopadhyay S. Heterotypic electrostatic interactions control complex phase separation of tau and prion into multiphasic condensates and co-aggregates. Proc Natl Acad Sci. 2023 Jan 10;120(2):e2216338120.

274. Hentze MW, Castello A, Schwarzl T, Preiss T. A brave new world of RNA-binding proteins. Nat Rev Mol Cell Biol. 2018 May;19(5):327–41.

275. Ripin N, Parker R. Formation, function, and pathology of RNP granules. Cell. 2023 Oct 26;186(22):4737–56.

276. Kedersha N, Ivanov P, Anderson P. Stress granules and cell signaling: more than just a passing phase? Trends Biochem Sci. 2013 Oct 1;38(10):494–506.

277. Banani SF, Lee HO, Hyman AA, Rosen MK. Biomolecular condensates: organizers of cellular biochemistry. Nat Rev Mol Cell Biol. 2017 May;18(5):285–98.

278. Wolozin B, Apicco D. RNA binding proteins and the genesis of neurodegenerative diseases. Adv Exp Med Biol. 2015;822:11–5.

279. Asadi MR, Sadat Moslehian M, Sabaie H, Jalaiei A, Ghafouri-Fard S, Taheri M, et al. Stress Granules and Neurodegenerative Disorders: A Scoping Review. Front Aging Neurosci. 2021 June 23;13:650740.

280. Kavanagh T, Halder A, Drummond E. Tau interactome and RNA binding proteins in neurodegenerative diseases. Mol Neurodegener. 2022 Oct 17;17(1):66.

281. Vanderweyde T, Yu H, Varnum M, Liu-Yesucevitz L, Citro A, Ikezu T, et al. Contrasting pathology of the stress granule proteins TIA-1 and G3BP in tauopathies. J Neurosci Off J Soc Neurosci. 2012 June 13;32(24):8270–83.

282. Vanderweyde T, Apicco DJ, Youmans-Kidder K, Ash PEA, Cook C, Lummertz da Rocha E, et al. Interaction of tau with the RNA-Binding Protein TIA1 Regulates tau Pathophysiology and Toxicity. Cell Rep. 2016 May 17;15(7):1455–66.

283. Maziuk BF, Apicco DJ, Cruz AL, Jiang L, Ash PEA, da Rocha EL, et al. RNA binding proteins co-localize with small tau inclusions in tauopathy. Acta Neuropathol Commun. 2018 Aug 1;6(1):71.

284. Apicco DJ, Ash PEA, Maziuk B, LeBlang C, Medalla M, Al Abdullatif A, et al. Reducing the RNA binding protein TIA1 protects against tau-mediated neurodegeneration in vivo. Nat Neurosci. 2018 Jan;21(1):72–80.

285. Kizhakkeduth ST, Abdul Vahid A, Oliyantakath Hassan MS, Parambil AK, Jain P, Vijayan V. Molecular Interactions between Tau Protein and TIA1: Distinguishing Physiological Condensates from Pathological Fibrils. ACS Chem Neurosci. 2024 Oct 7;acschemneuro.4c00456.

286. Kosmaoglou M, Schwarz N, Bett JS, Cheetham ME. Molecular chaperones and photoreceptor function. Prog Retin Eye Res. 2008 July;27(4):434–49.

287. Hu C, Yang J, Qi Z, Wu H, Wang B, Zou F, et al. Heat shock proteins: Biological functions, pathological roles, and therapeutic opportunities. MedComm. 2022 Aug 2;3(3):e161.

288. Ciechanover A, Kwon YT. Protein Quality Control by Molecular Chaperones in Neurodegeneration. Front Neurosci. 2017;11:185.

289. Nachman E, Wentink AS, Madiona K, Bousset L, Katsinelos T, Allinson K, et al. Disassembly of Tau fibrils by the human Hsp70 disaggregation machinery generates small seeding-competent species. J Biol Chem. 2020 July 10;295(28):9676–90.

290. Liu Z, Zhang S, Gu J, Tong Y, Li Y, Gui X, et al. Hsp27 chaperones FUS phase separation under the modulation of stress-induced phosphorylation. Nat Struct Mol Biol. 2020 Apr;27(4):363–72.

291. Mörman C, Leppert A, Pizzirusso G, Zheng Z, Sun X, Kumar R, et al. Chaperone-Mediated Regulation of Tau Phase Separation, Fibrillation, and Toxicity. J Am Chem Soc. 2025 July 9;147(27):23504–18.

292. Yu H, Lu S, Gasior K, Singh D, Vazquez-Sanchez S, Tapia O, et al. HSP70 chaperones RNA-free TDP-43 into anisotropic intranuclear liquid spherical shells. Science. 2021 Feb 5;371(6529):eabb4309.

293. Sun Y, MacRae TH. Small heat shock proteins: molecular structure and chaperone function. Cell Mol Life Sci CMLS. 2005 Nov 1;62(21):2460–76.

294. Darling AL, Dahrendorff J, Creodore SG, Dickey CA, Blair LJ, Uversky VN. Small heat shock protein 22 kDa can modulate the aggregation and liquid–liquid phase separation behavior of tau. Protein Sci. 2021;30(7):1350–9.

295. Mok SA, Condello C, Freilich R, Gillies A, Arhar T, Oroz J, et al. Mapping interactions with the chaperone network reveals factors that protect against tau aggregation. Nat Struct Mol Biol. 2018 May;25(5):384–93.

296. Rai SK, Khanna R, Sarbahi A, Joshi A, Mukhopadhyay S. Chaperone-mediated heterotypic phase separation regulates liquid-to-solid phase transitions of tau into amyloid fibrils. Sci Adv. 2025 June 6;11(23):eads1241.

297. Cristóvão JS, Morris VK, Cardoso I, Leal SS, Martínez J, Botelho HM, et al. The neuronal S100B protein is a calcium-tuned suppressor of amyloid-β aggregation. Sci Adv. 2018 June;4(6):eaaq1702.

298. Moreira GG, Cantrelle FX, Quezada A, Carvalho FS, Cristóvão JS, Sengupta U, et al. Dynamic interactions and Ca2+-binding modulate the holdase-type chaperone activity of S100B preventing tau aggregation and seeding. Nat Commun. 2021 Nov 1;12(1):6292.

299. Moreira GG, Gomes CM. Tau liquid–liquid phase separation is modulated by the Ca2+-switched chaperone activity of the S100B protein. J Neurochem. 2023;166(1):76–86.

300. Cau Y, Valensin D, Mori M, Draghi S, Botta M. Structure, Function, Involvement in Diseases and Targeting of 14-3-3 Proteins: An Update. Curr Med Chem. 25(1):5–21.

301. Chen Y, Chen X, Yao Z, Shi Y, Xiong J, Zhou J, et al. 14-3-3/Tau Interaction and Tau Amyloidogenesis. J Mol Neurosci MN. 2019 Aug;68(4):620–30.

302. Qureshi HY, Li T, MacDonald R, Cho CM, Leclerc N, Paudel HK. Interaction of 14-3-3ζ with Microtubule-Associated Protein Tau within Alzheimer's Disease Neurofibrillary Tangles. Biochemistry. 2013 Sept 17;52(37):6445–55.

303. Sluchanko NN, Gusev NB. Probable Participation of 14-3-3 in Tau Protein Oligomerization and Aggregation. J Alzheimer's Dis. 2011 Nov 29;27(3):467–76.

304. Layfield R, Fergusson J, Aitken A, Lowe J, Landon M, Mayer RJ. Neurofibrillary tangles of Alzheimer's disease brains contain 14-3-3 proteins. Neurosci Lett. 1996 May 3;209(1):57–60.

305. Hernández F, Cuadros R, Avila J. Zeta 14-3-3 protein favours the formation of human tau fibrillar polymers. Neurosci Lett. 2004 Mar 4;357(2):143–6.

306. Hashiguchi M, Sobue K, Paudel HK. 14-3-3ζ Is an Effector of Tau Protein Phosphorylation*. J Biol Chem. 2000 Aug 18;275(33):25247–54.

307. Sadik G, Tanaka T, Kato K, Yamamori H, Nessa BN, Morihara T, et al. Phosphorylation of tau at Ser214 mediates its interaction with 14-3-3 protein: implications for the mechanism of tau aggregation. J Neurochem. 2009;108(1):33–43.

308. Hochmair J, Oetelaar MCM van den, Ravatt L, Diez L, Lemmens LJM, Ponce-Lina R, et al. Stoichiometric 14-3-3ζ binding promotes phospho-Tau microtubule dissociation and reduces aggregation and condensation [Internet]. bioRxiv; 2025 [cited 2025 July 10]. p. 2024.03.15.585148. Available from: https://www.biorxiv.org/content/10.1101/2024.03.15.585148v2

309. Li T, Paudel HK. 14-3-3ζ Mediates Tau Aggregation in Human Neuroblastoma M17 Cells. PloS One. 2016;11(8):e0160635.

310. Wilkinson B, Gilbert HF. Protein disulfide isomerase. Biochim Biophys Acta BBA - Proteins Proteomics. 2004 June 1;1699(1):35–44.

311. Wang L, Wang X, Wang C chen. Protein disulfide–isomerase, a folding catalyst and a redox-regulated chaperone. Free Radic Biol Med. 2015 June 1;83:305–13.

312. Uehara T, Nakamura T, Yao D, Shi ZQ, Gu Z, Ma Y, et al. S-Nitrosylated protein-disulphide isomerase links protein misfolding to neurodegeneration. Nature. 2006 May;441(7092):513–7.

313. Walker AK, Farg MA, Bye CR, McLean CA, Horne MK, Atkin JD. Protein disulphide isomerase protects against protein aggregation and is S-nitrosylated in amyotrophic lateral sclerosis. Brain. 2010 Jan 1;133(1):105–16.

314. Andreu CI, Woehlbier U, Torres M, Hetz C. Protein disulfide isomerases in neurodegeneration: From disease mechanisms to biomedical applications. FEBS Lett. 2012 Aug 31;586(18):2826–34.

315. Honjo Y, Horibe T, Torisawa A, Ito H, Nakanishi A, Mori H, et al. Protein Disulfide Isomerase P5-Immunopositive Inclusions in Patients with Alzheimer's Disease. J Alzheimer's Dis. 2014 Jan 1;38(3):601–9.

316. Lee JH, Won SM, Suh J, Son SJ, Moon GJ, Park UJ, et al. Induction of the unfolded protein response and cell death pathway in Alzheimer's disease, but not in aged Tg2576 mice. Exp Mol Med. 2010 May;42(5):386–94.

317. Wang K, Liu JQ, Zhong T, Liu XL, Zeng Y, Qiao X, et al. Phase Separation and Cytotoxicity of Tau are Modulated by Protein Disulfide Isomerase and S-nitrosylation of this Molecular Chaperone. J Mol Biol. 2020 Mar 27;432(7):2141–63.

318. Vega IE. EFhd2, a Protein Linked to Alzheimer's Disease and Other Neurological Disorders. Front Neurosci. 2016 Mar 31;10:150.

319. Ferrer-Acosta Y, Rodríguez-Cruz EN, Orange F, De Jesús-Cortés H, Madera B, Vaquer-Alicea J, et al. EFhd2 is a novel amyloid protein associated with pathological tau in Alzheimer's disease. J Neurochem. 2013 June;125(6):921–31.

320. Vega IE, Traverso EE, Ferrer-Acosta Y, Matos E, Colon M, Gonzalez J, et al. A novel calcium-binding protein is associated with tau proteins in tauopathy. J Neurochem. 2008 July;106(1):96–106.

321. Vega IE, Sutter A, Parks L, Umstead A, Ivanova MI. Tau's Three-Repeat Domain and EFhd2 Co-incubation Leads to Increased Thioflavin Signal. Front Neurosci. 2018;12:879.

322. Vega IE, Umstead A, Kanaan NM. EFhd2 Affects Tau Liquid-Liquid Phase Separation. Front Neurosci. 2019;13:845.

323. Vega IE. EFhd2, a Protein Linked to Alzheimer's Disease and Other Neurological Disorders. Front Neurosci [Internet]. 2016 Mar 31 [cited 2025 June 25];10. Available from: https://www.frontiersin.org/journals/neuroscience/articles/10.3389/fnins.2016.00150/full

324. Dunyak BM, Gestwicki JE. Peptidyl-Proline Isomerases (PPIases): Targets for Natural Products and Natural Product-Inspired Compounds. J Med Chem. 2016 Nov 10;59(21):9622–44.

325. Cyclophilins as Modulators of Viral Replication [Internet]. [cited 2025 June 25]. Available from: https://www.mdpi.com/1999-4915/5/7/1684

326. Nigro P, Pompilio G, Capogrossi MC. Cyclophilin A: a key player for human disease. Cell Death Dis. 2013 Oct;4(10):e888–e888.

327. Koren J, Jinwal UK, Davey Z, Kiray J, Arulselvam K, Dickey CA. Bending tau into shape: the emerging role of peptidyl-prolyl isomerases in tauopathies. Mol Neurobiol. 2011 Aug;44(1):65–70.

328. Pasetto L, Grassano M, Pozzi S, Luotti S, Sammali E, Migazzi A, et al. Defective cyclophilin A induces TDP-43 proteinopathy: implications for amyotrophic lateral sclerosis and frontotemporal dementia. Brain J Neurol. 2021 Dec 31;144(12):3710–26.

329. Hattori Y, Kumashiro M, Kumeta H, Kyo T, Kawagoe S, Matsusaki M, et al. A Disease-Associated Mutation Impedes PPIA through Allosteric Dynamics Modulation. Biochemistry. 2025 June 30;

330. Babu M, Favretto F, Rankovic M, Zweckstetter M. Peptidyl Prolyl Isomerase A Modulates the Liquid–Liquid Phase Separation of Proline-Rich IDPs. J Am Chem Soc. 2022 Sept 7;144(35):16157–63.

331. Hill SE, Esquivel AR, Ospina SR, Rahal LM, Dickey CA, Blair LJ. Chaperoning activity of the cyclophilin family prevents tau aggregation. Protein Sci Publ Protein Soc. 2022 Nov;31(11):e4448.

332. Culibrk RA, Ebbert KA, Yeisley DJ, Chen R, Qureshi FA, Hahn J, et al. Impact of Suramin on Key Pathological Features of Sporadic Alzheimer's Disease-Derived Forebrain Neurons. J Alzheimers Dis JAD. 2024;98(1):301–18.

333. Exley C, Korchazhkina OV. Promotion of formation of amyloid fibrils by aluminium adenosine triphosphate (AlATP). J Inorg Biochem. 2001 Apr;84(3–4):215–24.

334. Majumder P, Trujillo CA, Lopes CG, Resende RR, Gomes KN, Yuahasi KK, et al. New insights into purinergic receptor signaling in neuronal differentiation, neuroprotection, and brain disorders. Purinergic Signal. 2007 Sept;3(4):317–31.

335. Prince PR, Hochmair J, Brognaro H, Gevorgyan S, Franck M, Schubert R, et al. Initiation and modulation of Tau protein phase separation by the drug suramin. Sci Rep. 2023 Mar 9;13(1):3963.

336. Oz M, Lorke DE, Hasan M, Petroianu GA. Cellular and molecular actions of Methylene Blue in the nervous system. Med Res Rev. 2011;31(1):93–117.

337. Medina DX, Caccamo A, Oddo S. Methylene Blue Reduces Aβ Levels and Rescues Early Cognitive Deficit by Increasing Proteasome Activity. Brain Pathol. 2011 Jan 27;21(2):140–9.

338. Wischik CM, Edwards PC, Lai RY, Roth M, Harrington CR. Selective inhibition of Alzheimer disease-like tau aggregation by phenothiazines. Proc Natl Acad Sci. 1996 Oct;93(20):11213–8.

339. Huang Y, Wen J, Ramirez LM, Gümüşdil E, Pokhrel P, Man VH, et al. Methylene blue accelerates liquid-to-gel transition of tau condensates impacting tau function and pathology. Nat Commun. 2023 Sept 6;14(1):5444.

340. Goedert M, Jakes R, Spillantini MG. The Synucleinopathies: Twenty Years On. J Park Dis. 2017 Mar 6;7(s1):S51–69.

341. Vidović M, Rikalovic MG. Alpha-Synuclein Aggregation Pathway in Parkinson's Disease: Current Status and Novel Therapeutic Approaches. Cells. 2022 Jan;11(11):1732.

342. Srinivasan E, Chandrasekhar G, Chandrasekar P, Anbarasu K, Vickram AS, Karunakaran R, et al. Alpha-Synuclein Aggregation in Parkinson's Disease. Front Med. 2021;8:736978.

343. Uversky VN. Neuropathology, biochemistry, and biophysics of α-synuclein aggregation. J Neurochem. 2007;103(1):17–37.

344. Fusco G, Pape T, Stephens AD, Mahou P, Costa AR, Kaminski CF, et al. Structural basis of synaptic vesicle assembly promoted by α-synuclein. Nat Commun. 2016 Sept 19;7(1):12563.

345. Maroteaux L, Campanelli JT, Scheller RH. Synuclein: a neuron-specific protein localized to the nucleus and presynaptic nerve terminal. J Neurosci. 1988 Aug 1;8(8):2804–15.

346. Calabresi P, Mechelli A, Natale G, Volpicelli-Daley L, Di Lazzaro G, Ghiglieri V. Alpha-synuclein in Parkinson's disease and other synucleinopathies: from overt neurodegeneration back to early synaptic dysfunction. Cell Death Dis. 2023 Mar 1;14(3):176.

347. Rocha EM, De Miranda B, Sanders LH. Alpha-synuclein: Pathology, mitochondrial dysfunction and neuroinflammation in Parkinson's disease. Neurobiol Dis. 2018 Jan 1;109:249–57.

348. Emamzadeh FN. Alpha-synuclein structure, functions, and interactions. J Res Med Sci. 2016;21(1):29.

349. Fauvet B, Mbefo MK, Fares MB, Desobry C, Michael S, Ardah MT, et al. α-Synuclein in Central Nervous System and from Erythrocytes, Mammalian Cells, and Escherichia coli Exists Predominantly as Disordered Monomer *. J Biol Chem. 2012 May 1;287(19):15345–64.

350. Alam P, Bousset L, Melki R, Otzen DE. α-synuclein oligomers and fibrils: a spectrum of species, a spectrum of toxicities. J Neurochem. 2019;150(5):522–34.

351. Danzer KM, Haasen D, Karow AR, Moussaud S, Habeck M, Giese A, et al. Different Species of α-Synuclein Oligomers Induce Calcium Influx and Seeding. J Neurosci. 2007 Aug 22;27(34):9220–32.

352. Du X yu, Xie X xiu, Liu R tian. The Role of α-Synuclein Oligomers in Parkinson's Disease. Int J Mol Sci. 2020 Nov 17;21(22):8645.

353. Cascella R, Bigi A, Cremades N, Cecchi C. Effects of oligomer toxicity, fibril toxicity and fibril spreading in synucleinopathies. Cell Mol Life Sci. 2022 Mar 4;79(3):174.

354. Winner B, Jappelli R, Maji SK, Desplats PA, Boyer L, Aigner S, et al. In vivo demonstration that α-synuclein oligomers are toxic. Proc Natl Acad Sci. 2011 Mar 8;108(10):4194–9.

355. Pieri L, Madiona K, Melki R. Structural and functional properties of prefibrillar α-synuclein oligomers. Sci Rep. 2016 Apr 14;6(1):24526.

356. Bigi A, Cascella R, Cecchi C. α-Synuclein oligomers and fibrils: partners in crime in synucleinopathies. Neural Regen Res. 2023 Nov;18(11):2332.

357. Fusco G, Chen SW, Williamson PTF, Cascella R, Perni M, Jarvis JA, et al. Structural basis of membrane disruption and cellular toxicity by α-synuclein oligomers. Science. 2017 Dec 15;358(6369):1440–3.

358. Ray S, Singh N, Kumar R, Patel K, Pandey S, Datta D, et al. α-Synuclein aggregation nucleates through liquid–liquid phase separation. Nat Chem. 2020 Aug;12(8):705–16.

359. Mukherjee S, Sakunthala A, Gadhe L, Poudyal M, Sawner AS, Kadu P, et al. Liquid-liquid Phase Separation of α-Synuclein: A New Mechanistic Insight for α-Synuclein Aggregation Associated with Parkinson's Disease Pathogenesis. J Mol Biol. 2023 Jan 15;435(1):167713.

360. Hardenberg MC, Sinnige T, Casford S, Dada ST, Poudel C, Robinson EA, et al. Observation of an α-synuclein liquid droplet state and its maturation into Lewy body-like assemblies. J Mol Cell Biol. 2021 Aug 4;13(4):282–94.

361. Sawner AS, Ray S, Yadav P, Mukherjee S, Panigrahi R, Poudyal M, et al. Modulating α-Synuclein Liquid–Liquid Phase Separation. Biochemistry. 2021 Dec 7;60(48):3676–96.

362. Piroska L, Fenyi A, Thomas S, Plamont MA, Redeker V, Melki R, et al. α-Synuclein liquid condensates fuel fibrillar α-synuclein growth. Sci Adv. 9(33):eadg5663.

363. Mahapatra A, Newberry RW. Liquid–liquid phase separation of α-synuclein is highly sensitive to sequence complexity. Protein Sci. 2024;33(4):e4951.

364. Hernandez SM, Tikhonova EB, Karamyshev AL. Protein-Protein Interactions in Alpha-Synuclein Biogenesis: New Potential Targets in Parkinson's Disease. Front Aging Neurosci. 2020;12:72.

365. Wakabayashi K, Tanji K, Mori F, Takahashi H. The Lewy body in Parkinson's disease: Molecules implicated in the formation and degradation of α-synuclein aggregates. Neuropathology. 2007;27(5):494–506.

366. Chánez-Cárdenas ME, Vázquez-Contreras E. The Aggregation of Huntingtin and α-Synuclein. J Biophys. 2012;2012:606172.

367. Dhakal S, Wyant CE, George HE, Morgan SE, Rangachari V. Prion-like C-Terminal Domain of TDP-43 and α-Synuclein Interact Synergistically to Generate Neurotoxic Hybrid Fibrils. J Mol Biol. 2021 May 14;433(10):166953.

368. Irwin DJ, Lee VMY, Trojanowski JQ. Parkinson's disease dementia: convergence of α-synuclein, tau and amyloid-β pathologies. Nat Rev Neurosci. 2013 Sept;14(9):626–36.

369. Spires-Jones TL, Attems J, Thal DR. Interactions of pathological proteins in neurodegenerative diseases. Acta Neuropathol (Berl). 2017 Aug 1;134(2):187–205.

370. Clinton LK, Blurton-Jones M, Myczek K, Trojanowski JQ, LaFerla FM. Synergistic Interactions between Aβ, Tau, and α-Synuclein: Acceleration of Neuropathology and Cognitive Decline. J Neurosci. 2010 May 26;30(21):7281–9.

371. Mackenzie IRA, Rademakers R. The role of TDP-43 in amyotrophic lateral sclerosis and frontotemporal dementia. Curr Opin Neurol. 2008 Dec;21(6):693–700.

372. Štalekar M, Yin X, Rebolj K, Darovic S, Troakes C, Mayr M, et al. Proteomic analyses reveal that loss of TDP-43 affects RNA processing and intracellular transport. Neuroscience. 2015 May 7;293:157–70.

373. Jo M, Lee S, Jeon YM, Kim S, Kwon Y, Kim HJ. The role of TDP-43 propagation in neurodegenerative diseases: integrating insights from clinical and experimental studies. Exp Mol Med. 2020 Oct;52(10):1652–62.

374. Yokota O, Davidson Y, Arai T, Hasegawa M, Akiyama H, Ishizu H, et al. Effect of topographical distribution of α-synuclein pathology on TDP-43 accumulation in Lewy body disease. Acta Neuropathol (Berl). 2010 Dec 1;120(6):789–801.

375. Meneses A, Koga S, O'Leary J, Dickson DW, Bu G, Zhao N. TDP-43 Pathology in Alzheimer's Disease. Mol Neurodegener. 2021 Dec 20;16(1):84.

376. Koga S, Lin WL, Walton RL, Ross OA, Dickson DW. TDP-43 pathology in multiple system atrophy: colocalization of TDP-43 and α-synuclein in glial cytoplasmic inclusions. Neuropathol Appl Neurobiol. 2018 Dec;44(7):707–21.

377. Dhakal S, Mondal M, Mirzazadeh A, Banerjee S, Ghosh A, Rangachari V. α-Synuclein emulsifies TDP-43 prion-like domain-RNA liquid droplets to promote heterotypic amyloid fibrils. Commun Biol. 2023 Dec 5;6(1):1227.

378. Thom T, Schmitz M, Fischer AL, Correia A, Correia S, Llorens F, et al. Cellular Prion Protein Mediates α-Synuclein Uptake, Localization, and Toxicity In Vitro and In Vivo. Mov Disord. 2022;37(1):39–51.

379. Vieira TCRG, Barros CA, Domingues R, Outeiro TF. PrP meets alpha-synuclein: Molecular mechanisms and implications for disease. J Neurochem. 2024;168(8):1625–39.

380. La Vitola P, Beeg M, Balducci C, Santamaria G, Restelli E, Colombo L, et al. Cellular prion protein neither binds to alpha-synuclein oligomers nor mediates their detrimental effects. Brain. 2019 Feb 1;142(2):249–54.

381. So RWL, Amano G, Stuart E, Ebrahim Amini A, Aguzzi A, Collingridge GL, et al. α-Synuclein strain propagation is independent of cellular prion protein expression in a transgenic synucleinopathy mouse model. PLOS Pathog. 2024 Sept 12;20(9):e1012517.

382. Agarwal A, Arora L, Rai SK, Avni A, Mukhopadhyay S. Spatiotemporal modulations in heterotypic condensates of prion and α-synuclein control phase transitions and amyloid conversion. Nat Commun. 2022 Mar 3;13(1):1154.

383. Jain MK, Singh P, Roy S, Bhat R. Comparative Analysis of the Conformation, Aggregation, Interaction, and Fibril Morphologies of Human α-, β-, and γ-Synuclein Proteins. Biochemistry. 2018 July 3;57(26):3830–48.

384. Brown JWP, Buell AK, Michaels TCT, Meisl G, Carozza J, Flagmeier P, et al. β-Synuclein suppresses both the initiation and amplification steps of α-synuclein aggregation via competitive binding to surfaces. Sci Rep. 2016 Nov 3;6(1):36010.

385. Hashimoto M, Rockenstein E, Mante M, Mallory M, Masliah E. β-Synuclein Inhibits α-Synuclein Aggregation: A Possible Role as an Anti-Parkinsonian Factor. Neuron. 2001 Oct 25;32(2):213–23.

386. Janowska MK, Wu KP, Baum J. Unveiling transient protein-protein interactions that modulate inhibition of alpha-synuclein aggregation by beta-synuclein, a pre-synaptic protein that co-localizes with alpha-synuclein. Sci Rep. 2015 Oct 19;5:15164.

387. Li X, Yu L, Liu X, Shi T, Zhang Y, Xiao Y, et al. β-synuclein regulates the phase transitions and amyloid conversion of α-synuclein. Nat Commun. 2024 Oct 9;15(1):8748.

388. Xu B, He W, Fan F, Chen S, Zhu M, Hou Y, et al. β-synuclein blocks α-synuclein condensate fusion to disrupt the maturation of phase separation. Cell Rep [Internet]. 2025 June 24 [cited 2025 June 30];44(6). Available from: https://www.cell.com/cell-reports/abstract/S2211-1247(25)00532-7

389. Hayashi J, Carver JA. β-Synuclein: An Enigmatic Protein with Diverse Functionality. Biomolecules. 2022 Jan 16;12(1):142.

390. Zhang C, Liu Y, Gilthorpe J, Maarel JRC van der. MRP14 (S100A9) Protein Interacts with Alzheimer Beta-Amyloid Peptide and Induces Its Fibrillization. PLOS ONE. 2012 Mar 22;7(3):e32953.

391. Horvath I, Iashchishyn IA, Moskalenko RA, Wang C, Wärmländer SKTS, Wallin C, et al. Co-aggregation of pro-inflammatory S100A9 with α-synuclein in Parkinson's disease: ex vivo and in vitro studies. J Neuroinflammation. 2018 June 4;15(1):172.

392. Veiveris D, Kopustas A, Sulskis D, Mikalauskaite K, Alsamsam MN, Tutkus M, et al. Heterotypic Droplet Formation by Pro-Inflammatory S100A9 and Neurodegenerative Disease-Related α-Synuclein. Biomacromolecules. 2025 June 9;26(6):3525–37.

393. Yan C, Jiang J, Yang Y, Geng X, Dong W. The function of VAMP2 in mediating membrane fusion: An overview. Front Mol Neurosci. 2022;15:948160.

394. Burré J, Sharma M, Tsetsenis T, Buchman V, Etherton M, Südhof TC. α-Synuclein Promotes SNARE-Complex Assembly in vivo and in vitro. Science. 2010 Sept 24;329(5999):1663–7.

395. Agarwal A, Chandran A, Raza F, Ungureanu IM, Hilcenko C, Stott K, et al. VAMP2 regulates phase separation of α-synuclein. Nat Cell Biol. 2024 Aug;26(8):1296–308.

396. Wang C, Zhang K, Cai B, Haller JE, Carnazza KE, Hu J, et al. VAMP2 chaperones α-synuclein in synaptic vesicle co-condensates. Nat Cell Biol. 2024 Aug;26(8):1287–95.

397. Sun J, Wang L, Bao H, Premi S, Das U, Chapman ER, et al. Functional cooperation of α-synuclein and VAMP2 in synaptic vesicle recycling. Proc Natl Acad Sci U S A. 2019 June 4;116(23):11113–5.

398. Sahoo BR, Bardwell JCA. SERF, a family of tiny highly conserved, highly charged proteins with enigmatic functions. FEBS J. 2023;290(17):4150–62.

399. Mitra R, Usher ET, Dedeoğlu S, Crotteau MJ, Fraser OA, Yennawar NH, et al. Molecular insights into the interaction between a disordered protein and a folded RNA. Proc Natl Acad Sci U S A. 2024 Dec 3;121(49):e2409139121.

400. Falsone SF, Meyer NH, Schrank E, Leitinger G, Pham CLL, Fodero-Tavoletti MT, et al. SERF Protein Is a Direct Modifier of Amyloid Fiber Assembly. Cell Rep. 2012 Aug 30;2(2):358–71.

401. Meinen BA, Gadkari VV, Stull F, Ruotolo BT, Bardwell JCA. SERF engages in a fuzzy complex that accelerates primary nucleation of amyloid proteins. Proc Natl Acad Sci U S A. 2019 Nov 12;116(46):23040–9.

402. Tsai TY, Jhang WT, Hsu HK, Chan YT, Chang CF, Chen YR. Amyloid Modifier SERF1a Accelerates Alzheimer's Amyloid-β Fibrillization and Exacerbates the Cytotoxicity. ACS Chem Neurosci. 2024 Feb 7;15(3):479–90.

403. Yoshimura Y, Holmberg MA, Kukic P, Andersen CB, Mata-Cabana A, Falsone SF, et al. MOAG-4 promotes the aggregation of α-synuclein by competing with self-protective electrostatic interactions. J Biol Chem. 2017 May 19;292(20):8269–78.

404. Merle DA, Witternigg A, Tam-Amersdorfer C, Hartlmüller C, Spreitzer E, Schrank E, et al. Increased Aggregation Tendency of Alpha-Synuclein in a Fully Disordered Protein Complex. J Mol Biol. 2019 June 28;431(14):2581–98.

405. Liu HN, Wang T, Hu JJ, Chen L, Shi X, Li YM, et al. The disordered protein SERF promotes α-Synuclein aggregation through liquid-liquid phase separation. J Biol Chem. 2024 Mar;300(3):105667.

406. Fornasiero EF, Bonanomi D, Benfenati F, Valtorta F. The role of synapsins in neuronal development. Cell Mol Life Sci CMLS. 2010 May;67(9):1383–96.

407. Milovanovic D, Wu Y, Bian X, De Camilli P. A Liquid Phase of Synapsin and Lipid Vesicles. Science. 2018 Aug 10;361(6402):604–7.

408. Mirza FJ, Zahid S. The Role of Synapsins in Neurological Disorders. Neurosci Bull. 2018 Apr 1;34(2):349–58.

409. Longhena F, Faustini G, Varanita T, Zaltieri M, Porrini V, Tessari I, et al. Synapsin III is a key component of α-synuclein fibrils in Lewy bodies of PD brains. Brain Pathol. 2018 Feb 23;28(6):875–88.

410. Zaltieri M, Grigoletto J, Longhena F, Navarria L, Favero G, Castrezzati S, et al. α-synuclein and synapsin III cooperatively regulate synaptic function in dopamine neurons. J Cell Sci. 2015 July 1;128(13):2231–43.

411. Hoffmann C, Sansevrino R, Morabito G, Logan C, Vabulas RM, Ulusoy A, et al. Synapsin Condensates Recruit alpha-Synuclein. J Mol Biol. 2021 June 11;433(12):166961.

412. Ross JA, Kasum CM. DIETARY FLAVONOIDS: Bioavailability, Metabolic Effects, and Safety. Annu Rev Nutr. 2002 July 1;22(Volume 22, 2002):19–34.

413. Ishige K, Schubert D, Sagara Y. Flavonoids protect neuronal cells from oxidative stress by three distinct mechanisms. Free Radic Biol Med. 2001 Feb 15;30(4):433–46.

414. Kimura AM, Tsuji M, Yasumoto T, Mori Y, Oguchi T, Tsuji Y, et al. Myricetin prevents high molecular weight Aβ1-42 oligomer-induced neurotoxicity through antioxidant effects in cell membranes and mitochondria. Free Radic Biol Med. 2021 Aug 1;171:232–44.

415. Takahashi R, Ono K, Takamura Y, Mizuguchi M, Ikeda T, Nishijo H, et al. Phenolic compounds prevent the oligomerization of α-synuclein and reduce synaptic toxicity. J Neurochem. 2015;134(5):943–55.

416. Prajapati KP, Singh AP, Dubey K, Ansari M, Temgire M, Anand BG, et al. Myricetin inhibits amyloid fibril formation of globular proteins by stabilizing the native structures. Colloids Surf B Biointerfaces. 2020 Feb 1;186:110640.

417. Sharma S, Tomar VR, Deep S. Myricetin: A Potent Anti-Amyloidogenic Polyphenol against Superoxide Dismutase 1 Aggregation. ACS Chem Neurosci. 2023 July 5;14(13):2461–75.

418. Caruana M, Högen T, Levin J, Hillmer A, Giese A, Vassallo N. Inhibition and disaggregation of α-synuclein oligomers by natural polyphenolic compounds. FEBS Lett. 2011;585(8):1113–20.

419. Xu B, Mo X, Chen J, Yu H, Liu Y. Myricetin Inhibits α-Synuclein Amyloid Aggregation by Delaying the Liquid-to-Solid Phase Transition. ChemBioChem. 2022;23(16):e202200216.

420. Zhang J, Zhang R, Jin S, Feng X. Curcumin, a plant polyphenol with multiple physiological functions of improving antioxidation, anti-inflammation, immunomodulation and its application in poultry production. J Anim Physiol Anim Nutr. 2024;108(6):1890–905.

421. He Y, Yue Y, Zheng X, Zhang K, Chen S, Du Z. Curcumin, Inflammation, and Chronic Diseases: How Are They Linked? Molecules. 2015 May;20(5):9183–213.

422. Nebrisi EE. Neuroprotective Activities of Curcumin in Parkinson's Disease: A Review of the Literature. Int J Mol Sci. 2021 Jan;22(20):11248.

423. Tang M, Taghibiglou C. The Mechanisms of Action of Curcumin in Alzheimer's Disease. J Alzheimer's Dis. 2017 June 23;58(4):1003–16.

424. Singh PK, Kotia V, Ghosh D, Mohite GM, Kumar A, Maji SK. Curcumin Modulates α-Synuclein Aggregation and Toxicity. ACS Chem Neurosci. 2013 Mar 20;4(3):393–407.

425. Pandey N, Strider J, Nolan WC, Yan SX, Galvin JE. Curcumin inhibits aggregation of α-synuclein. Acta Neuropathol (Berl). 2008 Apr 1;115(4):479–89.

426. Ono K, Yamada M. Expression of Concern: Antioxidant compounds have potent anti-fibrillogenic and fibril-destabilizing effects for α-synuclein fibrils in vitro. J Neurochem. 2006;97(1):105–15.

427. Xu B, Chen J, Liu Y. Curcumin Interacts with α-Synuclein Condensates To Inhibit Amyloid Aggregation under Phase Separation. ACS Omega. 2022 Aug 30;7(34):30281–90.

428. Craik DJ, Fairlie DP, Liras S, Price D. The Future of Peptide-based Drugs. Chem Biol Drug Des. 2013;81(1):136–47.

429. Armiento V, Spanopoulou A, Kapurniotu A. Peptide-Based Molecular Strategies To Interfere with Protein Misfolding, Aggregation, and Cell Degeneration. Angew Chem Int Ed. 2020;59(9):3372–84.

430. Ito K, Passioura T, Suga H. Technologies for the Synthesis of mRNA-Encoding Libraries and Discovery of Bioactive Natural Product-Inspired Non-Traditional Macrocyclic Peptides. Molecules. 2013 Mar;18(3):3502–28.

431. Ikenoue T, Oono M, So M, Yamakado H, Arata T, Takahashi R, et al. A RaPID Macrocyclic Peptide That Inhibits the Formation of α-Synuclein Amyloid Fibrils. ChemBioChem. 2023;24(12):e202300320.

432. Ikenoue T, So M, Terasaka N, Huang WE, Kawata Y, Miyanoiri Y, et al. De Novo Peptides That Induce the Liquid-Liquid Phase Separation of α-Synuclein. J Am Chem Soc. 2025 July 9;147(27):24113–26.

433. Lewandowski NM, Ju S, Verbitsky M, Ross B, Geddie ML, Rockenstein E, et al. Polyamine pathway contributes to the pathogenesis of Parkinson disease. Proc Natl Acad Sci. 2010 Sept 28;107(39):16970–5.

434. Handa AK, Fatima T, Mattoo AK. Polyamines: Bio-Molecules with Diverse Functions in Plant and Human Health and Disease. Front Chem. 2018;6:10.

435. Antony T, Hoyer W, Cherny D, Heim G, Jovin TM, Subramaniam V. Cellular Polyamines Promote the Aggregation of α-Synuclein*. J Biol Chem. 2003 Jan 31;278(5):3235–40.

436. Luo J, Yu CH, Yu H, Borstnar R, Kamerlin SCL, Gräslund A, et al. Cellular Polyamines Promote Amyloid-Beta (Aβ) Peptide Fibrillation and Modulate the Aggregation Pathways. ACS Chem Neurosci. 2013 Mar 20;4(3):454–62.

437. Percival M, Pantoja CF, Cima-Omori MS, Becker S, Zweckstetter M. Polyamines promote disordered protein phase separation [Internet]. bioRxiv; 2024 [cited 2025 Apr 21]. p. 2024.05.10.593468. Available from: https://www.biorxiv.org/content/10.1101/2024.05.10.593468v1

438. Rodríguez LC, Foressi NN, Celej MS. Modulation of α-synuclein phase separation by biomolecules. Biochim Biophys Acta BBA - Proteins Proteomics. 2023 Feb 1;1871(2):140885.

439. Jiang H, D'Agostino GD, Cole PA, Dempsey DR. Chapter Fifteen - Selective protein N-terminal labeling with N-hydroxysuccinimide esters. In: Chenoweth DM, editor. Methods in Enzymology [Internet]. Academic Press; 2020 [cited 2025 Aug 15]. p. 333–53. (Chemical Tools for Imaging, Manipulating, and Tracking Biological Systems: Diverse Methods for Optical Imaging and Conjugation; vol. 639). Available from: https://www.sciencedirect.com/science/article/pii/S0076687920301464

440. Koulouras G, Panagopoulos A, Rapsomaniki MA, Giakoumakis NN, Taraviras S, Lygerou Z. EasyFRAP-web: a web-based tool for the analysis of fluorescence recovery after photobleaching data. Nucleic Acids Res. 2018 July 2;46(W1):W467–72.

441. Zhao Y, Brener O, Andrzejewska E, Wei J, Reiß C, Tietz O, et al. Detecting and Tracking β-Amyloid Oligomeric Forms and Dynamics In Vitro by a High-Sensitivity Fluorescent-Based Assay. ACS Chem Neurosci. 2024 Dec 18;15(24):4383–9.

442. Düster R, Kaltheuner IH, Schmitz M, Geyer M. 1,6-Hexanediol, commonly used to dissolve liquid–liquid phase separated condensates, directly impairs kinase and phosphatase activities. J Biol Chem. 2021 Jan 8;296:100260.

443. Taylor NO, Wei MT, Stone HA, Brangwynne CP. Quantifying Dynamics in Phase-Separated Condensates Using Fluorescence Recovery after Photobleaching. Biophys J. 2019 Oct 1;117(7):1285–300.

444. Hayden EY, Teplow DB. Amyloid β-protein oligomers and Alzheimer's disease. Alzheimers Res Ther. 2013 Nov 29;5(6):60.

445. Gavini K, Parameshwaran K. Western Blot. In: StatPearls [Internet]. Treasure Island (FL): StatPearls Publishing; 2025 [cited 2025 Nov 18]. Available from: http://www.ncbi.nlm.nih.gov/books/NBK542290/

446. Akabayov B, Akabayov SR, Lee SJ, Wagner G, Richardson CC. Impact of macromolecular crowding on DNA replication. Nat Commun. 2013 Mar 19;4(1):1615.

447. Brzezinski M, Argudo PG, Scheidt T, Yu M, Hosseini E, Kaltbeitzel A, et al. Protein-Specific Crowding Accelerates Aging in Protein Condensates. Biomacromolecules. 2025 Apr 14;26(4):2060–75.

448. Liebau J, Laatsch BF, Rusnak J, Gunderson K, Finke B, Bargender K, et al. Polyethylene Glycol Impacts Conformation and Dynamics of Escherichia coli Prolyl-tRNA Synthetase Via Crowding and Confinement Effects. Biochemistry. 2024 July 2;63(13):1621–35.

449. Forman-Kay JD, Ditlev JA, Nosella ML, Lee HO. What are the distinguishing features and size requirements of biomolecular condensates and their implications for RNA-containing condensates? RNA. 2022 Jan;28(1):36–47.

450. Vosough F, Barth A. Characterization of Homogeneous and Heterogeneous Amyloid-β42 Oligomer Preparations with Biochemical Methods and Infrared Spectroscopy Reveals a Correlation between Infrared Spectrum and Oligomer Size. ACS Chem Neurosci. 2021 Jan 18;12(3):473–88.

451. Upadhaya AR, Lungrin I, Yamaguchi H, Fändrich M, Thal DR. High-molecular weight Aβ oligomers and protofibrils are the predominant Aβ species in the native soluble protein fraction of the AD brain. J Cell Mol Med. 2012 Feb;16(2):287–95.

452. Bramanti E, Fulgentini L, Bizzarri R, Lenci F, Sgarbossa A. β-Amyloid Amorphous Aggregates Induced by the Small Natural Molecule Ferulic Acid. J Phys Chem B. 2013 Nov 7;117(44):13816–21.

453. Meng JX, Zhang Y, Saman D, Haider AM, De S, Sang JC, et al. Hyperphosphorylated tau self-assembles into amorphous aggregates eliciting TLR4-dependent responses. Nat Commun. 2022 May 16;13(1):2692.

454. Kumar P, Nagarajan A, Uchil PD. Analysis of Cell Viability by the Lactate Dehydrogenase Assay. Cold Spring Harb Protoc. 2018 Jan 6;2018(6):pdb.prot095497.

455. Babinchak WM, Surewicz WK. Liquid-liquid phase separation and its mechanistic role in pathological protein aggregation. J Mol Biol. 2020 Mar 27;432(7):1910–25.

456. Biswas S, Hecht AL, Noble SA, Huang Q, Gillilan RE, Xu AY. Understanding the Impacts of Molecular and Macromolecular Crowding Agents on Protein–Polymer Complex Coacervates. Biomacromolecules. 2023 Nov 13;24(11):4771–82.

457. Phillip Y, Sherman E, Haran G, Schreiber G. Common Crowding Agents Have Only a Small Effect on Protein-Protein Interactions. Biophys J. 2009 Aug 5;97(3):875–85.

458. Chew PY, Joseph JA, Collepardo-Guevara R, Reinhardt A. Aromatic and arginine content drives multiphasic condensation of protein-RNA mixtures. Biophys J. 2024 June 4;123(11):1342–55.

459. King MR, Ruff KM, Lin AZ, Pant A, Farag M, Lalmansingh JM, et al. Macromolecular condensation organizes nucleolar sub-phases to set up a pH gradient. Cell. 2024 Apr 11;187(8):1889-1906.e24.

460. Sanders DW, Kedersha N, Lee DSW, Strom AR, Drake V, Riback JA, et al. Competing Protein-RNA Interaction Networks Control Multiphase Intracellular Organization. Cell. 2020 Apr 16;181(2):306-324.e28.

461. Ye S, Latham AP, Tang Y, Hsiung CH, Chen J, Luo F, et al. Micropolarity governs the structural organization of biomolecular condensates. Nat Chem Biol. 2024 Apr;20(4):443–51.

462. Lu T, Spruijt E. Multiphase Complex Coacervate Droplets. J Am Chem Soc. 2020 Feb 12;142(6):2905–14.

463. Kaur T, Raju M, Alshareedah I, Davis RB, Potoyan DA, Banerjee PR. Sequence-encoded and composition-dependent protein-RNA interactions control multiphasic condensate morphologies. Nat Commun. 2021 Feb 8;12(1):872.

464. Mountain GA, Keating CD. Formation of Multiphase Complex Coacervates and Partitioning of Biomolecules within them. Biomacromolecules. 2020 Feb 10;21(2):630–40.

465. ResearchGate [Internet]. [cited 2025 Nov 14]. (PDF) Heterotypic Protein Interactions Modulate the Condensate Dynamics and Aggregation of α-Synuclein. Available from: https://www.researchgate.net/publication/393761672_Heterotypic_Protein_Interactions_Modulate_the_Condensate_Dynamics_and_Aggregation_of_a-Synuclein

466. Meng F, Kim JY, Gopich IV, Chung HS. Single-molecule FRET and molecular diffusion analysis characterize stable oligomers of amyloid-β 42 of extremely low population. PNAS Nexus. 2023 Aug 1;2(8):pgad253.

467. Brzezinski M, Argudo PG, Scheidt T, Yu M, Lemke EA, Michels JJ, et al. Protein-specific crowding accelerates aging in phase-separated droplets [Internet]. bioRxiv; 2023 [cited 2025 Nov 5]. p. 2023.12.10.570970. Available from: https://www.biorxiv.org/content/10.1101/2023.12.10.570970v1

468. Takkella D, Vishwakarma J, Gavvala K. Effect of PEG-Induced Liquid–Liquid Phase Separation on DNA–Topotecan Interactions. J Phys Chem B [Internet]. 2025 Oct 29 [cited 2025 Nov 5]; Available from: https://doi.org/10.1021/acs.jpcb.5c04718

469. Juković M, Ratkaj I, Kalafatovic D, Bradshaw NJ. Amyloids, amorphous aggregates and assemblies of peptides – Assessing aggregation. Biophys Chem. 2024 May 1;308:107202.

470. Kuroda Y. Biophysical studies of amorphous protein aggregation and in vivo immunogenicity. Biophys Rev. 2022 Nov 23;14(6):1495–501.

471. Meng JX, Zhang Y, Saman D, Haider AM, De S, Sang JC, et al. Hyperphosphorylated tau self-assembles into amorphous aggregates eliciting TLR4-dependent responses. Nat Commun. 2022 May 16;13(1):2692.

472. Do TD, Economou NJ, Chamas A, Buratto SK, Shea JE, Bowers MT. Interactions between Amyloid-β and Tau Fragments Promote Aberrant Aggregates: Implications for Amyloid Toxicity. J Phys Chem B. 2014 Sept 25;118(38):11220–30.

473. Freyer D, Harms C. Kinetic Lactate Dehydrogenase Assay for Detection of Cell Damage in Primary Neuronal Cell Cultures. Bio-Protoc. 2017 June 5;7(11):e2308.

474. Raz Y, Miller Y. Interactions between Aβ and Mutated Tau Lead to Polymorphism and Induce Aggregation of Aβ-Mutated Tau Oligomeric Complexes. PLOS ONE. 2013 Aug 12;8(8):e73303.

475. Adhav VA, Saikrishnan K. The Realm of Unconventional Noncovalent Interactions in Proteins: Their Significance in Structure and Function. ACS Omega. 2023 June 13;8(25):22268–84.

476. Zhou HX, Pang X. Electrostatic Interactions in Protein Structure, Folding, Binding, and Condensation. Chem Rev. 2018 Feb 28;118(4):1691–741.

477. Ferenczy GG, Kellermayer M. Contribution of hydrophobic interactions to protein mechanical stability. Comput Struct Biotechnol J. 2022 Jan 1;20:1946–56.

478. Boyko S, Qi X, Chen TH, Surewicz K, Surewicz WK. Liquid–liquid phase separation of tau protein: The crucial role of electrostatic interactions. J Biol Chem. 2019 July 19;294(29):11054–9.

479. Beeg M, Battocchio E, De Luigi A, Colombo L, Natale C, Cagnotto A, et al. Nonphosphorylated tau slows down Aβ1–42 aggregation, binds to Aβ1–42 oligomers, and reduces Aβ1–42 toxicity. J Biol Chem. 2021 Apr 16;296:100664.

480. Wallin C, Hiruma Y, Wärmländer SKTS, Huvent I, Jarvet J, Abrahams JP, et al. The Neuronal Tau Protein Blocks in Vitro Fibrillation of the Amyloid-β (Aβ) Peptide at the Oligomeric Stage. J Am Chem Soc. 2018 July 5;140(26):8138–46.